



Final Report

Probing mechanisms of and improving *n*-butanol tolerance in *B. subtilis* using an untargeted metabolomics approach

By Nawaporn Vinayavekhin

Contract No. TRG5780194

Final Report

Probing mechanisms of and improving *n*-butanol tolerance in *B. subtilis* using an untargeted metabolomics approach

Dr. Nawaporn Vinayavekhin Department of Chemistry

Assoc. Prof. Dr. Alisa Vangnai Department of Biochemistry

Assoc. Prof. Dr. Polkit Sangvanich Department of Chemistry

Faculty of Science, Chulalongkorn University

This project was supported by the Thailand Research Fund and Chulalongkorn University

(The opinions expressed in this report are the sole responsibility of the authors and do not necessarily reflect those of the Thailand Research Fund or Chulalongkorn University.)

Abstract

Project Code: TRG5780194

Project Title: Probing mechanisms of and improving *n*-butanol tolerance in *B. subtilis* using an

untargeted metabolomics approach

Investigator:

Dr. Nawaporn Vinayavekhin

Department of Chemistry, Faculty of Science, CU

Assoc. Prof. Dr. Alisa Vangnai

Department of Biochemistry, Faculty of Science, CU

Assoc. Prof. Dr. Polkit Sangvanich

Department of Chemistry, Faculty of Science, CU

E-mail Address: nawaporn.v@chula.ac.th

Project Period: June 2, 2014 – June 1, 2016

Abstract:

1-Butanol has been utilized widely in industry and can be produced or transformed by microbes. However, current knowledge about the mechanisms of 1-butanol tolerance in bacteria remains quite limited. In this research project, we applied untargeted metabolomics to study Bacillus subtlis cells under 1-butanol stress and identified 55 and 37 ions with significantly increased and decreased levels, respectively. Using accurate mass determination, tandem mass spectra, and synthetic standards, 86% of these ions were characterized. The levels of phosphatidylethanolamine, diglucosyldiacylglycerol and phosphatidylserine were found to be upregulated upon 1-butanol treatment, whereas those of diacylglycerol and lysyl phosphatidylglycerol were downregulated. Most lipids contained 15:0/15:0, 16:0/15:0 and 17:0/15:0 acyl chains, and all were mapped to membrane lipid biosynthetic pathways. Subsequent two-stage quantitative real-time reverse transcriptase PCR analyses of genes in the two principal membrane lipid biosynthesis pathways revealed elevated levels of ywiE transcripts in the presence of 1-butanol and reduced expression levels of cdsA, pgsA, mprF, clsA and yfnI transcripts. Thus, the gene transcript levels showed agreement with the metabolomics data. Lastly, the cell morphology was investigated by scanning electron microscopy, which indicated that cells became almost two-fold longer after 1.4 % (v/v) 1-butanol stress for 12 h. Overall, the studies uncovered changes in the composition of glycerolipids and phospholipids in B. subtilis under 1-butanol stress, emphasizing the power of untargeted metabolomics in the discovery of new biological insights. The obtained knowledge from this project provides a good basis for further studying 1-butanol tolerance mechanisms, as well as engineering B. subtilis to be more tolerance to 1-butanol in the future.

(Most contents presented in this report were adapted from the published article; the final publication is available at Springer via http://dx.doi.org/10.1007/s00253-015-6692-0.)

Keywords: metabolomics, Bacillus subtilis, 1-butanol tolerance, membrane lipids

บทคัดย่อ

รหัสโครงการ: TRG5780194

ชื่อโครงการ: การศึกษากลไกและพัฒนาการทนต่อ *n-*butanol ของ *B. subtilis* โดยใช้วิธีการเมตาบอโลมิกส์

อย่างไม่เจาะจง

ชื่อนักวิจัย และสถาบัน:

อาจารย์ ดร.นวพร วินยเวคิน รองศาสตราจารย์ ดร.อลิสา วังใน

รองศาสตราจารย์ ดร.พลกฤษณ์ แสงวณิช

ภาควิชาเคมี คณะวิทยาศาสตร์ จุฬาลงกรณ์มหาวิทยาลัย ภาควิชาชีวเคมี คณะวิทยาศาสตร์ จุฬาลงกรณ์มหาวิทยาลัย ภาควิชาเคมี คณะวิทยาศาสตร์ จุฬาลงกรณ์มหาวิทยาลัย

อีเมล์: nawaporn.v@chula.ac.th

ระยะเวลาโครงการ: 2 มิถุนายน 2557 – 1 มิถุนายน 2559

บทคัดย่อ:

1-บิวทานอลเป็นสารที่ใช้แพร่หลายในอุตสาหกรรม และสามารถผลิตหรือเปลี่ยนรูปได้โดยใช้เชื้อจุลินทรีย์ อย่างไรก็ตาม ความรู้เกี่ยวกับกลไกความทนต่อ 1-บิวทานอลในแบคทีเรียยังค่อนข้างจำกัด โครงการวิจัยนี้จึง ประยุกต์ใช้วิธีเมตาบอโลมิกส์อย่างไม่เจาะจงเพื่อศึกษาเซลล์บาซิลลัส ซับทิลีส ภายใต้ความเครียดจาก 1-บิว ทานอล และระบุไอออนจำนวน 55 และ 37 ไอออนที่มีปริมาณเพิ่มขึ้นและน้อยลงเมื่ออยู่ใต้สภาวะนี้ ตามลำดับ 86 เปอร์เซ็นต์ของไอออนจำนวนนี้ได้รับการระบุเอกลักษณ์โดยใช้ข้อมูลค่ามวลแม่นยำ แทนเดม แมสสเปกตรัม และการเทียบค่ากับสารมาตรฐาน สารฟอสฟาทิดิลเอทานอลามีน ใดกลูโคซิลไดเอซิลกลีเซ อรอล และฟอสฟาทิดิลซีรีนมีปริมาณเพิ่มขึ้นเมื่อมี 1-บิวทานอล ในภาชนะเลี้ยงเชื้อ ส่วนไดเอซิลกลีเซอรอล และไลซิลฟอสฟาทิดิลกลีเซอรอลมีปริมาณลดลง ไขมันส่วนใหญ่ประกอบด้วยโซ่เอซิล 15:0/15:0, 16:0/15:0 และ 17:0/15:0 และอยู่ในวิถีชีวสังเคราะห์ของเมมเบรนลิพิด การวิเคราะห์ด้วยเทคนิคปฏิกิริยาลูกโซ่พอลิเมอ เรสแบบเวลาจริงของยืนในวิถีชีวสังเคราะห์ของเมมเบรนลิพิด 2 วิถีหลัก แสดงให้เห็นการเพิ่มขึ้นของยืน ywiE เมื่อมี 1-บิวทานอล และการลดลงของยืน cdsA, pgsA, mprF, clsA และ yfnI การเปลี่ยนแปลงของ ปริมาณยืนนี้สอดคล้องกับข้อมูลเมตาบอโลมิกส์ สุดท้าย การศึกษาสันฐานวิทยาของเซลล์ด้วยกล้อง จุลทรรศน์อิเล็กตรอนแบบส่องกราดทำให้ทราบว่า เซลล์ยาวขึ้นเกือบ 2 เท่า หลังอยู่ภายใต้ความเครียดจาก 1-บิวทานอล ปริมาณ 1.4 เปอร์เซ็นต์ เป็นเวลา 12 ชั่วโมง โดยภาพรวม การวิเคราะห์เมตาบอโลมิกส์อย่างไม่ เจาะจงแสดงให้เห็นการเปลี่ยนแปลงองค์ประกอบของกลีเซอโรลิพิดและฟอสโฟลิพิดในบาซิลลัส ซับทิลิส ภายใต้ความเครียดจาก 1-บิวทานอล ซึ่งเน้นย้ำให้เห็นถึงความสามารถของเมตาบอโลมิกส์อย่างไม่เจาะจงใน การค้นพบความเข้าใจอย่างลึกซึ้งทางชีววิทยาใหม่ ๆ องค์ความรู้ที่ได้ในงานวิจัยนี้จะเอื้อต่อการนำไปศึกษา กลไกและพัฒนาการทนต่อ 1-บิวทานอลของบาซิลลัส สับทิลีสในเชิงลึกต่อไป

คำหลัก: เมตาบอโลมิกส์, บาซิลลัส ซับทิลีส, การทนต่อ 1-บิวทานอล, เมมเบรนลิพิด

Executive Summary

1-butanol (or *n*-butanol) has been utilized in a wide variety of industries as a solvent and a stabilizer, and is considered currently as a promising second-generation biofuel. It is also a starting material for various valuable industrial products, such as paints, plastics, and polymers. Due to the recent lowering supply of petroleum oils, as well as the needs for highly efficient or specific transformation of chemicals, there are increasing efforts for finding strategies to produce, use, or transform 1-butanol. One attempt to approach this question is by using a genetically engineered microbe. However, the often-encountered problem here involves low yielding of desired products, which in most cases, are caused from inability of the microorganisms to tolerate high concentration of 1-butanol itself either as a starting material or product.

One way to improve 1-butanol tolerance of microbes is by understanding how they metabolically respond to and survive in an environment containing some amount of 1-butanol. In this proposal, liquid chromatography-mass spectrometry-based untargeted metabolomics analysis was therefore explored to identify lipophilic metabolites changed under 1-butanol stress in the cells of B. subtilis strain 168 (a model laboratory strain). After the characterization by bioinformatics, chemicals (using standards), tandem mass spectrometry, and comparison of retention time techniques, the levels of phosphatidylethanolamine, diglucosyldiacylglycerol and phosphatidylserine were found to be upregulated upon 6 hours of 1% (v/v) of 1-butanol treatment in Spizizen's minimal media (SMM). whereas those of diacylglycerol and lysyl phosphatidylglycerol were downregulated. Their levels were subsequently found by quantitative real-time reverse transcriptase PCR analyses (qRT-PCR) to correlate well with those of biosynthetic genes in the membrane lipid biosynthetic under 1-butanol stress, including upregulated ywiE gene and downregulated cdsA, pgsA, mprF, clsA and yfnI genes. Scanning electron microscope also revealed that the B. subtilis cells became almost two-fold longer $(3.91 \pm 0.66 \ \mu \text{m} \ vs. \ 1.98 \pm 0.27 \ \mu \text{m})$ when in contact with 1.4% (v/v) of 1-butanol in Luria-Bertani (LB) medium, which might help decrease surface-to-volume ratio, thereby alleviating their direct contacts with 1-butanol.

In summary, the research endeavors in this report not only uncover the metabolic responses of the microbe to 1-butanol stress, but also reveal metabolites and metabolic pathways responsible for improved tolerance of *B. subtilis* in 1-butanol. This knowledge will potentially allow us to better design an organism by perturbing their metabolic pathways or suggest novel strategies to achieve the desired outcomes. In a broader context, this project also leads to the establishment of untargeted metabolomics platforms for analyzing lipophilic metabolites, which can be applied to solve other biological and biochemical problems in the near future.

Introduction

Due to the decreasing supply of petroleum oil, increasing efforts have been spent on finding sustainably renewable resources for the production of fuels and related industrial chemicals in recent years. One such effort includes employing microorganisms to produce or transform compounds of interest, such as biofuels.

1-Butanol is a short chain alcohol, which has gained increasing attentions as a potential alternative biofuel^{1,2}, since it has many advantageous properties over ethanol, including its higher energy density and its lower vapor pressure, corrosiveness and solubility in water³. 1-Butanol has also been used widely in industries as a solvent, stabilizer and as a precursor in the production of paints, polymers and plastics⁴.

Microbial production of 1-butanol has long been possible industrially using the acetone-butanol-ethanol (ABE) production by suitable ABE microbes⁵. The process turns starch or sugars from molasses into 1-butanol, typically using the natural 1-butanol-producing strain, *Clostridium acetobutylicum*, as a fermentation host¹. However, one of the main problems is the low yield of 1-butanol, due to its toxicity even to the producing host. In fact, the bacterial growth is inhibited at only about 2 % (*v/v*) of 1-butanol⁶. The same problem with 1-butanol toxicity would need to be resolved as well, if microbes were to be employed for the conversion of 1-butanol to other industrially important compounds or in bioremediation.

Bacillus subtilis is one of the best-characterized Gram-positive bacteria⁷. It is non-pathogenic and has been considered an important industrial strain, especially for the synthesis of enzymes via heterologous expression. In terms of 1-butanol tolerance, it was shown that *B. subtilis* had the highest tolerance in 1-butanol of the other six commonly used mesophilic, facultatively anaerobic biofuel producing hosts⁸. *B. subtilis* strain GRSW2-B1 was also one of the microorganisms isolated from seawater samples in Thailand in a screen to find bacteria with a higher tolerance to 1-butanol⁹.

One way to aid obtaining a 1-butanol-tolerant strain of bacteria is by truly understanding how bacteria respond to 1-butanol-induced stress metabolically, since these metabolites might be crucial for the survival and tolerance of the microorganisms in 1-butanol. Consequently, supplementing such metabolites or their precursors into the growth medium or genetically engineering genes in the involved metabolic pathways to manipulate their levels might enhance the 1-butanol tolerance in bacteria.

Therefore, we set out to search for metabolite changes in response to 1-butanol stress in *B. subtilis* strain 168 (a laboratory strain) using an untargeted metabolomics approach to assay lipophilic compounds. The methods for the detection, quantitation and identification of lipophilic metabolites, and the observed changes in the levels of glycerolipids and phospholipids induced by 1-butanol are reported. Subsequent, two-stage quantitative real-time reverse transcriptase PCR (qrtRT-PCR) and scanning electron microscopy (SEM) were performed to attempt to link the observed changes in these metabolites to the expression level of their likely key gene transcripts and the changes in the cell morphology of *B. subtilis*, respectively.

Objectives

- I. Metabolomics analysis of B. subtilis strain 168 in the presence and absence of n- butanol. This aim is to use untargeted metabolomics strategies to measure lipophilic metabolite levels in B. subtilis incubated with and without n-butanol to enable the discovery of lipophilic metabolites potentially responsible for improving tolerance of B. subtilis in n-butanol.
- II. Characterization of metabolites whose levels are altered in n-butanol-treated samples. In this aim, we use various bioinformatics, chemical, analytical, and chromatographic techniques to characterize metabolite changes in aim 1, especially those elevated in n-butanol-treated samples.
- III. Linking metabolites with altering levels characterized in aim 2 to their biosynthetic pathways and thus to the related genes. The metabolites are searched on KEGG pathway database and in literature to find such connections.
- IV. Investigation of cell morphologies of *B. subtlis* strain 168 under *n*-butanol treatment.

Research Methodology

Bacterial Strains and Growth Conditions. *Bacillus subtilis* strain 168 was provided by the Bacillus Genetic Stock Center (BGSC). Unless otherwise stated, bacteria were grown aerobically at 200 rpm, 37 °C in Spizizen's minimal media (SMM; 2 g L⁻¹ (NH₄)₂SO₄, 14 g L⁻¹ K₂HPO₄, 6 g L⁻¹ KH₂PO₄, 1 g L⁻¹ sodium citrate and 1 mM MgSO₄) supplemented with carbon sources (5 g L⁻¹ glucose, 20 mg L⁻¹ L-tryptophan, and 18 mg L⁻¹ L-phenylalanine) and trace elements (5.5 mg L⁻¹ CaCl₂, 15.3 mg L⁻¹ FeCl₃·6H₂O, 1 mg L⁻¹ MnCl₂·4H₂O, 1.7 mg L⁻¹ ZnCl₂, 0.43 mg L⁻¹ CuCl₂·2H₂O, 0.6 mg L⁻¹ NaMoO₄·2H₂O and 0.47 mg L⁻¹ Na₂SeO₄) as reported previously¹⁰⁻¹².

Specifically, cultures (5 mL) of *B. subtilis* strain 168 were grown overnight and diluted 50-fold into 20 mL of fresh SMM medium. The cells were then allowed to grow to late lag phase (optical density at 600 nm (OD_{600}) of ~0.2–0.3), before they were treated with the indicated concentrations of 1-butanol (TCI > 99.0 %) or water as control and then grown further until the predetermined time. For the construction of growth curves, experiments were performed in triplicate and samples were collected every 3 h after treatment with 1-butanol to measure the OD_{600} . For the metabolomics and qrtRT-PCR analyses, cells were harvested 6 h after 1 % (v/v) 1-butanol was added to the culture.

Metabolites Extraction. Cell pellets were collected upon centrifugation of cultures (20 mL) at 4500g, 4 $^{\circ}$ C for 15 min, washed once with 20 mL of SMM medium without trace elements or carbon sources and then resuspended in 3 mL of fresh SMM. Extraction was then performed as described previously with slight modifications¹³. Briefly, the cell suspension was extracted with a 9 mL solution of 2:1 (v/v) ratio of chloroform (CHCl₃): methanol (MeOH) mixture in a glass vial and centrifuged at 1000g for 5 min to separate the organic layer (bottom) from the aqueous layer (top). Subsequently, the organic layer was carefully transferred to another vial and concentrated to dryness under a steam of nitrogen. Samples were stored at -20 $^{\circ}$ C and dissolved in 200 μ L CHCl₃ prior to analysis by liquid chromatography (LC)–mass spectrometry (MS).

LC–MS Analysis of Metabolomes. The LC–MS analysis was modified from that reported previously¹⁴. Briefly, the analysis was performed using Waters Alliance e2695 LC coupled to Bruker MicrOTOF Q-II MS instruments. For the LC analysis in the positive ion mode, a Luna C5 column (5 μm, 4.6 mm × 50 mm) was used together with a precolumn (Phenomenex). Mobile phase A was composed of 95/5 water/ MeOH, and mobile phase B was made up of a 60/35/5 isopropanol/ MeOH/ water mixture. In addition, 0.1 % (*v/v*) formic acid and 5 mM ammonium formate were added to both A and B to serve as solvent modifiers. The 60-min gradient started at 0 % B for 5 min at 0.1 mL min⁻¹ before abruptly changed to 20 % B and then increased linearly to 100 % B over 40 min at 0.4 mL min⁻¹. The gradient remained at 100 % B for 8 min at 0.5 mL min⁻¹ before ending with equilibration of the column at 0 % B for 7 min at 0.5 mL min⁻¹.

A similar LC analysis was performed in the negative ion mode except that samples were separated on a Gemini C18 column (5 μ m, 4.6 mm \times 50 mm; Phenomenex), and both mobile phases A and B were supplemented with 0.1 % (v/v) ammonium hydroxide as solvent modifiers instead. MS analysis was performed with an electrospray ionization source. The parameters were set as follows: end plate offset at -500 V, capillary voltage at 4000 V, Nebulizer pressure at 3 bar, dry gas at 8 L min⁻¹, dry temperature at 200 °C and collision RF at 150 Vpp. Data was collected in the profile mode with a mass range of 100–1500 Da. Mass axis calibration was performed for each individual analysis using 10 mM sodium formate solution. For each run, 40 μ L of metabolite extract was injected into the system for analysis.

LC–MS Untargeted Data Analysis. The total ion chromatograms were obtained for the two groups of samples (control *vs.* those stressed with 1 % (*v*/*v*) 1-butanol) in quadruplicate (giving a total of eight chromatograms in each ion mode). The chromatograms were analyzed in two steps. In the first step, automated data analysis by the XCMS program¹⁵ was performed to compare the metabolite profiles of the 1-butanol-treated samples with those of the untreated control samples so as to identify, match and quantify the ions in the LC–MS chromatographs of all samples. Then in the second stage, manual analysis of the XCMS output files was performed to obtain a final list of statistically-significant changing ions.

The automated data analysis step was performed as reported previously¹³. However, because of the differences in instruments employed, the conversion of the Bruker .d files to the mzXML format was achieved using the CompassXport software. The final XCMS output file contained the following information for each ion: average mass-to-charge ratio (m/z), average retention time, and integrated mass ion intensity (peak area; MSII) for each of the LC–MS chromatograms.

In the next step, manual analysis began with normalization of each ion by dividing the MSII of the ion by the OD_{600} of the culture from which it was derived to give a normalized MSII (nMSII) to control for any large differences in the cell number (as OD_{600} values) of the different samples (observed variance was 1.7- to 2.0-fold differences). To make each nMSII value closer to that of MSII, the nMSII was multiplied by the average OD_{600} of all eight samples in each mode to obtain the adjusted MSII (aMSII). The resulting values were then averaged within each group and subsequently

employed to calculate the fold changes (i.e., aMSII of control/ aMSII of 1-butanol-treated samples, or *vice versa*) for each ion.

To identify metabolites that were elevated or decreased upon addition of 1-butanol to B. subtilis cultures and not artifacts of differing cell numbers between cultures, certain criteria were set to filter out non-changing or unreal metabolites from the ion list. Specifically, these filters consisted of (i) a minimum fold changes of ≥ 4 , (ii) statistical significance (t-test with p < 0.05), and (iii) a minimum MSII of 30,000 in the elevated samples (which was approximately five times the limit of detection of the instruments). Subsequently, the remaining ions on the list were visually inspected for the peaks in the extracted ion chromatogram to eliminate isotopic ions or any false positives. Lastly, another set of experiments were repeated in triplicate for control and quadruplicate for 1-butanol-treated samples to confirm changes in the levels, as well as the presence of these ions in the final list.

Tandem MS Experiments. The MS/MS analyses were performed on every changing ion on the final list in previous part using a Waters Alliance e2695 instrument coupled to Bruker MicrOTOF Q-II instrument. The tandem MS analyses were performed in Auto MS/MS mode with instructions to include ions of interest in the precursor ion list using a target isolation width of 0.5. The number of precursor ions was set to 3 ions, and active exclusion was activated to exclude the ions after obtaining 3 MS/MS spectra and release the exclusion after 0.30 to 1.00 min. Collision energies were set at 35 V for m/z 500.00, 50 V for m/z 1000.00 and 70 V for m/z 2000.00. When an isolation mass was not exactly these values, the collision energies were then interpolated automatically from those of the two closest m/z values. Data were collected in the profile modes using a mass range of either 50–1500 Da or 100–1500 Da. Metabolites from the extract (40 μ L) or chemical standards (500 pmol) were separated using the same LC conditions as in the section "LC-MS analysis of metabolomes" before coupling to the tandem MS analyses.

Total RNA Isolation and Two-stage qrtRT-PCR Analysis. Cell pellets were collected by centrifugation of the cultures (5 mL for control and 10 mL for 1-butanol-stressed samples) at 4500g, 4° C for 15 min, and then washed once with SMM medium without trace elements or carbon sources using the same volumes as the cultures they were harvested from. Total RNA was isolated immediately from the washed cell pellets using the GF-1 Total RNA Extraction kit (Vivantis). In the first stage qrtRT-PCR, $4 \mu g$ of the total RNA was converted to cDNA using the RevertAid First Strand cDNA Synthesis kit (Thermo Scientific), according to the manufacturers' instructions. Subsequently, for each sample the respective cDNA solution was diluted 10- or 50-fold and then used as the template in the second stage qrtRT-PCR analysis using the SsoAdvancedTM SYBR® Green Supermix (Biorad). The primer sequences (Integrated DNA Technologies) for the amplification of the target genes are listed in Table 1, along with those of gyrase B (gyrB) that served as an internal control. Finally, data analysis was conducted by using the $2^{-\Delta\Delta_{\rm Ct}}$ method to calculate the relative amount of target mRNA in the 1-butanol-treated samples vs. the control. The Δ Ct values were subjected to Student's t-test, and only those with p < 0.05 were considered significant.

Table 1. Oligonucleotides Used for Amplification of Target Genes in the Second Stage qrtRT-PCR

Gene	Primer sequence (5' to 3')	Amplicon size (bp)
cdsA	TGG TTT CAC TGC CGG GTT TG GGA AAT CCC GTC CGC TTC AA	92
pssA	CAA AGC AAG CTC CCG ACG TT GCA AGT GCC GAT TGC CAG AA	108
psd	GGC AGC CGA AAT GTC CTG AT TCC TCG CCG ATC TCC AAT TCA	95
ugtP	GGC TAT GTG GAG CGC ATT GA TGG CTG TGG CTT CTG TCA AA	91
yfnI	TGA TGC CGA GCT GAC AAT GG AGG AAG CGA CTG GTA GGT GTT	94
yflE	CGC TGG CTG TTG GAC TTG AT AAC CTG GCA GTT GCG GAA TC	137
dgkB	ACG ACG TGC CAA GCA AAC TG ACG AAG TGA AGG CAG CAT TTC C	83
pgsA	AGA CTG GGT GGA CGG GTA TT CCA AGC TGG AGC GAG ATC AA	139
mprF	CAA TGA AGC GGC TCG AAA CGA ACC GCA CGC TGA ACA ACA AG	82
clsA	AGC CCG ATC ACG CCT TTG TA CTG TGC CGA CTG AAG CGA TTT	147
clsB	CCA ACA TTG CCC AAG CGA AGA CCA GCG GAT GGT CTG ATT TCA TC	147
ywiE	AAA TAG GGC GTG GCG ATC CA CCG TGG AAG GAG GAG GCA TTT A	127
gyrB (control)	AAG CTG GGC AAC TCA GAA GCA CGG AGC CAT TCT TGC TCT TGC CGC C	138

Cell Morphology. Cultures (20 mL) of *B. subtilis* strain 168 were prepared as detailed (Bacterial strains and growth conditions section), except that Luria-Bertani (LB) medium was used instead of SMM. Cells were allowed to grow in the absence (control) or presence of 1.4 % (*v/v*) 1-butanol for 12 h and then were harvested for cell morphology analysis by SEM as reported ¹⁶. In brief, to perform the SEM analysis, cells were collected by filtration through a 0.4 μm membrane and fixed with 2.5% glutaraldehyde in 0.1 M phosphate buffer (pH 7.2) for 2 h. The solution was then removed and the cells were washed twice with 0.1 M phosphate buffer (pH 7.2) and once with distilled water (5 min each). Next, specimens were prepared by dehydrating the cells in a graded ethanol series, followed by drying in a critical point dryer (Balzers, model no. CPD020) and gold-mounting and coating using a sputter coater (Balzers, model no. SCD040). Finally, a scanning

electron microscope (JEOL, model no. JSM-5410LV) was used to examine the specimens for any changes in their anhydrous morphology induced by the 1-butanol stress.

Results

Growth of *B. subtilis* 168 in SMM with varying amount of 1-butanol. To determine the appropriate culture conditions for the untargeted metabolomics analysis, we first monitored the growth of *B. subtilis* 168 in SMM medium with various concentrations of 1-butanol. The defined medium does not contain any unknown metabolites that might interfere with the subsequent LC–MS analyses, so it was appropriate for use as our culture conditions. Moreover, the addition of 1-butanol at an improper time can induce spore formation (data not shown). Thus, an overnight culture of *B. subtilis* in SMM medium was used to inoculate larger cultures (20 mL), which were allowed to grow to late lag phase $(OD_{600} \sim 0.25)$, prior to the addition of 1-butanol at concentrations up to 1.4% (v/v). The subsequent cell growth was then monitored by measuring the OD_{600} over 12 h.

The *B. subtilis* strain 168 was able to grow in 1-butanol at all tested concentrations (0.6–1.4 % (v/v)), albeit at lower growth rates than the 1-butanol free control (Figure 1). As expected when cells were induced to stress by 1-butanol, the OD₆₀₀ values at every measured time point were lower with increasing 1-butanol concentrations and lowest at 1.4% (v/v) 1-butanol. However, the fact that the final OD₆₀₀ of the cultures with 0.6% and 0.8% (v/v) of 1-butanol at 12 h did not differ noticeably from that of the control indicated that the level of stress subjected upon *B. subtilis* at these concentrations might be insignificant or insufficient over this 12 h time course.

From the results, because the lowest concentration of 1-butanol that moderately and continuously disrupted the growth of *B. subtilis* was 1% (v/v), this condition was selected for the metabolomics analysis. Since *B. subtilis* entered early stationary phase at 6 h in the presence of 1% (v/v) 1-butanol, this time point was selected, because by this time the cells would likely have already accumulated several stress-induced metabolites in respond to 1-butanol. At a 6 h time point, the OD₆₀₀ values of the 1-butanol-free control samples were approximately 1.7- to 2.0-fold higher than the samples cultured with 1% (v/v) 1-butanol.

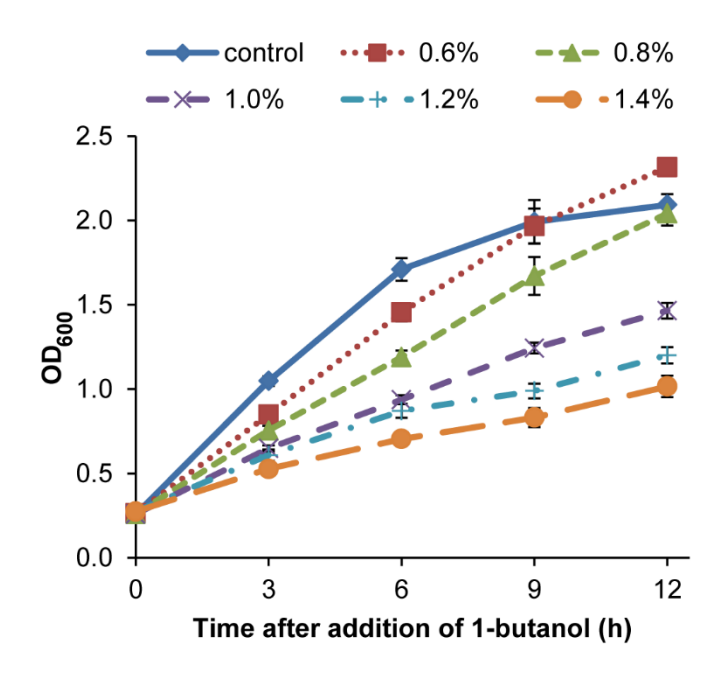


Figure 1. Growth curves of B. subtilis stain 168 in SMM medium with different concentrations of 1-butanol. Cultures were grown to late lag phase ($OD_{600} \sim 0.2-0.3$), before 1-butanol was added (all (VV)) at 0% (control; dark blue diamonds), 0.6% (red squares), 0.8% (green triangles), 1.0% (purple crosses), 1.2% (blue pluses) and 1.4% (orange circles). Data are shown as the average $OD_{600} \pm$ standard errors of the mean, derived from three experimental replicates per concentration.

Untargeted metabolomics of *B. subtilis* **168 under 1-butanol stress.** Untargeted metabolomics was performed on *B. subtilis* **168** cells cultured in the presence of 1% (*v*/*v*) 1-butanol for 6 h, along with those cultured without 1-butanol as the control. Hydrophobic metabolites, such as fatty acids, were then extracted from the cells using 2:1 (*v*/*v*) ratio CHCl₃: MeOH, and the extracts were then concentrated and subjected to LC–MS analysis using an untargeted metabolomics platform¹⁷.

To identify differentially changed metabolites associated with the 1-butanol stress response, the XCMS program was used to compare the metabolite profiles of the 1-butanol-treated samples with those of the untreated controls. The obtained MSII values were normalized to the OD_{600} value of each sample (aMSII) to account for differences in the cell numbers. To be certain that the differences were not merely artifacts of differing cell numbers, metabolite ions were labeled as likely to be involved in the 1-butanol stress response only if they were elevated or decreased by four-fold or more with statistical significance (p < 0.05) compared to in the control cells (Figure 2). The differential levels of the ions could clearly be observed in the extracted ion chromatograms (Figure 3). At the end, the unbiased comparative analyses identified 34 and 21 ions with increasing levels, and 30 and 7 ions with decreasing levels in the 1-butanol-treated samples in the positive and negative ion modes, respectively (Figure 2, Figure 3, and Tables 2–5).

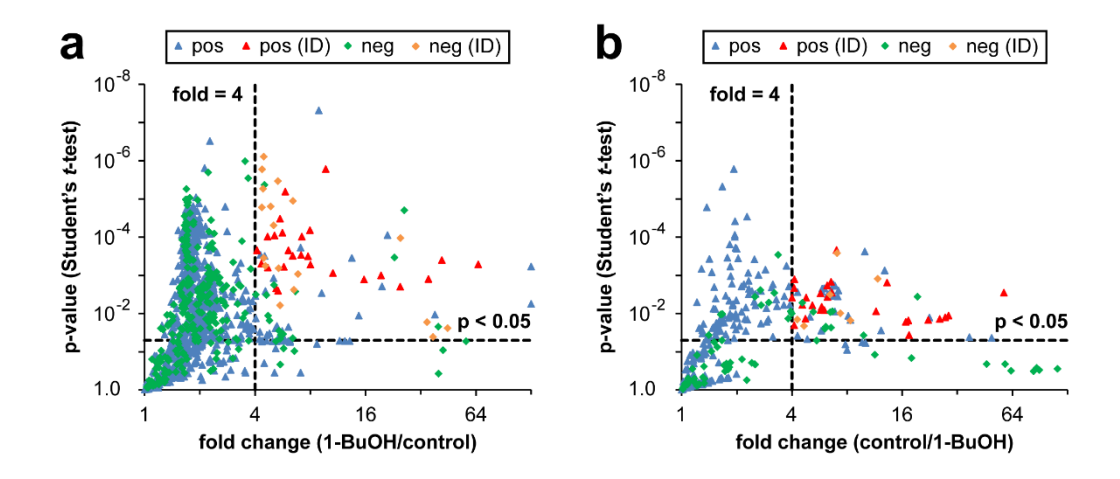


Figure 2. Results from the untargeted metabolomics analyses of hydrophobic cell components from *B. subtilis* 168 cells cultured in the absence (control) or presence of 1% (*v/v*) 1-butanol (1-BuOH) for 6 h. Each metabolite ion with an average MSII above 30,000 counts in the (**a**) 1-BuOH or (**b**) control group is plotted as its statistical significance against the fold change of (**a**) 1-BuOH over the control or (**b**) vice versa. Positive- and negative-mode MS ions are indicated by triangles and diamonds, respectively, with the red and orange colors representing statistically significant changing ions that could be characterized in this study.

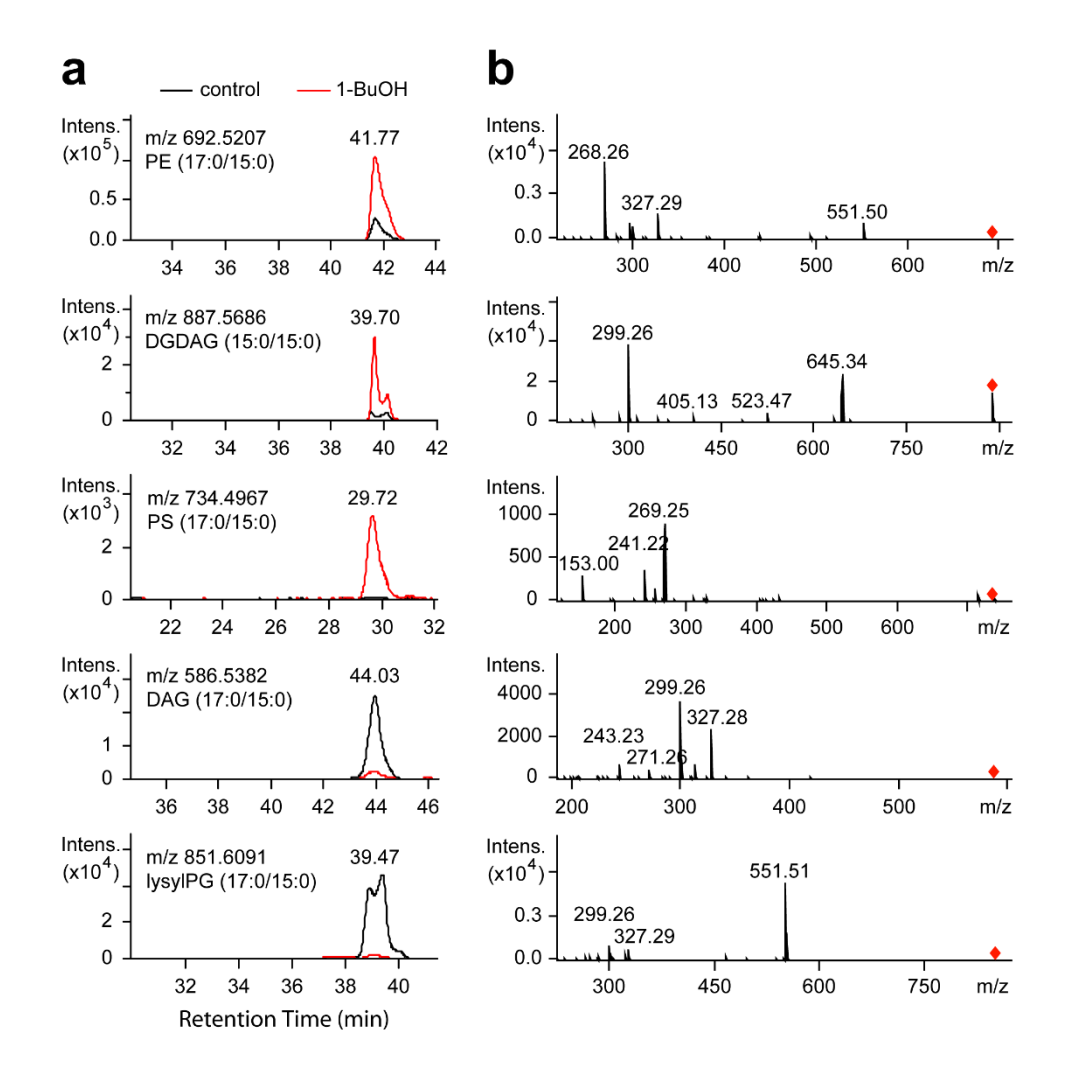


Figure 3. Representative differential detected ions between 1-butanol-stressed and unstressed *B. subtilis* cells, and their characterization as glycerolipids and phospholipids. (**a**) Extracted ion chromatograms of representative ions that showed highly elevated levels with m/z values of 692.5207, 887.5686 and 734.4967, or highly decreased levels with m/z values of 586.5382 and 851.6091 in the 1-butanol-treated samples (1-BuOH; dashed line) compared to the untreated control (solid line). Based on (**a**) accurate mass and (**b**) MS/MS spectra, they were characterized as PE (17:0/15:0), DGDAG (15:0/15:0), PS (17:0/15:0), DAG (17:0/15:0), and lysylPG (17:0/15:0), respectively, which are all membrane lipids. Precursor ions are denoted as diamonds in the MS/MS spectra. For a complete list of the changing ions, as well as identification of ions in the MS/MS spectra, see Tables 2–5.

Table 2. Positive-mode ions with significantly elevated levels in 1-butanol-treated *B. subtilis* compared to the untreated control showing the mass-to-charge ratio (m/z), retention time (RT), (a) potential identification, (b) integrated mass ion intensity (MSII), and (c) adjusted mass ion intensity (aMSII). (b) MSII and (c) aMSII data are for the four *B. subtilis* cultures without (Con-1–4) or with 1-butanol treatments (BuOH-1–4) and their respective averages (Con-avg and BuOH-avg, respectively).

(a) Significantly elevated positive-mode ions in 1-butanol-treated samples (potential identification)

#	m/z	RT (min)	lon	Potential identification
1	223.2024	35.6	?	?
2	243.2279	40.0	[M + H] ⁺	FFA (15:0) (a fragment of a larger compound?)
3	313.2492	34.7	?	?
4	337.2681	35.6	?	?
5	341.3200	38.5	?	?
6	381.3115	38.5	?	?
7	493.3491	39.6	?	?
8	517.4454	43.4	?	?
9	636.4574	39.3	[M + H] ⁺	PE (13:0/15:0)
10	650.4743	40.0	[M + H] ⁺	PE (14:0/15:0)
11	664.4893	40.6	[M + H] ⁺	PE (15:0/15:0) and some PE (14:0/16:0)
12	678.5045	41.2	[M + H] ⁺	PE (16:0/15:0)
13	686.4740	40.7	[M + Na] ⁺	PE (15:0/15:0) and some PE (14:0/16:0)
14	692.5207	41.7	[M + H] ⁺	PE (17:0/15:0)
15	700.4895	41.3	[M + Na] ⁺	PE (16:0/15:0)
16	706.5397	42.3	[M + H] ⁺	PE (18:0/15:0) and PE (16:0/17:0)
17	714.5043	41.8	[M + Na] ⁺	PE (17:0/15:0)
18	736.5072	42.0	[M + 2Na - H] ⁺	PE (17:0/15:0) and some PE (16:0/16:0)
19	887.5686	39.7	[M + Na] ⁺	DGDAG (15:0/15:0) and some DGDAG (14:0/16:0)
20	901.5840	40.7	[M + Na] ⁺	DGDAG (16:0/15:0) and some DGDAG (14:0/17:0)
21	903.5416	39.6	[M + K] ⁺	DGDAG (15:0/15:0) and some DGDAG (14:0/16:0)
22	1327.9713	40.6	[2M + H] ⁺	PE (15:0/15:0) and some PE (14:0/16:0)
23	1341.9807	41.1	[M + H] ⁺	PE (15:0/15:0) + PE (16:0/15:0)
24	1344.9465	39.9	[2M + HCONH ₂ + H] ⁺	PE (14:0/15:0)
25	1355.9990	41.2	[2M + H] ⁺	PE (16:0/15:0) or PE (14:0/17:0)
26	1358.9629	40.4	[M + HCONH ₂ + H] ⁺	PE (14:0/15:0) + PE (15:0/15:0)
27	1370.0164	41.6	[M + H] ⁺	PE (16:0/15:0) + PE (17:0/15:0)
28	1372.9808	40.6	[2M + HCONH ₂ + H] ⁺	PE (15:0/15:0) or PE (14:0/16:0)
29	1384.0328	41.7	[2M + H] ⁺	PE (17:0/15:0) or PE (16:0/16:0)
30	1386.9926	41.0	[M + HCONH ₂ + H] ⁺	PE (15:0/15:0) + PE (16:0/15:0)
31	1394.9604	40.7	[2M + HCONH ₂ + Na] ⁺	PE (15:0/15:0)
32	1401.0108	41.2	[2M + HCONH ₂ + H] ⁺	PE (16:0/15:0)
33	1406.0117	41.7	[M + Na] ⁺	PE (17:0/15:0)
34	1422.9911	41.3	[2M + HCONH ₂ + Na] ⁺	PE (16:0/15:0)

(b) Significantly elevated positive-mode ions in 1-butanol-treated samples (MSII)

ш		RT	RT Integrated mass ion intensity (MSII)										
#	m/z	(min)	BuOH-1	BuOH-2	BuOH-3	BuOH-4	BuOH- avg	Con-1	Con-2	Con-3	Con-4	Con-avg	
1	223.2024	35.6	3.8E+04	2.0E+04	2.5E+04	3.7E+04	3.0E+04	1.1E+02	1.1E+02	0.0E+00	0.0E+00	5.4E+01	
2	243.2279	40.0	6.7E+04	7.2E+04	6.9E+04	7.8E+04	7.2E+04	3.6E+03	6.4E+03	6.8E+03	6.3E+03	5.8E+03	
3	313.2492	34.7	7.9E+04	NA	4.9E+04	7.6E+04	6.8E+04	9.7E+03	1.0E+04	8.3E+03	9.8E+03	9.6E+03	
4	337.2681	35.6	1.6E+05	1.2E+05	1.1E+05	1.6E+05	1.4E+05	1.3E+04	1.1E+04	1.1E+04	1.3E+04	1.2E+04	
5	341.3200	38.5	5.3E+04	5.9E+04	4.9E+04	5.6E+04	5.4E+04	7.1E+03	7.6E+03	6.5E+03	6.5E+03	6.9E+03	
6	381.3115	38.5	1.3E+05	1.2E+05	1.4E+05	1.3E+05	1.3E+05	1.7E+04	2.8E+04	3.1E+04	2.3E+04	2.5E+04	
7	493.3491	39.6	3.1E+04	4.0E+04	5.7E+04	5.1E+04	4.5E+04	3.4E+03	6.5E+03	1.4E+04	8.9E+03	8.2E+03	
8	517.4454	43.4	5.6E+04	5.9E+04	5.5E+04	4.5E+04	5.4E+04	0.0E+00	0.0E+00	0.0E+00	0.0E+00	0.0E+00	
9	636.4574	39.3	8.1E+04	8.4E+04	7.9E+04	7.1E+04	7.9E+04	3.3E+04	3.1E+04	2.7E+04	2.4E+04	2.9E+04	
10	650.4743	40.0	4.0E+05	4.2E+05	3.8E+05	3.5E+05	3.9E+05	1.0E+05	9.7E+04	9.0E+04	8.5E+04	9.4E+04	
11	664.4893	40.6	1.5E+06	1.6E+06	1.6E+06	1.4E+06	1.5E+06	4.9E+05	4.8E+05	4.5E+05	4.2E+05	4.6E+05	
12	678.5045	41.2	2.7E+06	2.6E+06	2.8E+06	2.6E+06	2.7E+06	5.1E+05	5.1E+05	4.4E+05	4.4E+05	4.7E+05	
13	686.4740	40.7	2.6E+04	3.1E+04	3.4E+04	3.2E+04	3.1E+04	7.6E+03	7.9E+03	9.1E+03	8.2E+03	8.2E+03	
14	692.5207	41.7	2.7E+06	2.3E+06	2.4E+06	2.3E+06	2.4E+06	6.3E+05	6.5E+05	5.2E+05	5.1E+05	5.8E+05	
15	700.4895	41.3	8.0E+04	8.0E+04	9.4E+04	9.3E+04	8.7E+04	1.9E+04	1.8E+04	1.9E+04	1.9E+04	1.9E+04	
16	706.5397	42.3	2.1E+05	1.8E+05	1.6E+05	1.7E+05	1.8E+05	2.4E+04	3.4E+04	3.1E+04	2.7E+04	2.9E+04	
17	714.5043	41.8	1.6E+05	1.3E+05	1.5E+05	1.4E+05	1.5E+05	5.1E+04	4.9E+04	4.0E+04	4.3E+04	4.6E+04	
18	736.5072	42.0	3.2E+04	3.0E+04	3.3E+04	3.1E+04	3.1E+04	1.6E+04	1.6E+04	7.9E+03	1.2E+04	1.3E+04	
19	887.5686	39.7	4.4E+05	5.3E+05	6.1E+05	5.6E+05	5.3E+05	1.0E+05	8.6E+04	1.1E+05	1.6E+05	1.2E+05	
20	901.5840	40.7	1.7E+05	2.5E+05	2.7E+05	2.7E+05	2.4E+05	5.6E+04	5.9E+04	9.4E+04	9.7E+04	7.7E+04	
21	903.5416	39.6	4.0E+04	5.0E+04	5.8E+04	5.1E+04	5.0E+04	6.1E+03	8.1E+03	1.4E+04	1.6E+04	1.1E+04	
22	1327.9713	40.6	1.8E+05	2.0E+05	1.7E+05	1.4E+05	1.7E+05	1.7E+04	1.8E+04	1.4E+04	1.2E+04	1.5E+04	
23	1341.9807	41.1	9.8E+04	7.6E+04	1.1E+05	1.0E+05	9.5E+04	3.7E+03	4.0E+03	3.5E+03	4.4E+03	3.9E+03	
24	1344.9465	39.9	2.7E+05	2.8E+05	2.4E+05	1.9E+05	2.5E+05	8.7E+04	8.9E+04	7.6E+04	7.0E+04	8.1E+04	
25	1355.9990	41.2	5.1E+05	4.9E+05	4.4E+05	4.0E+05	4.6E+05	1.5E+04	1.4E+04	1.0E+04	9.3E+03	1.2E+04	
26	1358.9629	40.4	1.1E+05	9.8E+04	1.4E+05	1.2E+05	1.2E+05	4.5E+04	4.2E+04	4.6E+04	5.1E+04	4.6E+04	
27	1370.0164	41.6	3.3E+05	2.2E+05	2.6E+05	2.6E+05	2.7E+05	1.6E+04	1.5E+04	9.7E+03	1.2E+04	1.3E+04	
28	1372.9808	40.6	9.8E+05	9.6E+05	8.7E+05	7.6E+05	8.9E+05	3.9E+05	3.6E+05	2.9E+05	2.8E+05	3.3E+05	
29	1384.0328	41.7	4.3E+05	3.9E+05	3.2E+05	3.0E+05	3.6E+05	3.2E+04	3.1E+04	1.8E+04	1.9E+04	2.5E+04	
30	1386.9926	41.0	2.8E+05	2.3E+05	2.5E+05	2.8E+05	2.6E+05	9.7E+04	9.6E+04	7.5E+04	8.4E+04	8.8E+04	
31	1394.9604	40.7	3.1E+04	3.8E+04	4.1E+04	3.9E+04	3.7E+04	9.0E+03	9.8E+03	1.3E+04	1.1E+04	1.0E+04	
32	1401.0108	41.2	8.6E+05	7.3E+05	6.9E+05	6.7E+05	7.4E+05	2.6E+05	2.5E+05	1.8E+05	1.9E+05	2.2E+05	
33	1406.0117	41.7	3.3E+04	3.4E+04	2.9E+04	2.5E+04	3.0E+04	4.3E+03	3.8E+03	2.6E+03	2.7E+03	3.3E+03	
34	1422.9911	41.3	5.2E+04	5.1E+04	5.3E+04	4.8E+04	5.1E+04	1.5E+04	1.6E+04	1.4E+04	1.4E+04	1.5E+04	

(c) Significantly elevated positive-mode ions in 1-butanol-treated samples (aMSII)

	m/z	RT			Adj	usted inte	egrated mas	ss ion inte	ensity (alv	ISII)		
#	m/z	(min)	BuOH-1	BuOH-2	BuOH-3	BuOH-4	BuOH-avg	Con-1	Con-2	Con-3	Con-4	Con-avg
1	223.2024	35.6	5.2E+04	2.9E+04	3.3E+04	5.0E+04	4.1E+04	8.6E+01	8.7E+01	0.0E+00	0.0E+00	4.3E+01
2	243.2279	40.0	9.2E+04	1.0E+05	9.1E+04	1.1E+05	9.8E+04	2.7E+03	5.3E+03	6.0E+03	4.4E+03	4.6E+03
3	313.2492	34.7	1.2E+05	NA	8.7E+04	1.2E+05	1.1E+05	7.6E+03	7.3E+03	7.2E+03	7.5E+03	7.4E+03
4	337.2681	35.6	2.2E+05	1.7E+05	1.5E+05	2.1E+05	1.9E+05	1.0E+04	9.1E+03	1.0E+04	8.8E+03	9.5E+03
5	341.3200	38.5	7.3E+04	8.4E+04	6.5E+04	7.6E+04	7.4E+04	5.4E+03	6.3E+03	5.7E+03	4.5E+03	5.5E+03
6	381.3115	38.5	1.7E+05	1.8E+05	1.8E+05	1.8E+05	1.8E+05	1.3E+04	2.3E+04	2.7E+04	1.6E+04	2.0E+04
7	493.3491	39.6	4.3E+04	5.8E+04	7.5E+04	7.0E+04	6.1E+04	2.6E+03	5.4E+03	1.2E+04	6.2E+03	6.6E+03
8	517.4454	43.4	7.7E+04	8.4E+04	7.2E+04	6.2E+04	7.4E+04	0.0E+00	0.0E+00	0.0E+00	0.0E+00	0.0E+00
9	636.4574	39.3	1.1E+05	1.2E+05	1.0E+05	9.7E+04	1.1E+05	2.5E+04	2.6E+04	2.4E+04	1.7E+04	2.3E+04
10	650.4743	40.0	5.4E+05	6.0E+05	5.0E+05	4.8E+05	5.3E+05	8.0E+04	8.0E+04	7.9E+04	5.9E+04	7.5E+04
11	664.4893	40.6	2.0E+06	2.3E+06	2.1E+06	1.9E+06	2.1E+06	3.7E+05	4.0E+05	3.9E+05	3.0E+05	3.7E+05
12	678.5045	41.2	3.7E+06	3.8E+06	3.7E+06	3.5E+06	3.7E+06	3.9E+05	4.2E+05	3.9E+05	3.1E+05	3.8E+05
13	686.4740	40.7	3.5E+04	4.4E+04	4.4E+04	4.4E+04	4.2E+04	5.8E+03	6.5E+03	8.0E+03	5.7E+03	6.5E+03
14	692.5207	41.7	3.7E+06	3.3E+06	3.1E+06	3.1E+06	3.3E+06	4.9E+05	5.4E+05	4.6E+05	3.6E+05	4.6E+05
15	700.4895	41.3	1.1E+05	1.1E+05	1.2E+05	1.3E+05	1.2E+05	1.5E+04	1.5E+04	1.7E+04	1.3E+04	1.5E+04
16	706.5397	42.3	2.9E+05	2.5E+05	2.1E+05	2.2E+05	2.5E+05	1.9E+04	2.8E+04	2.7E+04	1.9E+04	2.3E+04
17	714.5043	41.8	2.2E+05	1.9E+05	2.0E+05	1.9E+05	2.0E+05	3.9E+04	4.1E+04	3.5E+04	3.0E+04	3.6E+04
18	736.5072	42.0	4.3E+04	4.3E+04	4.3E+04	4.2E+04	4.3E+04	1.3E+04	1.3E+04	6.9E+03	8.5E+03	1.0E+04
19	887.5686	39.7	5.9E+05	7.5E+05	8.0E+05	7.6E+05	7.3E+05	7.9E+04	7.1E+04	9.9E+04	1.1E+05	9.1E+04
20	901.5840	40.7	2.3E+05	3.5E+05	3.5E+05	3.7E+05	3.3E+05	4.4E+04	4.9E+04	8.3E+04	6.8E+04	6.1E+04
21	903.5416	39.6	5.5E+04	7.2E+04	7.6E+04	6.9E+04	6.8E+04	4.7E+03	6.7E+03	1.2E+04	1.1E+04	8.7E+03
22	1327.9713	40.6	2.4E+05	2.8E+05	2.3E+05	2.0E+05	2.4E+05	1.3E+04	1.5E+04	1.2E+04	8.7E+03	1.2E+04
23	1341.9807	41.1	1.3E+05	1.1E+05	1.4E+05	1.4E+05	1.3E+05	2.9E+03	3.3E+03	3.1E+03	3.1E+03	3.1E+03
24	1344.9465	39.9	3.7E+05	4.0E+05	3.2E+05	2.6E+05	3.4E+05	6.7E+04	7.4E+04	6.7E+04	4.9E+04	6.4E+04
25	1355.9990	41.2	6.9E+05	7.0E+05	5.8E+05	5.5E+05	6.3E+05	1.1E+04	1.2E+04	9.0E+03	6.5E+03	9.6E+03
26	1358.9629	40.4	1.5E+05	1.4E+05	1.8E+05	1.7E+05	1.6E+05	3.5E+04	3.5E+04	4.1E+04	3.5E+04	3.7E+04
27	1370.0164	41.6	4.5E+05	3.1E+05	3.4E+05	3.5E+05	3.6E+05	1.2E+04	1.2E+04	8.6E+03	8.1E+03	1.0E+04
28	1372.9808	40.6	1.3E+06	1.4E+06	1.1E+06	1.0E+06	1.2E+06	3.0E+05	2.9E+05	2.5E+05	1.9E+05	2.6E+05
29	1384.0328	41.7	5.9E+05	5.5E+05	4.2E+05	4.0E+05	4.9E+05	2.5E+04	2.5E+04	1.6E+04	1.3E+04	2.0E+04
30	1386.9926	41.0	3.8E+05	3.3E+05	3.3E+05	3.8E+05	3.6E+05	7.5E+04	7.9E+04	6.7E+04	5.8E+04	7.0E+04
31	1394.9604	40.7	4.3E+04	5.4E+04	5.4E+04	5.3E+04	5.1E+04	7.0E+03	8.1E+03	1.1E+04	7.3E+03	8.4E+03
32	1401.0108	41.2	1.2E+06	1.0E+06	9.0E+05	9.1E+05	1.0E+06	2.0E+05	2.0E+05	1.6E+05	1.3E+05	1.8E+05
33	1406.0117	41.7	4.5E+04	4.9E+04	3.8E+04	3.4E+04	4.2E+04	3.3E+03	3.1E+03	2.3E+03	1.9E+03	2.7E+03
34	1422.9911	41.3	7.1E+04	7.2E+04	6.9E+04	6.5E+04	6.9E+04	1.2E+04	1.3E+04	1.3E+04	1.0E+04	1.2E+04

Table 3. Negative-mode ions with significantly elevated levels in 1-butanol-treated *B. subtilis* compared to the untreated control showing the mass-to-charge ratio (m/z), retention time (RT), (a) potential identification, (b) integrated mass ion intensity (MSII), and (c) adjusted mass ion intensity (aMSII). (b) MSII and (c) aMSII data are for the four *B. subtilis* cultures without (Con-1–4) or with 1-butanol treatments (BuOH-1–4) and their respective averages (Con-avg and BuOH-avg, respectively).

(a) Significantly elevated negative-mode ions in 1-butanol-treated samples (potential identification)

#	m/z	RT (min)	lon	Potential identification
1	474.2599	37.5	[M + Na - 2H] ⁻	Fragment of PE (16:0/15:0)
2	488.2762	38.5	[M + Na - 2H] ⁻	Fragment of PE (17:0/15:0)
3	572.2569	38.5	[M + Na - 2H + 84] ⁻	Fragment of PE (17:0/15:0)?
4	648.4608	35.7	[M - H] ⁻	PE (14:0/15:0) and some PE (13:0/16:0)
5	662.4753	37.9	[M - H] ⁻	PE (15:0/15:0) and PE (14:0/16:0)
6	670.4420	35.7	[M + Na - 2H] ⁻	PE (14:0/15:0) and some PE (13:0/16:0)
7	676.4917	37.6	[M - H] ⁻	PE (16:0/15:0) and some PE (14:0/17:0)
8	684.4578	37.9	[M + Na - 2H] ⁻	PE (15:0/15:0) and PE (14:0/16:0)
9	690.5084	38.5	[M - H] ⁻	PE (17:0/15:0) and some PE (16:0/16:0)
10	698.4726	37.5	[M + Na - 2H] ⁻	PE (16:0/15:0) and some PE (14:0/17:0)
11	704.5251	39.6	[M - H] ⁻	PE (18:0/15:0) and some PE (16:0/17:0)
12	706.4664	28.6	[M - H] ⁻	PS (15:0/15:0) and some PS (14:0/16:0)
13	712.4893	38.5	[M + Na - 2H] ⁻	PE (17:0/15:0) and some PE (16:0/16:0)
14	720.4817	29.5	[M - H] ⁻	PS (16:0/15:0) and some PS (14:0/17:0)
15	723.4289	32.7	?	?
16	734.4967	30.4	[M - H] ⁻	PS (17:0/15:0) and some PS (16:0/16:0)
17	760.4695	37.6	[M - H + 84] ⁻	PE (16:0/15:0)
18	774.4860	38.5	[M - H + 84] ⁻	PE (17:0/15:0)
19	905.6164	46.7	?	?
20	1031.5878	33.3	?	?
21	1325.9568	36.5	[2M - H] ⁻	PE (15:0/15:0) and PE (14:0/16:0)

(b) Significantly elevated negative-mode ions in 1-butanol-treated samples (MSII)

	,	RT				Integrat	ed mass io	n intensit	y (MSII)			
#	m/z	(min)	BuOH-1	BuOH-2	BuOH-3	BuOH-4	BuOH-avg	Con-1	Con-2	Con-3	Con-4	Con-avg
1	474.2599	37.5	5.8E+04	5.5E+04	5.2E+04	5.6E+04	5.5E+04	1.4E+04	2.1E+04	1.9E+04	1.8E+04	1.8E+04
2	488.2762	38.5	3.6E+04	3.5E+04	3.2E+04	3.1E+04	3.3E+04	7.7E+03	1.4E+04	1.3E+04	1.2E+04	1.2E+04
3	572.2569	38.5	4.2E+04	4.5E+04	4.5E+04	4.2E+04	4.4E+04	1.1E+04	2.0E+04	1.8E+04	1.9E+04	1.7E+04
4	648.4608	35.7	3.0E+05	4.0E+05	4.7E+05	4.3E+05	4.0E+05	3.9E+04	1.1E+05	1.2E+05	1.3E+05	1.0E+05
5	662.4753	37.9	1.2E+06	NA	1.2E+06	1.2E+06	1.2E+06	3.1E+05	6.8E+05	4.2E+05	4.4E+05	4.6E+05
6	670.4420	35.7	2.8E+04	4.2E+04	4.9E+04	4.4E+04	4.1E+04	4.0E+03	1.2E+04	1.2E+04	1.5E+04	1.1E+04
7	676.4917	37.6	1.7E+06	1.8E+06	1.7E+06	1.7E+06	1.7E+06	6.8E+05	7.1E+05	6.3E+05	6.9E+05	6.8E+05
8	684.4578	37.9	1.0E+05	NA	1.0E+05	9.3E+04	9.9E+04	3.1E+04	5.2E+04	3.5E+04	3.5E+04	3.8E+04
9	690.5084	38.5	1.2E+06	1.1E+06	9.7E+05	9.9E+05	1.1E+06	4.3E+05	3.7E+05	4.0E+05	3.8E+05	4.0E+05
10	698.4726	37.5	1.7E+05	1.7E+05	1.7E+05	1.8E+05	1.7E+05	7.5E+04	6.9E+04	6.1E+04	6.1E+04	6.6E+04
11	704.5251	39.6	1.5E+05	1.3E+05	1.3E+05	1.4E+05	1.3E+05	5.7E+03	1.0E+04	1.1E+04	1.0E+04	9.2E+03
12	706.4664	28.6	3.9E+04	4.3E+04	7.1E+04	9.4E+04	6.2E+04	2.6E+03	3.5E+03	2.5E+03	3.6E+03	3.1E+03
13	712.4893	38.5	1.3E+05	1.1E+05	1.1E+05	1.1E+05	1.1E+05	5.1E+04	4.3E+04	4.1E+04	3.9E+04	4.4E+04
14	720.4817	29.5	6.5E+04	6.7E+04	1.2E+05	1.7E+05	1.1E+05	2.7E+03	5.3E+03	2.9E+03	5.3E+03	4.1E+03
15	723.4289	32.7	6.0E+04	7.0E+04	6.9E+04	6.1E+04	6.5E+04	0.0E+00	0.0E+00	9.7E+03	7.2E+03	4.2E+03
16	734.4967	30.4	2.5E+04	2.5E+04	5.6E+04	8.1E+04	4.7E+04	1.3E+03	2.4E+03	1.9E+03	3.1E+03	2.2E+03
17	760.4695	37.6	6.4E+04	6.5E+04	6.8E+04	6.7E+04	6.6E+04	1.7E+04	3.1E+04	2.6E+04	3.1E+04	2.6E+04
18	774.4860	38.5	5.3E+04	5.1E+04	4.7E+04	4.5E+04	4.9E+04	1.1E+04	1.9E+04	1.8E+04	1.7E+04	1.6E+04
19	905.6164	46.7	7.5E+04	6.7E+04	5.8E+04	5.5E+04	6.4E+04	2.2E+04	2.4E+04	1.8E+04	2.2E+04	2.2E+04
20	1031.5878	33.3	2.2E+05	1.8E+05	1.4E+05	1.8E+05	1.8E+05	8.0E+04	6.8E+04	6.1E+04	6.2E+04	6.8E+04
21	1325.9568	36.5	2.8E+04	2.6E+04	3.2E+04	3.4E+04	3.0E+04	1.4E+03	9.8E+03	9.5E+03	1.1E+04	8.0E+03

(c) Significantly elevated negative-mode ions in 1-butanol-treated samples (aMSII)

	,	RT			Adj	usted inte	grated mas	ss ion inte	ensity (aM	ISII)		
#	m/z	(min)	BuOH-1	BuOH-2	BuOH-3	BuOH-4	BuOH-avg	Con-1	Con-2	Con-3	Con-4	Con-avg
1	474.2599	37.5	7.9E+04	7.8E+04	6.8E+04	7.6E+04	7.5E+04	1.1E+04	1.7E+04	1.6E+04	1.2E+04	1.4E+04
2	488.2762	38.5	4.9E+04	5.0E+04	4.2E+04	4.2E+04	4.6E+04	6.0E+03	1.2E+04	1.2E+04	8.3E+03	9.4E+03
3	572.2569	38.5	5.8E+04	6.4E+04	6.0E+04	5.7E+04	6.0E+04	8.5E+03	1.6E+04	1.6E+04	1.4E+04	1.4E+04
4	648.4608	35.7	4.1E+05	5.7E+05	6.2E+05	5.8E+05	5.4E+05	3.0E+04	9.1E+04	1.0E+05	9.2E+04	7.9E+04
5	662.4753	37.9	1.8E+06	NA	2.1E+06	1.9E+06	1.9E+06	2.5E+05	4.7E+05	3.7E+05	3.4E+05	3.6E+05
6	670.4420	35.7	3.8E+04	6.0E+04	6.4E+04	5.9E+04	5.5E+04	3.1E+03	9.7E+03	1.1E+04	1.0E+04	8.5E+03
7	676.4917	37.6	2.4E+06	2.5E+06	2.3E+06	2.3E+06	2.4E+06	5.2E+05	5.8E+05	5.6E+05	4.8E+05	5.4E+05
8	684.4578	37.9	1.6E+05	NA	1.9E+05	1.5E+05	1.6E+05	2.4E+04	3.6E+04	3.1E+04	2.7E+04	3.0E+04
9	690.5084	38.5	1.6E+06	1.5E+06	1.3E+06	1.3E+06	1.4E+06	3.3E+05	3.1E+05	3.5E+05	2.7E+05	3.2E+05
10	698.4726	37.5	2.4E+05	2.4E+05	2.2E+05	2.4E+05	2.4E+05	5.8E+04	5.7E+04	5.4E+04	4.2E+04	5.3E+04
11	704.5251	39.6	2.0E+05	1.8E+05	1.7E+05	1.8E+05	1.8E+05	4.4E+03	8.4E+03	9.6E+03	7.2E+03	7.4E+03
12	706.4664	28.6	5.4E+04	6.1E+04	9.3E+04	1.3E+05	8.4E+04	2.0E+03	2.9E+03	2.2E+03	2.5E+03	2.4E+03
13	712.4893	38.5	1.8E+05	1.6E+05	1.4E+05	1.4E+05	1.5E+05	4.0E+04	3.5E+04	3.6E+04	2.8E+04	3.5E+04
14	720.4817	29.5	8.8E+04	9.6E+04	1.6E+05	2.3E+05	1.4E+05	2.1E+03	4.4E+03	2.6E+03	3.7E+03	3.2E+03
15	723.4289	32.7	8.2E+04	1.0E+05	9.0E+04	8.3E+04	8.9E+04	0.0E+00	0.0E+00	8.6E+03	5.0E+03	3.4E+03
16	734.4967	30.4	3.4E+04	3.6E+04	7.3E+04	1.1E+05	6.3E+04	1.0E+03	1.9E+03	1.7E+03	2.1E+03	1.7E+03
17	760.4695	37.6	8.8E+04	9.3E+04	9.0E+04	9.1E+04	9.0E+04	1.3E+04	2.5E+04	2.3E+04	2.1E+04	2.1E+04
18	774.4860	38.5	7.2E+04	7.2E+04	6.1E+04	6.1E+04	6.7E+04	8.5E+03	1.6E+04	1.6E+04	1.2E+04	1.3E+04
19	905.6164	46.7	1.0E+05	9.5E+04	7.6E+04	7.5E+04	8.7E+04	1.7E+04	2.0E+04	1.6E+04	1.5E+04	1.7E+04
20	1031.5878	33.3	3.0E+05	2.6E+05	1.9E+05	2.5E+05	2.5E+05	6.2E+04	5.6E+04	5.4E+04	4.3E+04	5.4E+04
21	1325.9568	36.5	3.8E+04	3.8E+04	4.2E+04	4.6E+04	4.1E+04	1.1E+03	8.1E+03	8.4E+03	7.9E+03	6.4E+03

Table 4. Positive-mode ions with significantly decreased levels in 1-butanol-treated *B. subtilis* compared to the untreated control showing the mass-to-charge ratio (m/z), retention time (RT), (a) potential identification, (b) integrated mass ion intensity (MSII), and (c) adjusted mass ion intensity (aMSII). (b) MSII and (c) aMSII data are for the four *B. subtilis* cultures without (Con-1–4) or with 1-butanol treatments (BuOH-1–4) and their respective averages (Con-avg and BuOH-avg, respectively).

(a) Significantly decreased positive-mode ions in 1-butanol-treated samples (potential identification)

	/-	DT (:-)	I	Data wild idea wife a time
#	m/z	RT (min)	ion	Potential identification
1	299.2563	43.6	[M + H] ⁺	Fragment of DAG (17:0/15:0)
2	327.2871	43.6	[M + H] ⁺	Fragment of DAG (17:0/15:0)
3	523.4691	42.7	[M - H2O + H] ⁺	DAG (15:0/15:0) and some DAG (14:0/16:0)
4	541.4820	42.6	[M + H] ⁺	DAG (15:0/15:0) and some DAG (14:0/16:0) and DAG (13:0/17:0)
5	551.5029	43.6	[M - H2O + H] ⁺	DAG (17:0/15:0) and some DAG (16:0/16:0)
6	555.4968	43.2	[M + H] ⁺	DAG (16:0/15:0)
7	558.5066	42.9	$[M + NH_4]^+$	DAG (15:0/15:0) and some DAG (14:0/16:0)
8	569.5127	43.6	[M + H] ⁺	DAG (17:0/15:0) and some DAG (16:0/16:0)
9	572.5192	43.2	$[M + NH_4]^+$	DAG (16:0/15:0) and some DAG (14:0/17:0)
10	586.5382	43.9	$[M + NH_4]^+$	DAG (17:0/15:0) and some DAG (16:0/16:0)
11	600.5474	44.1	$[M + NH_4]^+$	DAG (18:0/15:0) and DAG (16:0/17:0)
12	795.5458	36.3	[M + H] ⁺	lysylPG (13:0/15:0)
13	809.5604	37.1	[M + H] ⁺	lysylPG (14:0/15:0)
14	823.5780	37.7	[M + H] ⁺	lysylPG (15:0/15:0)
15	831.5400	37.1	[M + Na] ⁺	lysylPG (14:0/15:0)
16	837.5934	38.4	[M + H] ⁺	lysylPG (16:0/15:0)
17	845.5584	37.8	[M + Na] ⁺	lysylPG (15:0/15:0)
18	851.6091	39.1	[M + H] ⁺	lysylPG (17:0/15:0)
19	853.5358	37.1	[M + 2Na - H] ⁺	lysylPG (14:0/15:0)
20	853.5865	36.4	?	?
21	861.5338	37.8	[M + K] ⁺	lysylPG (15:0/15:0)
22	867.5506	37.5	[M + 2Na - H] ⁺	lysylPG (15:0/15:0)
23	867.5964	37.0	?	?
24	881.5621	38.4	[M + 2Na - H] ⁺	lysylPG (16:0/15:0)
25	1103.9358	42.9	[2M + Na] ⁺	DAG (15:0/15:0) and some DAG (14:0/16:0)
26	1117.9517	43.2	[M + Na] ⁺	DAG (15:0/15:0) + DAG (16:0/15:0)
27	1145.9819	43.7	[M + Na] ⁺	DAG (16:0/15:0) + DAG (17:0/15:0)
28	1159.9972	43.9	[2M + Na] ⁺	DAG (17:0/15:0)
29	1174.0098	44.3	[M + Na] ⁺	DAG (17:0/15:0) + DAG (16:0/17:0)
30	1419.9666	39.4	?	?

(b) Significantly decreased positive-mode ions in 1-butanol-treated samples (MSII)

		RT Integrated mass ion intensity (MSII)										
#	m/z	(min)	BuOH-1	BuOH-2	BuOH-3	BuOH-4	BuOH-avg	Con-1	Con-2	Con-3	Con-4	Con-avg
1	299.2563	43.6	9.6E+05	NA	9.9E+05	5.6E+05	8.3E+05	1.0E+07	5.2E+06	9.1E+06	8.1E+06	8.2E+06
2	327.2871	43.6	2.4E+05	NA	2.7E+05	1.9E+05	2.3E+05	3.2E+06	2.1E+06	2.6E+06	2.2E+06	2.5E+06
3	523.4691	42.7	2.8E+05	NA	2.6E+05	2.0E+05	2.5E+05	2.3E+06	1.8E+06	2.3E+06	1.8E+06	2.1E+06
4	541.4820	42.6	7.2E+03	NA	6.9E+03	4.8E+03	6.3E+03	9.7E+04	5.8E+04	7.9E+04	6.6E+04	7.5E+04
5	551.5029	43.6	4.0E+05	NA	4.0E+05	3.3E+05	3.8E+05	4.4E+06	3.0E+06	3.7E+06	3.2E+06	3.6E+06
6	555.4968	43.2	1.2E+04	NA	1.2E+04	9.8E+03	1.1E+04	1.8E+05	1.1E+05	1.4E+05	1.2E+05	1.4E+05
7	558.5066	42.9	4.4E+04	4.5E+04	4.2E+04	3.7E+04	4.2E+04	4.4E+05	5.0E+05	3.2E+05	5.8E+05	4.6E+05
8	569.5127	43.6	1.1E+04	NA	1.2E+04	9.5E+03	1.1E+04	1.7E+05	1.0E+05	1.5E+05	1.2E+05	1.4E+05
9	572.5192	43.2	7.0E+04	NA	7.8E+04	5.0E+04	6.6E+04	2.1E+06	1.2E+06	1.7E+06	1.3E+06	1.6E+06
10	586.5382	43.9	7.3E+04	7.5E+04	6.7E+04	6.4E+04	7.0E+04	6.5E+05	8.1E+05	5.5E+05	1.0E+06	7.6E+05
11	600.5474	44.1	8.3E+03	NA	9.2E+03	7.8E+03	8.4E+03	1.0E+05	4.9E+04	7.2E+04	6.4E+04	7.2E+04
12	795.5458	36.3	2.8E+03	4.1E+03	1.9E+03	1.9E+02	2.2E+03	1.3E+05	1.0E+05	6.3E+04	5.7E+04	8.7E+04
13	809.5604	37.1	1.6E+04	2.7E+04	1.8E+04	7.7E+03	1.7E+04	1.2E+06	9.9E+05	6.5E+05	5.9E+05	8.6E+05
14	823.5780	37.7	9.1E+04	1.6E+05	9.5E+04	3.9E+04	9.6E+04	6.6E+06	5.3E+06	3.3E+06	3.1E+06	4.6E+06
15	831.5400	37.1	4.0E+03	3.1E+03	2.1E+03	1.8E+03	2.8E+03	1.2E+05	8.7E+04	5.5E+04	5.6E+04	8.0E+04
16	837.5934	38.4	1.0E+05	1.7E+05	9.1E+04	4.2E+04	1.0E+05	4.6E+06	3.3E+06	2.1E+06	2.2E+06	3.1E+06
17	845.5584	37.8	9.1E+03	1.4E+04	9.4E+03	3.9E+03	9.1E+03	5.8E+05	4.8E+05	2.7E+05	2.9E+05	4.1E+05
18	851.6091	39.1	6.5E+04	1.0E+05	6.2E+04	3.4E+04	6.6E+04	1.9E+06	1.5E+06	1.3E+06	1.4E+06	1.5E+06
19	853.5358	37.1	0.0E+00	0.0E+00	0.0E+00	0.0E+00	0.0E+00	7.7E+04	5.3E+04	3.3E+04	3.3E+04	4.9E+04
20	853.5865	36.4	2.6E+03	3.1E+03	2.0E+03	1.9E+03	2.4E+03	4.9E+04	3.9E+04	2.5E+04	2.4E+04	3.4E+04
21	861.5338	37.8	6.2E+02	4.9E+01	6.6E+02	2.5E+01	3.4E+02	3.8E+04	3.9E+04	2.6E+04	2.8E+04	3.3E+04
22	867.5506	37.5	1.3E+04	NA	1.5E+04	1.2E+04	1.3E+04	1.1E+05	1.4E+05	1.6E+05	1.3E+05	1.3E+05
23	867.5964	37.0	1.5E+04	9.7E+03	9.7E+03	1.2E+04	1.1E+04	9.8E+04	1.4E+05	9.7E+04	3.8E+04	9.3E+04
24	881.5621	38.4	6.7E+03	1.1E+04	5.4E+03	3.9E+03	6.6E+03	7.5E+04	7.0E+04	8.7E+04	9.1E+04	8.1E+04
25	1103.9358	42.9	3.1E+04	3.2E+04	3.2E+04	2.4E+04	3.0E+04	4.0E+05	3.2E+05	2.2E+05	4.3E+05	3.4E+05
26	1117.9517	43.2	3.2E+04	3.5E+04	3.3E+04	2.5E+04	3.1E+04	2.7E+05	2.2E+05	1.5E+05	2.5E+05	2.2E+05
27	1145.9819	43.7	4.0E+04	4.4E+04	3.8E+04	3.4E+04	3.9E+04	3.3E+05	2.8E+05	2.0E+05	3.2E+05	2.8E+05
28	1159.9972	43.9	3.2E+04	2.8E+04	3.0E+04	2.7E+04	2.9E+04	3.5E+05	3.1E+05	2.4E+05	4.4E+05	3.4E+05
29	1174.0098	44.3	5.1E+03	4.6E+03	5.0E+03	4.5E+03	4.8E+03	5.0E+04	4.5E+04	3.2E+04	6.6E+04	4.8E+04
30	1419.9666	39.4	2.4E+03	5.4E+03	3.3E+03	2.0E+03	3.3E+03	5.4E+04	4.3E+04	3.1E+04	2.9E+04	3.9E+04

(c) Significantly decreased positive-mode ions in 1-butanol-treated samples (aMSII)

.,		RT			Adj	usted inte	egrated mas	ss ion inte	ensity (aM	1SII)		
#	m/z	(min)	BuOH-1	BuOH-2	BuOH-3	BuOH-4	BuOH-avg	Con-1	Con-2	Con-3	Con-4	Con-avg
1	299.2563	43.6	1.5E+06	NA	1.8E+06	8.7E+05	1.4E+06	8.1E+06	3.6E+06	8.0E+06	6.2E+06	6.5E+06
2	327.2871	43.6	3.7E+05	NA	4.8E+05	3.0E+05	3.9E+05	2.5E+06	1.5E+06	2.3E+06	1.7E+06	2.0E+06
3	523.4691	42.7	4.4E+05	NA	4.6E+05	3.2E+05	4.1E+05	1.8E+06	1.3E+06	2.0E+06	1.4E+06	1.6E+06
4	541.4820	42.6	1.1E+04	NA	1.2E+04	7.5E+03	1.0E+04	7.6E+04	4.1E+04	6.9E+04	5.1E+04	5.9E+04
5	551.5029	43.6	6.2E+05	NA	7.0E+05	5.2E+05	6.2E+05	3.4E+06	2.1E+06	3.3E+06	2.5E+06	2.8E+06
6	555.4968	43.2	1.8E+04	NA	2.2E+04	1.5E+04	1.9E+04	1.4E+05	7.7E+04	1.2E+05	9.5E+04	1.1E+05
7	558.5066	42.9	6.1E+04	6.4E+04	5.5E+04	5.1E+04	5.8E+04	3.4E+05	4.1E+05	2.9E+05	4.0E+05	3.6E+05
8	569.5127	43.6	1.7E+04	NA	2.1E+04	1.5E+04	1.8E+04	1.4E+05	7.3E+04	1.3E+05	9.4E+04	1.1E+05
9	572.5192	43.2	1.1E+05	NA	1.4E+05	7.8E+04	1.1E+05	1.6E+06	8.4E+05	1.5E+06	1.0E+06	1.2E+06
10	586.5382	43.9	9.9E+04	1.1E+05	8.8E+04	8.7E+04	9.5E+04	5.0E+05	6.7E+05	4.8E+05	7.3E+05	6.0E+05
11	600.5474	44.1	1.3E+04	NA	1.6E+04	1.2E+04	1.4E+04	7.9E+04	3.4E+04	6.3E+04	4.9E+04	5.7E+04
12	795.5458	36.3	3.8E+03	5.9E+03	2.5E+03	2.6E+02	3.1E+03	9.7E+04	8.4E+04	5.6E+04	3.9E+04	6.9E+04
13	809.5604	37.1	2.2E+04	3.9E+04	2.4E+04	1.0E+04	2.4E+04	9.4E+05	8.2E+05	5.8E+05	4.1E+05	6.9E+05
14	823.5780	37.7	1.2E+05	2.3E+05	1.2E+05	5.2E+04	1.3E+05	5.1E+06	4.4E+06	3.0E+06	2.2E+06	3.7E+06
15	831.5400	37.1	5.5E+03	4.4E+03	2.8E+03	2.4E+03	3.8E+03	9.4E+04	7.2E+04	4.9E+04	3.9E+04	6.3E+04
16	837.5934	38.4	1.4E+05	2.5E+05	1.2E+05	5.6E+04	1.4E+05	3.6E+06	2.8E+06	1.9E+06	1.5E+06	2.4E+06
17	845.5584	37.8	1.2E+04	2.0E+04	1.2E+04	5.3E+03	1.2E+04	4.5E+05	4.0E+05	2.3E+05	2.0E+05	3.2E+05
18	851.6091	39.1	8.9E+04	1.5E+05	8.2E+04	4.7E+04	9.1E+04	1.5E+06	1.2E+06	1.1E+06	9.7E+05	1.2E+06
19	853.5358	37.1	0.0E+00	0.0E+00	0.0E+00	0.0E+00	0.0E+00	6.0E+04	4.4E+04	2.9E+04	2.3E+04	3.9E+04
20	853.5865	36.4	3.5E+03	4.4E+03	2.6E+03	2.6E+03	3.3E+03	3.8E+04	3.2E+04	2.2E+04	1.7E+04	2.7E+04
21	861.5338	37.8	8.5E+02	7.0E+01	8.6E+02	3.4E+01	4.5E+02	2.9E+04	3.3E+04	2.3E+04	2.0E+04	2.6E+04
22	867.5506	37.5	2.0E+04	NA	2.7E+04	1.9E+04	2.2E+04	8.7E+04	9.4E+04	1.4E+05	1.0E+05	1.1E+05
23	867.5964	37.0	2.0E+04	1.4E+04	1.3E+04	1.6E+04	1.6E+04	7.6E+04	1.2E+05	8.6E+04	2.7E+04	7.6E+04
24	881.5621	38.4	9.2E+03	1.5E+04	7.1E+03	5.3E+03	9.2E+03	5.8E+04	5.8E+04	7.7E+04	6.4E+04	6.4E+04
25	1103.9358	42.9	4.2E+04	4.6E+04	4.2E+04	3.2E+04	4.1E+04	3.1E+05	2.7E+05	2.0E+05	3.0E+05	2.7E+05
26	1117.9517	43.2	4.3E+04	5.0E+04	4.3E+04	3.4E+04	4.2E+04	2.1E+05	1.8E+05	1.4E+05	1.7E+05	1.7E+05
27	1145.9819	43.7	5.4E+04	6.3E+04	5.0E+04	4.7E+04	5.3E+04	2.5E+05	2.3E+05	1.8E+05	2.2E+05	2.2E+05
28	1159.9972	43.9	4.3E+04	4.0E+04	4.0E+04	3.7E+04	4.0E+04	2.7E+05	2.6E+05	2.1E+05	3.1E+05	2.6E+05
29	1174.0098	44.3	6.9E+03	6.5E+03	6.6E+03	6.2E+03	6.5E+03	3.8E+04	3.7E+04	2.9E+04	4.6E+04	3.8E+04
30	1419.9666	39.4	3.3E+03	7.7E+03	4.4E+03	2.8E+03	4.5E+03	4.1E+04	3.6E+04	2.7E+04	2.0E+04	3.1E+04

Table 5. Negative-mode ions with significantly decreased levels in 1-butanol-treated *B. subtilis* compared to the untreated control showing the mass-to-charge ratio (m/z), retention time (RT), (a) potential identification, (b) integrated mass ion intensity (MSII), and (c) adjusted mass ion intensity (aMSII). (b) MSII and (c) aMSII data are for the four B. subtilis cultures without (Con-1–4) or with 1-butanol treatments (BuOH-1–4) and their respective averages (Con-avg and BuOH-avg, respectively).

(a) Significantly decreased negative-mode ions in 1-butanol-treated samples (potential identification)

#	m/z	RT (min)	lon	Potential identification
1	807.5488	39.5	[M - H] ⁻	lysylPG (14:0/15:0) and some lysylPG (13:0/16:0)
2	821.5670	40.5	[M - H] ⁻	lysylPG (15:0/15:0) and some lysylPG (14:0/16:0)
3	835.5818	41.6	[M - H] ⁻	lysylPG (16:0/15:0) and some lysylPG (14:0/17:0) and lysylPG (13:0/18:0)
4	843.5483	40.5	[M + Na - 2H]	lysylPG (15:0/15:0) and some lysylPG (14:0/16:0)
5	849.5976	42.5	[M - H] ⁻	lysylPG (17:0/15:0)
6	857.5603	41.6	[M + Na - 2H]	lysylPG (16:0/15:0) and some lysylPG (14:0/17:0)
7	871.5775	42.5	[M + Na - 2H] ⁻	lysylPG (17:0/15:0) and some lysylPG (16:0/16:0)

(b) Significantly decreased negative-mode ions in 1-butanol-treated samples (MSII)

ш	/	RT				Integrat	ed mass io	n intensit	y (MSII)			
#	m/z	(min)	BuOH-1	BuOH-2	BuOH-3	BuOH-4	BuOH-avg	Con-1	Con-2	Con-3	Con-4	Con-avg
1	807.5488	39.5	5.7E+03	9.6E+03	6.5E+03	3.1E+03	6.2E+03	1.2E+05	1.4E+05	1.2E+05	1.1E+05	1.3E+05
2	821.5670	40.5	2.8E+04	4.0E+04	2.2E+04	1.5E+04	2.6E+04	5.4E+05	4.4E+05	2.5E+05	2.8E+05	3.8E+05
3	835.5818	41.6	4.3E+04	5.9E+04	2.2E+04	1.6E+04	3.5E+04	3.7E+05	3.0E+05	1.9E+05	1.8E+05	2.6E+05
4	843.5483	40.5	4.3E+03	5.6E+03	4.2E+03	2.5E+03	4.2E+03	4.1E+04	7.0E+04	5.4E+04	4.5E+04	5.2E+04
5	849.5976	42.5	3.4E+04	5.8E+04	4.7E+04	2.4E+04	4.1E+04	2.5E+05	4.4E+05	3.6E+05	2.4E+05	3.2E+05
6	857.5603	41.6	3.3E+03	6.4E+03	2.1E+03	1.3E+03	3.3E+03	4.0E+04	4.7E+04	2.9E+04	3.1E+04	3.7E+04
7	871.5775	42.5	2.2E+03	4.9E+03	3.5E+03	1.7E+03	3.1E+03	3.7E+04	4.1E+04	3.6E+04	3.5E+04	3.7E+04

(c) Significantly decreased negative-mode ions in 1-butanol-treated samples (aMSII)

ш	/	RT	Adjusted integrated mass ion intensity (aMSII)										
#	m/z	(min)	BuOH-1	BuOH-2	BuOH-3	BuOH-4	BuOH-avg	Con-1	Con-2	Con-3	Con-4	Con-avg	
1	807.5488	39.5	7.8E+03	1.4E+04	8.5E+03	4.1E+03	8.5E+03	9.4E+04	1.2E+05	1.1E+05	8.0E+04	1.0E+05	
2	821.5670	40.5	3.8E+04	5.7E+04	2.9E+04	2.0E+04	3.6E+04	4.2E+05	3.6E+05	2.2E+05	2.0E+05	3.0E+05	
3	835.5818	41.6	5.9E+04	8.5E+04	2.9E+04	2.2E+04	4.9E+04	2.9E+05	2.5E+05	1.7E+05	1.3E+05	2.1E+05	
4	843.5483	40.5	5.9E+03	8.1E+03	5.6E+03	3.3E+03	5.7E+03	3.2E+04	5.8E+04	4.8E+04	3.1E+04	4.2E+04	
5	849.5976	42.5	4.7E+04	8.4E+04	6.1E+04	3.3E+04	5.6E+04	1.9E+05	3.7E+05	3.2E+05	1.7E+05	2.6E+05	
6	857.5603	41.6	4.5E+03	9.1E+03	2.7E+03	1.8E+03	4.5E+03	3.1E+04	3.9E+04	2.6E+04	2.2E+04	2.9E+04	
7	871.5775	42.5	3.0E+03	7.0E+03	4.7E+03	2.2E+03	4.2E+03	2.9E+04	3.4E+04	3.2E+04	2.4E+04	3.0E+04	

Characterization of metabolite ions potentially involved in the 1-butanol stress response. To connect the observation to biological significance, the statistically-significant changing metabolite ions need to be characterized for their structures. Upon using the accurate mass of each of the ions with the as-yet unidentified adducts to search on the Metlin¹⁸ database (Tables 2–5), we found so many hits to known metabolites that unfortunately, it was impossible to extract any useful information. Therefore, the data was used for assigning possible molecular formulas to the ions instead.

To obtain more structural clues, we obtained tandem mass spectra of all the involved ions. The resulting MS/MS spectra were interpreted manually one by one to construct the likely structures from all the identifiable fragments (Tables 2–5). As a result, the most probable identification could be assigned to 27 and 18 ions with increasing levels, and 27 and 7 ions with decreasing levels in the 1-butanol-treated samples in the positive and negative ion modes, respectively (Tables 2–5). Together, 86% of the changing ions could be given potential identification. While several ions originated from the same metabolites and differed only by their ion adducts, the number of potentially identifiable ions was higher than previously anticipated for an untargeted metabolomics analysis.

In general, the characterized ions belonged to five classes of metabolites (Figure 3, and Tables 2–6). The classes with elevated levels in the 1-butanol-treated samples were phosphatidylethanolamine (PE), diglucosyldiacylglycerol (DGDAG) and phosphatidylserine (PS), whereas diacylglycerol (DAG) and lysyl phosphatidylglycerol (lysylPG) showed decreased levels. Although the MS/MS method did not allow distinction between the *sn*-1 acyl substituents from those at the *sn*-2 position, they were useful for identification of the acyl chains present in the molecules. Notably, we found that all the differentially changed metabolites contained only *saturated* fatty acyl chains, and that most were comprised of 15:0/15:0, 16:0/15:0 or 17:0/15:0 acyl chains (listed in random order without regarding the *sn*-1 or *sn*-2 positions).

To further confirm the identification of some of the glycerolipids and phospholipids, synthetic standards of PE (16:0/16:0), PS (16:0/16:0) and DAG (16:0/16:0) were examined. As expected if the identification was correct, the MS/MS fragmentation data of the standards (Table 8) exhibited the same patterns as those of the bacterial samples (Tables 2–5). In addition, while co-injection experiments were not performed due to the fact that the commercially-available synthetic standards contained different acyl chains from those that were most abundant in our *B. subtilis* samples, the standards were found to elute off of the columns at a sufficiently close retention time to the corresponding classes of metabolites in the natural samples (Tables 2–8). Together, the data with synthetic standards supported our prior identification of the metabolites.

Table 6. Relative levels of representative membrane lipids, measured by metabolomics analysis of *B. subtilis* 168 cultured with and without 1% (v/v) 1-butanol for 6 h.

Lipid class			RT	ah
acyl chain	lon	m/z	(min)	Fold ^{a,b}
Elevated lipids in 1-butano	l-treated samples ^c			
PE				
15:0/15:0	[M + H] ⁺	664.5	40.6	5.6***
16:0/15:0	[M + H] ⁺	678.5	41.2	9.7***
17:0/15:0	[M + H] ⁺	692.5	41.7	7.2***
DGDAG				
15:0/15:0	[M + Na] ⁺	887.6	39.7	8.0***
16:0/15:0	[M + Na]⁺	901.6	40.7	5.3***
PS				
15:0/15:0	[M - H] ⁻	706.5	28.6	34.6*
16:0/15:0	[M - H] ⁻	720.5	29.5	44.8*
17:0/15:0	[M - H] ⁻	734.5	30.4	37.4*
Decreased lipids in 1-buta	nol-treated sample:	s ^c		
DAG		550.5	40.0	0.0444
15:0/15:0	[M + NH₄] ⁺	558.5	42.9	6.2***
16:0/15:0	[M + NH₄] ⁺	572.5	43.2	11.5**
17:0/15:0	[M + NH₄] ⁺	586.5	43.9	6.3***
LysylPG	FR.4 . 1.17+	000.0	07.7	07.5*
15:0/15:0	[M + H] ⁺	823.6	37.7	27.5*
16:0/15:0	[M + H] ⁺	837.6	38.4	17.3*
17:0/15:0	[M + H] ⁺	851.6	39.1	13.2***
Other Lipids (fold ≤ 2 or p	> 0.05)			
15:0/15:0/15:0/15:0	[M - H]⁻	1295.9	39.0	0.5*
16:0/16:0/15:0/15:0	[M - H] ⁻	1323.9	40.1	1.4
17:0/17:0/15:0/15:0	[M - H] ⁻	1352.0	41.1	2.0*
CDP-DAG				
15:0/15:0	[M - H]⁻	924.5	24.9	1.1
16:0/15:0	[M - H]⁻	938.5	25.6	1.4
17:0/15:0	[M - H]⁻	952.5	26.3	1.0
PA				
15:0/15:0	[M - H]⁻	619.4	26.0	1.1
16:0/15:0	[M - H] ⁻	633.5	26.8	1.9***
17:0/15:0	[M - H] ⁻	647.5	27.6	1.3
PG				
15:0/15:0	[M - H] ⁻	693.5	33.2	0.9
16:0/15:0	[M - H] ⁻	707.5	34.1	1.4*
17:0/15:0	[M - H]⁻	721.5	35.0	1.2
PGP				
15:0/15:0	[M - H] ⁻	773.4	21.7	1.4
16:0/15:0	[M - H]⁻	787.5	22.4	2.3
17:0/15:0	[M - H] ⁻	801.5	23.0	1.5
MGDAG				
16:0/15:0	[M + Na] ⁺	739.5	41.9	1.0
17:0/15:0	[M + Na]⁺	753.5	42.3	1.2

^aFold value represents the ratio of the average aMSII of 1-butanol-treated samples and that of the control, and *vice versa* (underlined).

^bStudent's *t*-test: *, p < 0.05; **, p < 0.01; ***, p < 0.005; N = 3-4.

^clons identified from untargeted metabolomics analysis; only the three most abundant ions in each class of lipids are presented here (see Tables 2-5 for a more complete list).

Table 7. Other lipids in the membrane lipid biosynthetic pathways. Lipids are listed in terms of their lipid class and acyl chain as (a) detected ions, theoretical mass-to-charge ratio (m/z), retention time (RT), (b) integrated mass ion intensity (MSII), and (c) adjusted mass ion intensity (aMSII). (b) MSII and (c) aMSII data are for the four B. subtilis cultures without (Con-1–4) or with 1-butanol treatments (BuOH-1–4) and their respective averages (Con-avg and BuOH-avg, respectively).

(a) Other lipids in membrane lipid biosynthetic pathways (ions, m/z, RT)

#	Lipid class	lons	m/z	PT (min)	
#	acyl chain	IONS	111/2	RT (min)	
	CL				
1	15:0/15:0/15:0/15:0	[M - H] ⁻	1295.9018	39.0	
2	16:0/16:0/15:0/15:0	[M - H] ⁻	1323.9331	40.1	
3	17:0/17:0/15:0/15:0	[M - H] ⁻	1351.9644	41.1	
	CDP-DAG				
4	15:0/15:0	[M - H] ⁻	924.4757	24.9	
5	16:0/15:0	[M - H] ⁻	938.4914	25.6	
6	17:0/15:0	[M - H] ⁻	952.5070	26.3	
	PA				
7	15:0/15:0	[M - H] ⁻	619.4344	26.0	
8	16:0/15:0	[M - H] ⁻	633.4501	26.8	
9	17:0/15:0	[M - H] ⁻	647.4657	27.6	
	PG				
10	15:0/15:0	[M - H] ⁻	693.4712	33.2	
11	16:0/15:0	[M - H] ⁻	707.4869	34.1	
12	17:0/15:0	[M - H] ⁻	721.5025	35.0	
	PGP				

[M - H]⁻

[M - H]

[M - H]

[M + Na]⁺

[M + Na]⁺

773.4375

787.4532

801.4688

739.5331

753.5487

21.7

22.4

23.0

41.9

42.3

13

14

15

16

17

15:0/15:0

16:0/15:0

17:0/15:0

16:0/15:0

17:0/15:0

MGDAG

(b) Other lipids in membrane lipid biosynthetic pathways (MSII)

#	Lipid class	Integrated mass ion intensity (MSII)									
#	acyl chain	BuOH-1 Bu	iOH-2 Bu	OH-3 E	BuOH-4	BuOH-avg	Con-1	Con-2	Con-3	Con-4	Con-avg
	CL										
1	15:0/15:0/15:0/15:0	1.5E+04 2.6	6E+04 2.5	E+04 1	.6E+04	2.1E+04	4.4E+04	6.5E+04	8.3E+04	9.1E+04	7.1E+04
2	16:0/16:0/15:0/15:0	5.8E+04 8.0	E+04 1.1	E+05 1	.2E+05	9.1E+04	6.9E+04	1.2E+05	1.2E+05	1.4E+05	1.1E+05
3	17:0/17:0/15:0/15:0 CDP-DAG	2.7E+04 4.1	IE+04 5.0	E+04 6	.4E+04	4.6E+04	2.0E+04	3.4E+04	4.5E+04	6.0E+04	3.9E+04
4	15:0/15:0	4.2E+03 3.0	E+03 2.9	E+03 4	.8E+03	3.7E+03	7.7E+03	5.7E+03	4.6E+03	4.9E+03	5.7E+03
5	16:0/15:0	8.7E+03 8.3	BE+03 7.7	E+03 1	.1E+04	9.0E+03	1.7E+04	1.1E+04	7.6E+03	1.0E+04	1.1E+04
6	17:0/15:0	6.6E+03 5.2	2E+03 5.7	E+03 7	.3E+03	6.2E+03	1.6E+04	1.1E+04	7.5E+03	9.9E+03	1.1E+04
	PA										
7	15:0/15:0	1.4E+05 1.1	E+05 9.8	E+04 1	.2E+05	1.2E+05	2.7E+05	1.7E+05	1.6E+05	1.5E+05	1.9E+05
8	16:0/15:0	4.3E+05 3.0	E+05 3.2	E+05 3	.6E+05	3.5E+05	4.1E+05	3.0E+05	3.1E+05	2.4E+05	3.2E+05
9	17:0/15:0	2.7E+05 2.0	E+05 1.8	E+05 1	.9E+05	2.1E+05	4.0E+05	2.6E+05	2.3E+05	2.2E+05	2.8E+05
	PG										
10	15:0/15:0	9.0E+06 8.7	E+06 8.0	E+06 7	.2E+06	8.2E+06	1.8E+07	1.7E+07	1.5E+07	1.2E+07	1.5E+07
11	16:0/15:0	1.2E+07 1.1	E+07 9.5	E+06 9	.6E+06	1.0E+07	1.4E+07	1.4E+07	1.2E+07	1.0E+07	1.3E+07
12	17:0/15:0 PGP	6.9E+06 5.5	5E+06 5.2	E+06 5	.8E+06	5.8E+06	7.8E+06	9.3E+06	8.3E+06	7.6E+06	8.3E+06
13	15:0/15:0	1.2E+04 8.7	E+03 6.3	E+03 5	.1E+03	8.0E+03	1.3E+04	1.1E+04	7.4E+03	7.4E+03	9.7E+03
14	16:0/15:0	3.1E+04 2.4	E+04 1.8	E+04 1	.0E+04	2.1E+04	2.3E+04	1.7E+04	1.3E+04	1.1E+04	1.6E+04
15	17:0/15:0 MGDAG	2.2E+04 1.6	6E+04 1.3	E+04 6	.4E+03	1.4E+04	6.8E+03	2.5E+04	1.7E+04	1.4E+04	1.6E+04
16	16:0/15:0	6.1E+04 6.1	E+04 5.6	E+04 5	.5E+04	5.8E+04	1.2E+05	9.6E+04	8.5E+04	1.1E+05	1.0E+05
17	17:0/15:0	6.7E+04 4.9	E+04 4.8	E+04 4	.8E+04	5.3E+04	9.4E+04	8.0E+04	6.1E+04	8.1E+04	7.9E+04

(c) Other lipids in membrane lipid biosynthetic pathways (aMSII)

#	Lipid class	Adjusted integrated mass ion intensity (aMSII)									
#	acyl chain	BuOH-1	BuOH-2	BuOH-3	BuOH-4	BuOH-avg	Con-1	Con-2	Con-3	Con-4	Con-avg
	CL										
1	15:0/15:0/15:0/15:0	2.0E+04	3.8E+04	3.3E+04	2.2E+04	2.8E+04	3.4E+04	5.4E+04	7.3E+04	6.3E+04	5.6E+04
2	16:0/16:0/15:0/15:0	7.9E+04	1.1E+05	1.4E+05	1.7E+05	1.2E+05	5.3E+04	9.6E+04	1.0E+05	1.0E+05	8.8E+04
3	17:0/17:0/15:0/15:0 CDP-DAG	3.7E+04	5.9E+04	6.6E+04	8.7E+04	6.2E+04	1.5E+04	2.8E+04	3.9E+04	4.2E+04	3.1E+04
4	15:0/15:0	5.8E+03	4.2E+03	3.8E+03	6.5E+03	5.1E+03	6.0E+03	4.7E+03	4.0E+03	3.4E+03	4.5E+03
5	16:0/15:0	1.2E+04	1.2E+04	1.0E+04	1.5E+04	1.2E+04	1.3E+04	9.3E+03	6.7E+03	7.0E+03	9.0E+03
6	17:0/15:0	9.1E+03	7.5E+03	7.5E+03	9.8E+03	8.5E+03	1.2E+04	8.8E+03	6.6E+03	6.9E+03	8.6E+03
	PA										
7	15:0/15:0	1.9E+05	1.6E+05	1.3E+05	1.7E+05	1.6E+05	2.1E+05	1.4E+05	1.4E+05	1.1E+05	1.5E+05
8	16:0/15:0	5.8E+05	4.3E+05	4.3E+05	4.9E+05	4.8E+05	3.2E+05	2.5E+05	2.7E+05	1.7E+05	2.5E+05
9	17:0/15:0	3.7E+05	2.9E+05	2.4E+05	2.6E+05	2.9E+05	3.1E+05	2.2E+05	2.0E+05	1.6E+05	2.2E+05
	PG										
10	15:0/15:0	1.2E+07	1.2E+07	1.0E+07	9.8E+06	1.1E+07	1.4E+07	1.4E+07	1.3E+07	8.2E+06	1.2E+07
11	16:0/15:0	1.6E+07	1.5E+07	1.2E+07	1.3E+07	1.4E+07	1.1E+07	1.1E+07	1.1E+07	7.1E+06	1.0E+07
12	17:0/15:0	9.4E+06	7.9E+06	6.8E+06	7.9E+06	8.0E+06	6.0E+06	7.7E+06	7.3E+06	5.3E+06	6.6E+06
	PGP										
13	15:0/15:0	1.6E+04	1.2E+04	8.2E+03	7.0E+03	1.1E+04	1.0E+04	8.8E+03	6.5E+03	5.1E+03	7.7E+03
14	16:0/15:0	4.2E+04	3.4E+04	2.4E+04	1.4E+04	2.8E+04	1.8E+04	1.4E+04	1.1E+04	7.6E+03	1.3E+04
15	17:0/15:0	2.9E+04	2.3E+04	1.7E+04	8.6E+03	1.9E+04	5.2E+03	2.0E+04	1.5E+04	9.6E+03	1.3E+04
	MGDAG										
16	16:0/15:0	8.4E+04	8.8E+04	7.3E+04	7.4E+04	8.0E+04	9.6E+04	7.9E+04	7.5E+04	7.4E+04	8.1E+04
17	17:0/15:0	9.2E+04	7.0E+04	6.4E+04	6.5E+04	7.3E+04	7.2E+04	6.6E+04	5.4E+04	5.6E+04	6.2E+04

Table 8. List of lipid standards and other membrane lipids in the positive and negative ion modes

Lipid	lon	m/z
Lipid standards in the positive ion m	ode	
DAG (16:0/16:0)	[M + H] ⁺	569.5145
DAG (16:0/16:0)	$[M + NH_4]^+$	586.5405
PE (16:0/16:0)	[M + H] ⁺	692.5230
Lipid standards in the negative ion r	node	
PG (14:0/14:0)	[M - H] ⁻	665.4394
PE (16:0/16:0)	[M - H] ⁻	690.5074
PS (16:0/16:0)	[M - H] ⁻	734.4972
CL (18:2/18:2/18:2/18:2)	[M - H] ⁻	1447.9644
Other membrane lipids in the positiv	e ion mode	
MGDAG (17:0/15:0)	[M + Na] ⁺	753.5487
Other membrane lipids in the negati	ve ion mode	
PA (15:0/15:0)	[M - H] ⁻	619.4344
PA (16:0/15:0)	[M - H] ⁻	633.4501
PA (17:0/15:0)	[M - H] ⁻	647.4657
PG (16:0/15:0)	[M - H] ⁻	707.4849
PG (17:0/15:0)	[M - H] ⁻	721.5006
CDP-DAG (16:0/15:0)	[M - H] ⁻	938.4914
CL (16:0/16:0/15:0/15:0)	[M - H] ⁻	1323.9331

Mapping metabolites to biosynthetic pathways. The five classes of glycerolipids and phospholipids that showed significantly altered cellular levels are known constituents of cell membranes. The biosynthetic pathways of these lipids are shown in Figure 4^{19,20}, which begins with phosphatidic acid (PA). In the pathways, PA reacts with cytidine triphosphate (CTP) catalyzed by CDP-diglyceride synthase (CdsA) to produce cytidine diphosphate-DAG (CDP-DAG) as an intermediate. Subsequently, the CDP-DAG intermediate has two possible fates. In the first, it reacts with serine to give PS under the catalysis of phosphatidylserine synthase (PssA), which is then decarboxylated by phosphatidylserine decarboxylase (Psd) to PE. In the second, in the presence of phosphatidylglycerophosphate synthase (PgsA), CDP-DAG reacts with glycerol phosphate to yield phosphatidylglycerol phosphate (PGP) and then phosphatidylglycerol (PG). In turn, PG can also serve as the starting material in the synthesis of either lysylPG, catalyzed by phosphatidylglycerol lysyltransferase (MprF), or cardiolipins (CL) catalyzed by the CL synthase enzymes (ClsA, ClsB and potentially YwiE).

The other pathway utilizes PA as the precursor for the synthesis of lipoteichoic acid (LTA), which is a major component of the cell wall of Gram-positive bacteria²¹. In this pathway, PA is first dephosphorylated by an as-yet unknown enzyme to form DAG, which in turn is then converted to monoglucosyl-diacylglycerol (MGDAG) and DGDAG by the enzyme UgtP. In the final step, the LTA

synthase enzymes (YfnI and YflE) then mediate coupling between DGDAG and PG to produce LTA as well as DAG as a by-product in the process that is then either reused for synthesizing DGDAG or phosphorylated by DgkB to revert to its precursor, PA.

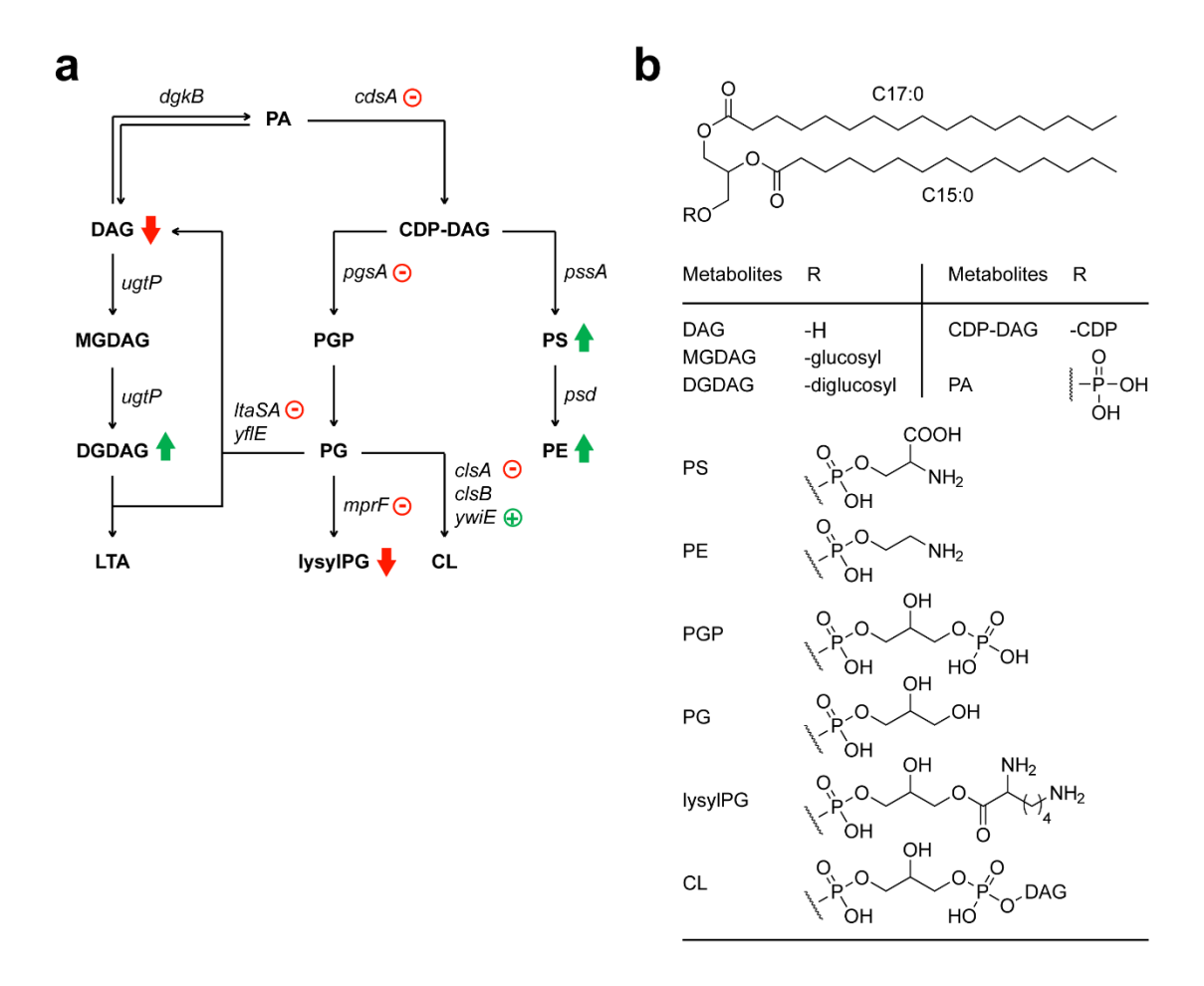


Figure 4. Biosynthesis of membrane lipids in *B. subtilis*. (a) Pathways showing the key intermediates and enzyme-encoding genes for the biosynthesis of membrane lipids, starting from PA. The block arrows indicate lipids in the metabolomics analysis that had significantly elevated (upward arrows) or decreased (downward arrows) levels under 1-butanol stress, whereas the arithmetic symbols represent up- (pluses) or down- (minuses) regulated gene transcript expression levels as determined from the qrtRT-PCR analysis. (b) Chemical structures of all the lipids shown in the pathways in (a). All are derivatives of DAG.

Relative levels of other lipids in membrane lipid biosynthetic pathways. Since many other lipids in the membrane lipid biosynthetic pathways showed no significant changes in their levels in the untargeted metabolomics analysis, we questioned if this was because these lipids were not detected in our platform or because their levels remained truly unaltered under 1-butanol stress. From the untargeted metabolomics analysis above, the data suggested that most glycerolipids and phospholipids in *B. subtilis* were made up of 15:0/15:0, 16:0/15:0, and 17:0/15:0 acyl chains.

Therefore, the levels of other membrane lipids that contained these acyl substituents were evaluated by searching for CL, CDP-DAG, PA, PG, PGP and MGDAG in the LC-MS chromatograms. Based on the accurate mass measurements and retention times, we could identify an ion peak that likely corresponded to each of these metabolites. To be certain of the identification, the matches were further validated using tandem mass spectra, which were obtained for at least one metabolite in each class whenever possible (e.g., when MSII of the metabolite was high enough) (Tables 2–5). In addition, commercially-available standards of CL from bovine heart (mostly 18:2/18:2/18:2/18:2) and PG (14:0/14:0) were also acquired to compare their MS/MS fragmentation patterns and approximate retention times (Table 8). Because we could characterize most peaks in the tandem mass spectra, and because the fragmentation patterns as well as the retention time of the synthetic and natural samples were comparable for CL and PG, this supported the identification of the ion peaks derived from these membrane lipids.

To quantify the membrane lipids, the levels of these ions in the 1-butanol-treated samples were compared to those in control groups, similar to the untargeted analysis above. As expected when the metabolites were not associated with 1-butanol stress response, all lipids under examination either changed statistically insignificantly (p > 0.05) or had two-fold or lower changes (Tables 6–7). The data therefore confirmed that 1-butanol only caused a significant alteration in the levels of PE, DGDAG, PS, DAG and lysylPG, but not *any* of the other lipids in the two biosynthetic pathways.

Expression levels of the key enzyme-encoding genes in membrane lipid biosynthetic pathways, as determined by qrtRT-PCR analysis. How the stress-induced metabolites correlated to the regulation of the genes in the membrane lipid biosynthetic pathways of *B. subtilis* was examined by two-stage qrtRT-PCR analysis on the total mRNA isolated from *B. subtilis* 168 cells grown under the same conditions as those for the untargeted metabolomics experiments. The relative mRNA expression level was determined for the genes in the memebrane lipid biosynthetic pathways (Figure 4: cdsA, pssA, psd, pgsA, mprF, clsA, clsB, ywiE, dgkB, ugtP, yfnI and yflE).

The presence of 1-butanol significantly downregulated five of these 11 target genes, *cdsA* (3.4-fold), *pgsA* (1.9-fold), *mprF* (2.7-fold), *clsA* (2.5-fold) and *yfnI* (1.5-fold), and upregulated one, *ywiE* (22.3-fold), whereas the rest of the genes remained unaltered (Figure 5). Interestingly, while *ywiE* was the only gene in the pathways found to be significantly upregulated, it had by far the highest magnitude (22.3-fold) of change. Together with the metabolomics data (Figure 4), the results demonstrated an agreement between the gene transcript expression level and detected metabolite levels.

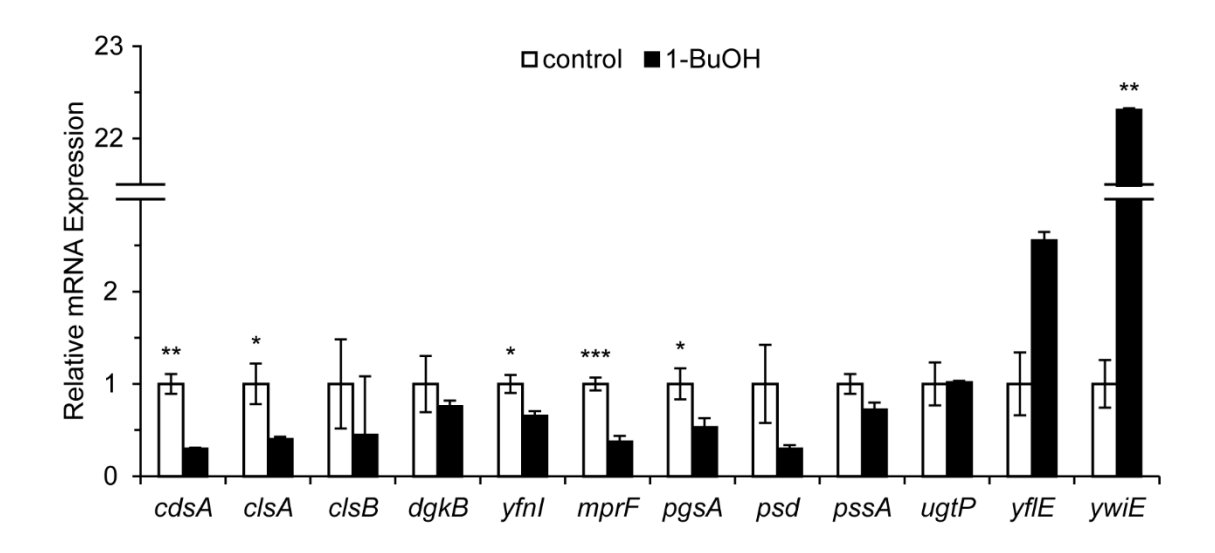


Figure 5. Relative transcript expression level of the genes involved in the biosynthesis of membrane lipids in *B. subtilis* after treatment without (control; white bars) or with 1% (v/v) 1-butanol (1-BuOH; black bars) for 6 h. The mRNA expression level was determined by two-stage qrtRT-PCR using the $2^{-\Delta\Delta_{\rm Ct}}$ method and standardized against the gyrB transcript expression level as an internal control. The graph indicates the fold changes in the indicated mRNA levels in 1-butanol-treated samples relative to that in the control. Data are shown as the average \pm standard errors of the mean, derived from three independent experiments. Student's t-test: *, p < 0.05; **, p < 0.01; ***, p < 0.005.

Cell morphologies of *B. subtilis* 168 under 1-butanol stress. Mutant *B. subtilis* cells with an altered membrane lipid composition have been shown to display aberrant cell morphologies¹⁹, and therefore, whether the differential levels of glycerolipids and phospholipids observed in our studies led to changes in the cell morphology under 1-butanol stress was examined using SEM analysis. The studies clearly demonstrated the lengthening of stationary-phase cells after being exposed to 1.4% (v/v) of 1-butanol for 12 h in LB medium (the same medium as in the previous literature and at the concentration that resulted in a similar growth rate of *B. subtilis* as in SMM medium). The cells showed an almost two-fold increased length (3.91 ± 0.66 μ m vs. 1.98 ± 0.27 μ m) compared to the control cells (Figure 6). Taken together, the findings suggested a potential correlation between the cell morphology, glycerolipid and phospholipid composition, and 1-butanol stress.

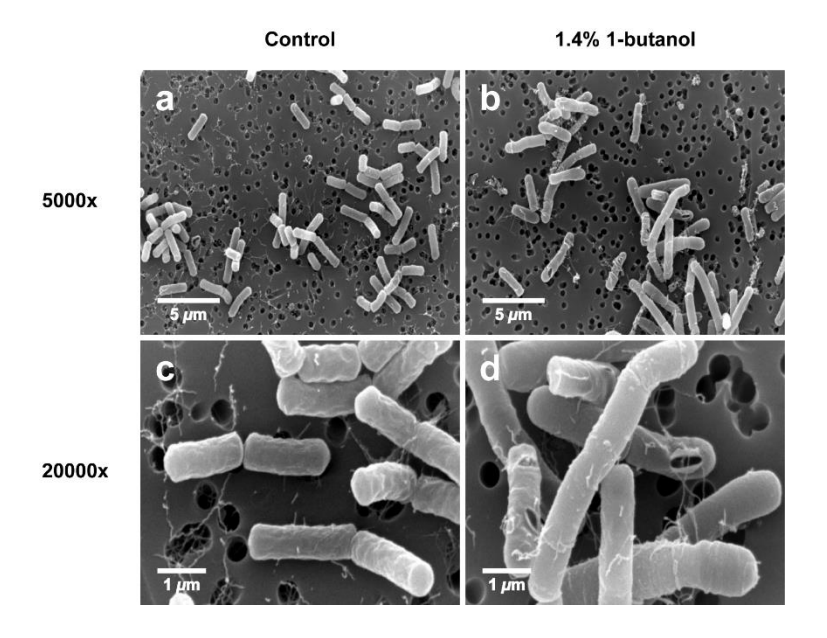


Figure 6. Representative SEM images of *B. subtilis* 168 cells after being cultured (a, c) without or (b, d) with 1.4% (v/v) of 1-butanol in LB medium for 12 h. 1-Butanol was supplemented into the *B. subtilis* 168 cultures during the late lag phase ($OD_{600} \sim 0.2-0.3$). Images shown are at (a, b) $5000 \times$ (scale bar is 5 μ m) and (c, d) $20000 \times$ (scale bar is 1 μ m) magnification.

Discussion and Conclusion

Organic solvent-tolerant bacteria have the potential to be utilized in industrial and environmental biotechnology applications that range from biofuel and chemical production to biocatalysis and bioremediation²². With these premises, various studies have previously been conducted to elucidate the mechanisms of organic solvent tolerance²³. Some of the response mechanisms include the induction of stress proteins²⁴, inhibition of sporulation²⁵, deactivation of organic solvents²⁶, changes in cell morphology^{27,28}, modification of the cell surface and cell membrane²⁹⁻³¹, and solvent excretion through efflux pumps³². The knowledge of these mechanisms helps accelerate the acquisition of bacterial strains with a higher tolerance to organic solvents by allowing the genetic engineering of relevant pathways or by changing the levels of key culture factors that are altered when the organisms adapt to stress³³.

1-Butanol is one of the organic solvents that have been used widely in industry. However, because 1-butanol is highly toxic to microorganisms, the possibilities of applying microbial fermentation to produce or transform 1-butanol to other important chemicals or for bioremediation are still quite limited in scope. In the hope of obtaining bacteria with an enhanced tolerance to 1-butanol in the near future, the present study was aimed at elucidating the metabolic responses of *B. subtilis* in a 1-butanol-stressed environment using an untargeted metabolomics approach.

Accordingly, *B. subtilis* was exposed to 1-butanol during the early growing condition (late lag phase), which was earlier than in most previous reports. During this vulnerable early stage of growth, the bacteria are able to tolerate lower concentrations of 1-butanol than when 1-butanol is

added at a later stage with an already high cell density⁹. However, the late lag to early log phase condition was chosen in this study, because the common practice in fermentation process is to have the toxic substrates present as early as possible, and the toxic products gradually formed.

We used an untargeted metabolomics analysis since, in contrast to targeted analysis that limits its scope to selected metabolites, untargeted analysis can detect and quantitate all ionizing metabolites based on their MSII, allowing measurement of both known and novel metabolites simultaneously³⁴. The untargeted metabolomics analysis identified the zwitterionic PE, neutral PS, and neutral DGDAG to be differentially upregulated in 1-butanol-stressed *B. subtilis*, whereas the positively-charged lysylPG and neutral DAG were downregulated. If the whole-cell measurement of lipids in this work were directly correlated with the amount of these lipids in the *B. subtilis* membrane, it would mean that there is a decrease in the ratio of ionic to neutral lipids under 1-butanol stress. However, this interpretation does not explain our findings, because one would expect ionic lipids to repel with the nonpolar alkyl chain of 1-butanol better than neutral lipids.

Alternatively, the metabolomics data also indicates an increase in the ratio of neutral and anionic to cationic membrane lipids under 1-butanol stress. While no report has previously demonstrated the importance of maintaining this ratio, an increase in the anionic phospholipid contents has been shown previously to allow the adaptation of *B. subtilis* in a high salinity environment³⁵, whereas cationic lipids generally played a role in attenuating the membrane perturbation of cationic compounds³⁶. Since 1-butanol is a neutral compound, both anionic and cationic lipids should not provide any extra protection for *B. subtilis* via charge-charge repulsion with the uncharged solvent. Thus, we speculated that if the altered amount of these charged lipids did not affect growth of the organism, their production might become unnecessary and was reduced in this environment, as observed in the case of the cationic lysylPG. On the other hand, the presence of the major anionic membrane lipid, PG, is essential for overall viability of the organism³⁵, and therefore its levels might be kept unaltered. Yet, it is also possible that the charged membrane lipids themselves might not interact directly with 1-butanol at all but affect the activities of integral membrane proteins, such as transporters, instead³⁷. In any cases, more data points with other neutral organic solvents are needed, before any generalization can be drawn upon.

One of the known mechanisms of bacteria for dealing with organic solvent stress involves changing their membrane fluidity, which in many cases, can be achieved by changing their saturated-to-unsaturated fatty acid composition. For example, ethanol stress was reported to cause an increased level of unsaturated fatty acids in the membrane of *E. coli*³⁸ and *S. cerevisiae*³⁹, and to increase the level of saturated fatty acids in *B. subtilis*⁴⁰ and *C. acetobutylicum*^{41,42}. Interestingly, we did not detect these changes in our metabolomics experiments with either the fatty acids themselves or as acyl chains of glycerolipids or phospholipids. One of the factors that may account for this discrepancy is that the earlier literature only described changes in fatty acid contents in *B. subtilis* under stress induced by methanol or ethanol, but not 1-butanol⁴⁰. Despite all three compounds being short-chain alcohols, they could affect lipid metabolism differently. For example, some fatty acid compositions were only modified by ethanol stress, but remained unchanged with methanol stress⁴⁰.

Alternatively, our results might simply be specific to the choices of the *B. subtilis* strain, growth medium and conditions employed in this study. Further experiments are needed to test their generality.

The LC-MS/MS analyses of differentially altered lipids suggested that the most abundant acyl chains present were 15:0/15:0, 16:0/15:0 and 17:0/15:0. Although the results might look surprising without any *a priori* knowledge of the acyl chains of *B. subtilis*, the data was consistent with a previous report on the fatty acid distribution of the total membrane lipid extracts from *B. subtilis*, which indicated C15:0 as the most frequently found acyl chain⁴³. Additional support for this observation also comes from a study on the lipid composition during various growth stages of *B. subtilis* by matrix-assisted laser desorption/ionization coupled to time-of-flight/time-of-flight (MALDI-TOF/TOF) mass spectrometry⁴⁴. In this work, the authors reported the detection of sodiated PE, PG, lysylPG and DGDAG in *B. subtilis* lipid extracts and applied tandem MS to identify the exact acyl chain combinations for DGDAG as observed here.

The LC–MS platform as used in this study was not without faults, however, since the system could not separate nor distinguish branched-chain lipids from straight-chain lipids. Since *B. subtilis* has previously been described to have C15:0 and C17:0 fatty acyl chains as mostly the iso-and anteiso-derivatives⁴³, it was likely that these branched-chain isomers constituted major components of our detected lipids. Nevertheless, except for the case of DGDAG above, our results demonstrated for the first time that glycerolipids and phospholipids in *B. subtilis* comprised mostly of 15:0/15:0, 16:0/15:0, and 17:0/15:0 acyl chains. Furthermore, the extensive list of MS/MS spectra of these lipids (see supplementary information in the full publication) could serve as informative guides for the identification and characterization of these glycerolipids and phospholipids in the future.

Assuming that the levels of gene transcript expression correlate linearly with the activity of their encoded enzymes, the observed changes in the levels of glycerolipids and phospholipids could be partially explained by the changes in the relative mRNA expression levels. While the levels of the immediate enzymes for synthesis of PS and PE, PssA and Psd, were unaffected by 1-butanol, the level of PgsA, which also utilized CDP-DAG as its substrate, was decreased (Figure 4). Consequently, more CDP-DAG might flux in the direction of PS and PE causing in their increased levels. On the other hand, the decreased levels of lysylPG could simply be due to the fact that the level of *mprF* was reduced.

Without differential expression of ugtP, the changes in the levels of DAG and DGDAG might seem uncorrelated to gene expression levels at first. However, because the YfnI enzyme can use DGDAG and PG as its substrate to release LTA and DAG as products⁴⁵, the downregulation of the yfnI gene should lead to the heightened levels of substrates and lowered levels of products, which is consistent with that observed for DGDAG and DAG, respectively. Interestingly, the main LTA synthase enzyme (YfIE), an ortholog of YfnI^{46,47}, exhibited no significant change in its transcript expression levels. The transcription of yfnI is regulated by the sigma factor σ^{M} , which is involved in various stress tolerance responses, such as high salt and ethanol^{48,49}. Albeit in the opposite direction, our work suggested that YfnI is potentially associated with the 1-butanol stress response

as well. More importantly, while there are enzyme-encoding genes that were not evaluated in this study, especially in the intersecting pathways, the qrtRT-PCR data already demonstrated a strong correlation between gene regulation and metabolite production.

The *B. subtilis* 168 cells were shown to elongate almost two-fold under 1-butanol stress in our studies. There are two membrane lipids-related genes that might be linked to the regulation of cell length, namely the *ugtP* and *yflE* genes. Deletion of the former gene was shown to shorten cells¹⁹. The UgtP enzyme converts DAG into MGDAG and DGDAG in the membrane lipid biosynthetic pathway, and therefore, in the *ugtP* mutant, the levels of DAG and DGDAG should be elevated and decreased, respectively. While no significant changes in the transcript levels of *ugtP* were found in this study, the DAG and DGDAG levels were decreased and increased, respectively, under 1-butanol stress, corroborating the observed cell morphologies.

The deletion of the *yflE* gene was previously shown to increase the cell or cell chain length of *B. subtilis*⁴⁷. Although YflE is the major LTA synthase enzyme in *B. subtilis*, another LTA synthase enzyme, YfnI, and not YflE showed a marked change in transcript expression levels under 1-butanol stress. A single deletion in the *yfnI* gene did not lead to the same morphological effects as the *yflE* mutant, but it is possible that its downregulation might affect the amount or structure of LTA⁴⁵ or the same metabolites in the pathway as the *yflE* mutant, leading to the observed morphologies. Nevertheless, it is also possible that the observed longer cell phenotype under 1-butanol stress might be unrelated to these genes, and further experiments are required to pin down any effects of these genes on 1-butanol tolerance of *B. subtilis*.

In total, applying untargeted metabolomics to study the hydrophobic or lipid-soluble cell components of B. subtilis under 1-butanol stress led to the identification of a moderate number of stress-associated membrane lipids. Using a combination of accurate mass determination, tandem mass spectra and partial comparison with synthetic standards, more than 85% of the ions could be characterized and were found to belong to five classes of glycerolipids and phospholipids in the membrane lipid biosynthetic pathways. These methods also revealed for the first time that the most frequently-found acyl chains of these lipids in B. subtilis were 15:0/15:0, 16:0/15:0 and 17:0/15:0. The downstream targeted grtRT-PCR and SEM analyses further supported this discovery. The former revealed six lipid metabolism genes with significant altered transcript expression levels that were strongly correlated with the observed metabolite changes, whilst the latter showed cell elongation morphologies that were potentially associated with the pathways. Together, this study revealed changes in the composition of glycerolipids and phospholipids in B. subtilis in response to 1-butanol stress. Future work will aim to determine the relevance of these changes in glycerolipids and phospholipids levels on 1-butanol tolerance. More generally, the results highlighted the importance of metabolite identification in metabolomics experiments, as well as the utility of linking metabolites to metabolic pathways in uncovering novel biological insights.

Output (Acknowledging the Thailand Research Fund)

1. International Journal Publication

Published in 1 international journal (Vinayavekhin N*, Mahipant G, Vangnai AS, Sangvanich P (2015). Untargeted metabolomics analysis revealed changes in the composition of glycerolipids and phospholipids in *Bacillus subtilis* under 1-butanol stress. *Appl. Microbiol. Biotechnol.* 99: 5971–5983.)

2. Application

Academic application – This project led to the novel discovery of metabolic responses of *B. subtilis* to 1-butanol. The knowledge can be applied for rationally engineering *B. subtilis* to have higher tolerance to 1-butanol in the future, which would be useful for processes involving 1-butanol, such as in microbial bioremediation, biocatalysis, and metabolic engineering of 1-butanol. This project was also used as a mean to train an undergraduate student to do research in the "Applied Chemistry Project" course.

3. Others (e.g., national journal publication, proceeding, international conference, book chapter, patent)

Oral presentation in international symposia, such as with Academia Sinica, Taiwan; Gifu University, Japan; Nagaoka University of Technology, Japan; and Yamaguchi University, Japan.

References

- Durre, P. Fermentative production of butanol--the academic perspective. *Current opinion in biotechnology* **22**, 331–336, doi:10.1016/j.copbio.2011.04.010 (2011).
- Fortman, J. L. *et al.* Biofuel alternatives to ethanol: pumping the microbial well. *Trends in Biotechnology* **26**, 375–381, doi:http://dx.doi.org/10.1016/j.tibtech.2008.03.008 (2008).
- 3 Connor, M. R. & Liao, J. C. Microbial production of advanced transportation fuels in non-natural hosts. *Current opinion in biotechnology* **20**, 307–315, doi:10.1016/j.copbio.2009.04.002 (2009).
- 4 Green, E. M. Fermentative production of butanol--the industrial perspective. *Current opinion in biotechnology* **22**, 337–343, doi:10.1016/j.copbio.2011.02.004 (2011).
- Ni, Y. & Sun, Z. Recent progress on industrial fermentative production of acetone-butanolethanol by *Clostridium acetobutylicum* in China. *Applied microbiology and biotechnology* **83**, 415–423, doi:10.1007/s00253-009-2003-y (2009).
- 6 Liu, S. & Qureshi, N. How microbes tolerate ethanol and butanol. *New Biotechnology* **26**, 117–121, doi:http://dx.doi.org/10.1016/j.nbt.2009.06.984 (2009).
- 7 Kunst, F. et al. The complete genome sequence of the Gram-positive bacterium *Bacillus* subtilis. Nature **390**, 249–256 (1997).
- Fischer, C. R., Klein-Marcuschamer, D. & Stephanopoulos, G. Selection and optimization of microbial hosts for biofuels production. *Metabolic engineering* **10**, 295–304, doi:10.1016/j.ymben.2008.06.009 (2008).
- 9 Kataoka, N., Tajima, T., Kato, J., Rachadech, W. & Vangnai, A. S. Development of butanol-tolerant *Bacillus subtilis* strain GRSW2-B1 as a potential bioproduction host. *AMB Express* 1, 10, doi:10.1186/2191-0855-1-10 (2011).
- Boch, J., Kempf, B. & Bremer, E. Osmoregulation in *Bacillus subtilis*: synthesis of the osmoprotectant glycine betaine from exogenously provided choline. *Journal of bacteriology* **176**, 5364–5371 (1994).
- Nakano, M. M., Dailly, Y. P., Zuber, P. & Clark, D. P. Characterization of anaerobic fermentative growth of *Bacillus subtilis*: identification of fermentation end products and genes required for growth. *Journal of bacteriology* **179**, 6749–6755 (1997).
- Spizizen, J. Transformation of biochemically deficient strains of *Bacillus subtilis* by deoxyribonucleate. *Proceedings of the National Academy of Sciences of the United States of America* **44**, 1072–1078 (1958).
- Vinayavekhin, N. & Saghatelian, A. Discovery of a protein-metabolite interaction between unsaturated fatty acids and the nuclear receptor Nur77 using a metabolomics approach. *Journal of the American Chemical Society* **133**, 17168–17171, doi:10.1021/ja208199h (2011).
- Vinayavekhin, N. & Saghatelian, A. Regulation of alkyl-dihydrothiazole-carboxylates (ATCs) by iron and the pyochelin gene cluster in *Pseudomonas aeruginosa*. ACS chemical biology 4, 617–623, doi:10.1021/cb900075n (2009).

- Smith, C. A., Want, E. J., O'Maille, G., Abagyan, R. & Siuzdak, G. XCMS: processing mass spectrometry data for metabolite profiling using nonlinear peak alignment, matching, and identification. *Analytical chemistry* **78**, 779–787, doi:10.1021/ac051437y (2006).
- Kongpol, A., Kato, J. & Vangnai, A. S. Isolation and characterization of *Deinococcus geothermalis* T27, a slightly thermophilic and organic solvent-tolerant bacterium able to survive in the presence of high concentrations of ethyl acetate. *FEMS microbiology letters* **286**, 227–235, doi:10.1111/j.1574-6968.2008.01273.x (2008).
- Vinayavekhin, N. & Saghatelian, A. Untargeted metabolomics. *Curr Protoc Mol Biol Chapter* 30, Unit 30 31 31–24, doi:10.1002/0471142727.mb3001s90 (2010).
- Smith, C. A. *et al.* METLIN: a metabolite mass spectral database. *Ther Drug Monit* **27**, 747–751, doi:Export Date 26 August 2013 (2005).
- Salzberg, L. I. & Helmann, J. D. Phenotypic and transcriptomic characterization of *Bacillus* subtilis mutants with grossly altered membrane composition. *Journal of bacteriology* **190**, 7797–7807, doi:10.1128/JB.00720-08 (2008).
- 20 Matsuoka, S. *et al.* The *Bacillus subtilis* essential gene dgkB is dispensable in mutants with defective lipoteichoic acid synthesis. *Genes & genetic systems* **86**, 365–376 (2011).
- 21 Matias, V. R. & Beveridge, T. J. Lipoteichoic acid is a major component of the *Bacillus* subtilis periplasm. *Journal of bacteriology* **190**, 7414–7418, doi:10.1128/JB.00581-08 (2008).
- Nicolaou, S. A., Gaida, S. M. & Papoutsakis, E. T. A comparative view of metabolite and substrate stress and tolerance in microbial bioprocessing: from biofuels and chemicals, to biocatalysis and bioremediation. *Metabolic engineering* **12**, 307–331, doi:10.1016/j.ymben.2010.03.004 (2010).
- Torres, S., Pandey, A. & Castro, G. R. Organic solvent adaptation of Gram positive bacteria: applications and biotechnological potentials. *Biotechnology advances* **29**, 442–452, doi:10.1016/j.biotechadv.2011.04.002 (2011).
- 24 Petersohn, A. et al. Global analysis of the general stress response of *Bacillus subtilis*.

 Journal of bacteriology **183**, 5617–5631, doi:10.1128/JB.183.19.5617-5631.2001 (2001).
- Bohin, J. P., Rigomier, D. & Schaeffer, P. Ethanol sensitivity of sporulation in *Bacillus subtilis*: a new tool for the analysis of the sporulation process. *Journal of bacteriology* **127**, 934–940 (1976).
- Bustard, M. T., Whiting, S., Cowan, D. A. & Wright, P. C. Biodegradation of high-concentration isopropanol by a solvent-tolerant thermophile, *Bacillus pallidus*. *Extremophiles*: life under extreme conditions **6**, 319–323, doi:10.1007/s00792-001-0260-5 (2002).
- Nielsen, L. E., Kadavy, D. R., Rajagopal, S., Drijber, R. & Nickerson, K. W. Survey of extreme solvent tolerance in gram-positive cocci: membrane fatty acid changes in *Staphylococcus haemolyticus* grown in toluene. *Applied and environmental microbiology* **71**, 5171–5176, doi:10.1128/AEM.71.9.5171-5176.2005 (2005).

- Neumann, G. et al. Cells of *Pseudomonas putida* and *Enterobacter* sp. adapt to toxic organic compounds by increasing their size. *Extremophiles : life under extreme conditions* **9**, 163–168, doi:10.1007/s00792-005-0431-x (2005).
- Aono, R. & Kobayashi, H. Cell surface properties of organic solvent-tolerant mutants of Escherichia coli K-12. Applied and environmental microbiology **63**, 3637–3642 (1997).
- 30 Kabelitz, N., Santos, P. M. & Heipieper, H. J. Effect of aliphatic alcohols on growth and degree of saturation of membrane lipids in *Acinetobacter calcoaceticus*. *FEMS microbiology letters* **220**, 223–227 (2003).
- Weber, F. J. & de Bont, J. A. Adaptation mechanisms of microorganisms to the toxic effects of organic solvents on membranes. *Biochimica et biophysica acta* **1286**, 225–245 (1996).
- Matsumoto, M., de Bont, J. A. & Isken, S. Isolation and characterization of the solvent-tolerant *Bacillus cereus* strain R1. *Journal of bioscience and bioengineering* **94**, 45–51 (2002).
- Zingaro, K. A. & Papoutsakis, E. T. Toward a semisynthetic stress response system to engineer microbial solvent tolerance. *mBio* **3**, doi:10.1128/mBio.00308-12 (2012).
- 34 Saghatelian, A. *et al.* Assignment of endogenous substrates to enzymes by global metabolite profiling. *Biochemistry* **43**, 14332–14339, doi:Export Date 26 August 2013 (2004).
- Lopez, C. S., Alice, A. F., Heras, H., Rivas, E. A. & Sanchez-Rivas, C. Role of anionic phospholipids in the adaptation of *Bacillus subtilis* to high salinity. *Microbiology* **152**, 605–616, doi:10.1099/mic.0.28345-0 (2006).
- Kilelee, E., Pokorny, A., Yeaman, M. R. & Bayer, A. S. Lysyl-phosphatidylglycerol attenuates membrane perturbation rather than surface association of the cationic antimicrobial peptide 6W-RP-1 in a model membrane system: implications for daptomycin resistance. *Antimicrobial agents and chemotherapy* **54**, 4476–4479, doi:10.1128/AAC.00191-10 (2010).
- Lee, A. G. How lipids affect the activities of integral membrane proteins. *Biochimica et biophysica acta* **1666**, 62-87, doi:10.1016/j.bbamem.2004.05.012 (2004).
- Ingram, L. O. Adaptation of membrane lipids to alcohols. *Journal of bacteriology* **125**, 670–678 (1976).
- 39 Beaven, M. J., Charpentier, C. & Rose, A. H. Production and tolerance of ethanol in relation to phospholipid fatty-acyl composition in *Saccharomyces cerevisiae* NCYC 431. *Journal of general microbiology* **128**, 1447–1455 (1982).
- 40 Rigomier, D., Bohin, J. P. & Lubochinsky, B. Effects of ethanol and methanol on lipid metabolism in *Bacillus subtilis*. *Journal of general microbiology* **121**, 139–149 (1980).
- Borden, J. R. & Papoutsakis, E. T. Dynamics of genomic-library enrichment and identification of solvent tolerance genes for *Clostridium acetobutylicum*. *Applied and environmental microbiology* **73**, 3061–3068, doi:10.1128/AEM.02296-06 (2007).

- Lepage, C., Fayolle, F., Hermann, M. & Vandecasteele, J. P. Changes in membrane lipid composition of *Clostridium acetobutylicum* during acetone-butanol fermentation: effects of solvents, growth temperature and pH. *Journal of general microbiology* **133**, 103–110 (1987).
- Clejan, S., Krulwich, T. A., Mondrus, K. R. & Seto-Young, D. Membrane lipid composition of obligately and facultatively alkalophilic strains of *Bacillus* spp. *Journal of bacteriology* **168**, 334–340 (1986).
- Gidden, J., Denson, J., Liyanage, R., Ivey, D. M. & Lay, J. O. Lipid compositions in *Escherichia coli* and *Bacillus subtilis* during growth as determined by MALDI-TOF and TOF/TOF mass spectrometry. *International journal of mass spectrometry* **283**, 178–184, doi:10.1016/j.ijms.2009.03.005 (2009).
- Wormann, M. E., Corrigan, R. M., Simpson, P. J., Matthews, S. J. & Grundling, A. Enzymatic activities and functional interdependencies of *Bacillus subtilis* lipoteichoic acid synthesis enzymes. *Mol Microbiol* **79**, 566–583, doi:DOI 10.1111/j.1365-2958.2010.07472.x (2011).
- Grundling, A. & Schneewind, O. Synthesis of glycerol phosphate lipoteichoic acid in Staphylococcus aureus. Proceedings of the National Academy of Sciences of the United States of America **104**, 8478–8483, doi:10.1073/pnas.0701821104 (2007).
- Schirner, K., Marles-Wright, J., Lewis, R. J. & Errington, J. Distinct and essential morphogenic functions for wall- and lipo-teichoic acids in *Bacillus subtilis*. *The EMBO journal* **28**, 830–842, doi:10.1038/emboj.2009.25 (2009).
- Jervis, A. J., Thackray, P. D., Houston, C. W., Horsburgh, M. J. & Moir, A. SigM-responsive genes of *Bacillus subtilis* and their promoters. *Journal of bacteriology* **189**, 4534–4538, doi:Doi 10.1128/Jb.00130-07 (2007).
- Thackray, P. D. & Moir, A. SigM, an extracytoplasmic function sigma factor of *Bacillus subtilis*, is activated in response to cell wall antibiotics, ethanol, heat, acid, and superoxide stress. *Journal of bacteriology* **185**, 3491–3498, doi:Doi 10.1128/Jb.185.12.3491-3498.2003 (2003).

Appendix

GENOMICS, TRANSCRIPTOMICS, PROTEOMICS

Untargeted metabolomics analysis revealed changes in the composition of glycerolipids and phospholipids in Bacillus subtilis under 1-butanol stress

Nawaporn Vinayavekhin¹ · Gumpanat Mahipant^{2,3} · Alisa S. Vangnai^{3,4} · Polkit Sangvanich¹

Received: 3 February 2015 / Revised: 18 April 2015 / Accepted: 15 May 2015 / Published online: 30 May 2015 © Springer-Verlag Berlin Heidelberg 2015

Abstract 1-Butanol has been utilized widely in industry and can be produced or transformed by microbes. However, current knowledge about the mechanisms of 1-butanol tolerance in bacteria remains quite limited. Here, we applied untargeted metabolomics to study Bacillus subtilis cells under 1-butanol stress and identified 55 and 37 ions with significantly increased and decreased levels, respectively. Using accurate mass determination, tandem mass spectra, and synthetic standards, 86 % of these ions were characterized. The levels of phosphatidylethanolamine, diglucosyldiacylglycerol, and phosphatidylserine were found to be upregulated upon 1butanol treatment, whereas those of diacylglycerol and lysyl phosphatidylglycerol were downregulated. Most lipids contained 15:0/15:0, 16:0/15:0, and 17:0/15:0 acyl chains, and all were mapped to membrane lipid biosynthetic pathways. Subsequent two-stage quantitative real-time reverse transcriptase PCR analyses of genes in the two principal membrane lipid biosynthesis pathways revealed elevated levels of

Electronic supplementary material The online version of this article (doi:10.1007/s00253-015-6692-0) contains supplementary material, which is available to authorized users.

- Nawaporn Vinayavekhin nawaporn.v@chula.ac.th
- Department of Chemistry, Faculty of Science, Chulalongkorn University, Bangkok 10330, Thailand
- Biological Sciences Program, Faculty of Science, Chulalongkorn University, Bangkok 10330, Thailand
- Department of Biochemistry, Faculty of Science, Chulalongkom University, Bangkok 10330, Thailand
- Center of Excellence on Hazardous Substance Management (HSM), Chulalongkorn University, Bangkok 10330, Thailand

ywiE transcripts in the presence of 1-butanol and reduced expression levels of cdsA, pgsA, mprF, clsA, and yfnI transcripts. Thus, the gene transcript levels showed agreement with the metabolomics data. Lastly, the cell morphology was investigated by scanning electron microscopy, which indicated that cells became almost twofold longer after 1.4% (v/v) 1-butanol stress for 12 h. Overall, the studies uncovered changes in the composition of glycerolipids and phospholipids in B. subtilis under 1-butanol stress, emphasizing the power of untargeted metabolomics in the discovery of new biological insights.

Keywords Metabolomics · *Bacillus subtilis* · 1-Butanol tolerance · Glycerolipids · Phospholipids · Membrane lipids

Introduction

Due to the decreasing supply of petroleum oil, increasing efforts have been spent on finding sustainably renewable resources for the production of fuels and related industrial chemicals in recent years. One such effort includes employing microorganisms to produce or transform compounds of interest, such as biofuels.

1-Butanol is a short-chain alcohol, which has gained increasing attentions as a potential alternative biofuel (Durre 2011; Fortman et al. 2008), since it has many advantageous properties over ethanol, including its higher energy density and its lower vapor pressure, corrosiveness, and solubility in water (Connor and Liao 2009). 1-Butanol has also been used widely in industries as a solvent, stabilizer, and precursor in the production of paints, polymers, and plastics (Green 2011).

Microbial production of 1-butanol has long been possible industrially using the acetone-butanol-ethanol (ABE) production by suitable ABE microbes (Ni and Sun 2009). The



process turns starch or sugars from molasses into 1-butanol, typically using the natural 1-butanol-producing strain, *Clostridium acetobutylicum*, as a fermentation host (Durre 2011). However, one of the main problems is the low yield of 1-butanol, due to its toxicity even to the producing host. In fact, the bacterial growth is inhibited at only about 2 % (v/v) of 1-butanol (Liu and Qureshi 2009). The same problem with 1-butanol toxicity would need to be resolved as well, if microbes were to be employed for the conversion of 1-butanol to other industrially important compounds or in bioremediation.

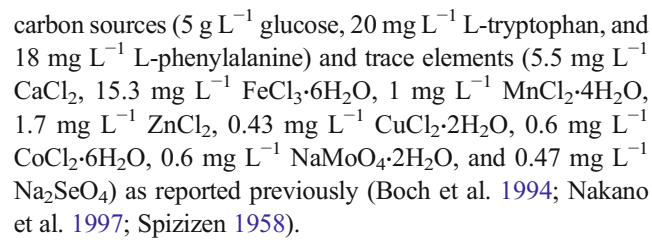
Bacillus subtilis is one of the best-characterized Gram-positive bacteria (Kunst et al. 1997). It is nonpathogenic and has been considered an important industrial strain, especially for the synthesis of enzymes via heterologous expression. In terms of 1-butanol tolerance, it was shown that B. subtilis had the highest tolerance in 1-butanol of the other six commonly used mesophilic, facultatively anaerobic biofuel-producing hosts (Fischer et al. 2008). B. subtilis strain GRSW2-B1 was also one of the microorganisms isolated from seawater samples in Thailand in a screen to find bacteria with a higher tolerance to 1-butanol (Kataoka et al. 2011).

One way to aid obtaining a 1-butanol-tolerant strain of bacteria is by truly understanding how bacteria respond to 1-butanol-induced stress metabolically, since these metabolites might be crucial for the survival and tolerance of the microorganisms in 1-butanol. Consequently, supplementing such metabolites or their precursors into the growth medium or genetically engineering genes in the involved metabolic pathways to manipulate their levels might enhance the 1-butanol tolerance in bacteria.

Therefore, we set out to search for metabolite changes in response to 1-butanol stress in *B. subtilis* strain 168 (a laboratory strain) using an untargeted metabolomics approach to assay lipophilic compounds. The methods for the detection, quantitation, and identification of lipophilic metabolites and the observed changes in the levels of glycerolipids and phospholipids induced by 1-butanol are reported. Subsequently, two-stage quantitative real-time reverse transcriptase PCR (qrtRT-PCR) and scanning electron microscopy (SEM) were performed to attempt to link the observed changes in these metabolites to the expression level of their likely key gene transcripts and the changes in the cell morphology of *B. subtilis*, respectively.

Materials and methods

Bacterial strains and growth conditions *B. subtilis* strain 168 was provided by the Bacillus Genetic Stock Center (BGSC). Unless otherwise stated, bacteria were grown aerobically at 200 rpm, 37 °C in Spizizen's minimal media (SMM; 2 g L⁻¹ (NH₄)₂SO₄, 14 g L⁻¹ K₂HPO₄, 6 g L⁻¹ KH₂PO₄, 1 g L⁻¹ sodium citrate, and 1 mM MgSO₄) supplemented with



Specifically, cultures (5 mL) of *B. subtilis* strain 168 were grown overnight and diluted 50-fold into 20 mL of fresh SMM. The cells were then allowed to grow to late lag phase (optical density at 600 nm (OD_{600}) of \sim 0.2–0.3), before they were treated with the indicated concentrations of 1-butanol (TCI>99.0%) or water as control and then grown further until the predetermined time. For the construction of growth curves, experiments were performed in triplicate and samples were collected every 3 h after treatment with 1-butanol to measure the OD_{600} . For the metabolomics and qrtRT-PCR analyses, cells were harvested 6 h after 1% (ν/ν) 1-butanol was added to the culture.

Metabolites extraction Cell pellets were collected upon centrifugation of cultures (20 mL) at 4500g, 4 °C for 15 min, washed once with 20 mL of SMM without trace elements or carbon sources, and then resuspended in 3 mL of fresh SMM. Extraction was then performed as described previously with slight modifications (Vinayavekhin and Saghatelian 2011). Briefly, the cell suspension was extracted with a 9-mL solution of 2:1 (v/v) ratio of chloroform (CHCl₃)/methanol (MeOH) mixture in a glass vial and centrifuged at 1000g for 5 min to separate the organic layer (bottom) from the aqueous layer (top). Subsequently, the organic layer was carefully transferred to another vial and concentrated to dryness under a steam of nitrogen. Samples were stored at -20 °C and dissolved in 200 μ L CHCl₃ prior to analysis by liquid chromatography (LC)–mass spectrometry (MS).

LC-MS analysis of metabolomes The LC-MS analysis was modified from that reported previously (Vinayavekhin and Saghatelian 2009). Briefly, the analysis was performed using Waters Alliance e2695 LC coupled to Bruker MicrOTOF Q-II MS instruments. For the LC analysis in the positive ion mode, a Luna C5 column (5 μm, 4.6 mm × 50 mm) was used together with a precolumn (Phenomenex). Mobile phase A was composed of 95/5 water/MeOH, and mobile phase B was made up of a 60/35/5 isopropanol/MeOH/water mixture. In addition, 0.1 % (v/v) formic acid and 5 mM ammonium formate were added to both A and B to serve as solvent modifiers. The 60min gradient started at 0 % B for 5 min at 0.1 mL min⁻¹ before abruptly changed to 20 % B and then increased linearly to 100 % B over 40 min at 0.4 mL min⁻¹. The gradient remained at 100 % B for 8 min at 0.5 mL min⁻¹ before ending with equilibration of the column at 0 % B for 7 min at 0.5 mL min^{-1} .



A similar LC analysis was performed in the negative ion mode except that samples were separated on a Gemini C18 column (5 μ m, 4.6 mm \times 50 mm; Phenomenex), and both mobile phases A and B were supplemented with 0.1 % (ν / ν) ammonium hydroxide as solvent modifiers instead. MS analysis was performed with an electrospray ionization source. The parameters were set as follows: end plate offset at -500 V, capillary voltage at 4000 V, nebulizer pressure at 3 bar, dry gas at 8 L min⁻¹, dry temperature at 200 °C, and collision RF at 150 Vpp. Data was collected in the profile mode with a mass range of 100–1500 Da. Mass axis calibration was performed for each individual analysis using 10 mM sodium formate solution. For each run, 40 μ L of metabolite extract was injected into the system for analysis.

LC–MS untargeted data analysis The total ion chromatograms were obtained for the two groups of samples (control vs. those stressed with 1 % (v/v) 1-butanol) in quadruplicate (giving a total of eight chromatograms in each ion mode). The chromatograms were analyzed in two steps. In the first step, automated data analysis by the XCMS program (Smith et al. 2006) was performed to compare the metabolite profiles of the 1-butanol-treated samples with those of the untreated control samples so as to identify, match, and quantify the ions in the LC–MS chromatographs of all samples. Then in the second stage, manual analysis of the XCMS output files was performed to obtain a final list of statistically significant changing ions.

The automated data analysis step was performed as reported previously (Vinayavekhin and Saghatelian 2011). However, because of the differences in instruments employed, the conversion of the Bruker .d files to the mzXML format was achieved using the CompassXport software. The final XCMS output file contained the following information for each ion: average mass-to-charge ratio (m/z), average retention time, and integrated mass ion intensity (peak area; MSII) for each of the LC–MS chromatograms.

In the next step, manual analysis began with normalization of each ion by dividing the MSII of the ion by the OD_{600} of the culture from which it was derived to give a normalized MSII (nMSII) to control for any large differences in the cell number (as OD_{600} values) of the different samples (observed variance was 1.7- to 2.0-fold differences). To make each nMSII value closer to that of MSII, the nMSII was multiplied by the average OD_{600} of all eight samples in each mode to obtain the adjusted MSII (aMSII). The resulting values were then averaged within each group and subsequently employed to calculate the fold changes (i.e., aMSII of control/aMSII of 1-butanol-treated samples or vice versa) for each ion.

To identify metabolites that were elevated or decreased upon addition of 1-butanol to *B. subtilis* cultures and not artifacts of differing cell numbers between cultures, certain criteria were set to filter out nonchanging or unreal

metabolites from the ion list. Specifically, these filters consisted of (i) a minimum fold changes of \geq 4, (ii) statistical significance (t test with p < 0.05), and (iii) a minimum MSII of 30,000 in the elevated samples (which was approximately five times the limit of detection of the instruments). Subsequently, the remaining ions on the list were visually inspected for the peaks in the extracted ion chromatogram to eliminate isotopic ions or any false positives. Lastly, another set of experiments were repeated in triplicate for control and quadruplicate for 1-butanol-treated samples to confirm changes in the levels, as well as the presence of these ions in the final list.

Tandem MS experiments The MS/MS analyses were performed on every changing ion on the final list in previous part using a Waters Alliance e2695 instrument coupled to Bruker MicrOTOF Q-II instrument. The tandem MS analyses were performed in auto MS/MS mode with instructions to include ions of interest in the precursor ion list using a target isolation width of 0.5. The number of precursor ions was set to 3 ions, and active exclusion was activated to exclude the ions after obtaining 3 MS/MS spectra and release the exclusion after 0.30 to 1.00 min. Collision energies were set at 35 V for m/z500.00, 50 V for m/z 1000.00, and 70 V for m/z 2000.00. When an isolation mass was not exactly these values, the collision energies were then interpolated automatically from those of the two closest m/z values. Data were collected in the profile modes using a mass range of either 50-1500 or 100-1500 Da. Metabolites from the extract (40 µL) or chemical standards (500 pmol) were separated using the same LC conditions as in the "LC-MS analysis of metabolomes" section before coupling to the tandem MS analyses.

Total RNA isolation and two-stage qrtRT-PCR analysis Cell pellets were collected by centrifugation of the cultures (5 mL for control and 10 mL for 1-butanol-stressed samples) at 4500g, 4 °C for 15 min, and then washed once with SMM medium without trace elements or carbon sources using the same volumes as the cultures they were harvested from. Total RNA was isolated immediately from the washed cell pellets using the GF-1 Total RNA Extraction kit (Vivantis). In the first-stage qrtRT-PCR, 4 µg of the total RNA was converted to cDNA using the RevertAid First Strand cDNA Synthesis kit (Thermo Scientific), according to manufacturers' instructions. Subsequently, for each sample, the respective cDNA solution was diluted 10- or 50-fold and then used as the template in the second-stage qrtRT-PCR analysis using the SsoAdvancedTM SYBR® Green Supermix (Biorad). The primer sequences (Integrated DNA Technologies) for the amplification of the target genes are listed in Table 1, along with those of gyrase B (gyrB) that served as an internal control. Finally, data analysis was conducted by using the $2^{-\Delta\Delta Ct}$ method to calculate the relative amount of target mRNA in the 1-butanol-treated samples vs. the control.



 Table 1
 Oligonucleotides used for amplification of target genes in the second-stage qrtRT-PCR

Gene	Primer sequence (5' to 3')	Amplicon size (bp)
cdsA	TGG TTT CAC TGC CGG GTT TG GGA AAT CCC GTC CGC TTC AA	92
pssA	CAA AGC AAG CTC CCG ACG TT GCA AGT GCC GAT TGC CAG AA	108
psd	GGC AGC CGA AAT GTC CTG AT TCC TCG CCG ATC TCC AAT TCA	95
ugtP	GGC TAT GTG GAG CGC ATT GA TGG CTG TGG CTT CTG TCA AA	91
yfnI	TGA TGC CGA GCT GAC AAT GG AGG AAG CGA CTG GTA GGT GTT	94
yflE	CGC TGG CTG TTG GAC TTG AT AAC CTG GCA GTT GCG GAA TC	137
dgkB	ACG ACG TGC CAA GCA AAC TG ACG AAG TGA AGG CAG CAT TTC C	83
pgsA	AGA CTG GGT GGA CGG GTA TT CCA AGC TGG AGC GAG ATC AA	139
mprF	CAA TGA AGC GGC TCG AAA CGA ACC GCA CGC TGA ACA ACA AG	82
clsA	AGC CCG ATC ACG CCT TTG TA CTG TGC CGA CTG AAG CGA TTT	147
clsB	CCA ACA TTG CCC AAG CGA AGA CCA GCG GAT GGT CTG ATT TCA TC	147
ywiE	AAA TAG GGC GTG GCG ATC CA CCG TGG AAG GAG GAG GCA TTT A	127
gyrB (control)	AAG CTG GGC AAC TCA GAA GCA CGG AGC CAT TCT TGC TCT TGC CGC C	138

The Δ Ct values were subjected to Student's t test, and only those with p < 0.05 were considered significant.

Cell morphology Cultures (20 mL) of *B. subtilis* strain 168 were prepared as detailed (Bacterial strains and growth conditions section), except that Luria-Bertani (LB) medium was used instead of SMM. Cells were allowed to grow in the absence (control) or presence of 1.4 % (ν/ν) 1-butanol for 12 h and then were harvested for cell morphology analysis by SEM as reported (Kongpol et al. 2008). In brief, to perform the SEM analysis, cells were collected by filtration through a 0.4-µm membrane and fixed with 2.5 % glutaraldehyde in 0.1 M phosphate buffer (pH 7.2) for 2 h. The solution was then removed, and the cells were washed twice with 0.1 M phosphate buffer (pH 7.2) and once with distilled water (5 min each). Next, specimens were prepared by dehydrating the cells in a graded ethanol series, followed by drying in a critical point dryer (Balzers, model no. CPD020) and gold-mounting and coating using a sputter coater (Balzers, model no. SCD040). Finally, a scanning electron microscope (JEOL, model no. JSM-5410LV) was used to examine the specimens for any changes in their anhydrous morphology induced by the 1-butanol stress.



Growth of *B. subtilis* **168 in SMM with varying amount of 1-butanol** To determine the appropriate culture conditions for the untargeted metabolomics analysis, we first monitored the growth of *B. subtilis* 168 in SMM with various concentrations of 1-butanol. The defined medium does not contain any unknown metabolites that might interfere with the subsequent LC–MS analyses, so it was appropriate for use as our culture conditions. Moreover, the addition of 1-butanol at an improper time can induce spore formation (data not shown). Thus, an overnight culture of *B. subtilis* in SMM was used to inoculate larger cultures (20 mL), which were allowed to grow to late lag phase (OD₆₀₀ ~ 0.25), prior to the addition of 1-butanol at concentrations up to 1.4 % (ν/ν). The subsequent cell growth was then monitored by measuring the OD₆₀₀ over 12 h.

The *B. subtilis* strain 168 was able to grow in 1-butanol at all tested concentrations (0.6-1.4% (v/v)), albeit at lower growth rates than the 1-butanol-free control (Fig. 1). As expected when cells were induced to stress by 1-butanol, the OD_{600} values at every measured time point were lower with increasing 1-butanol concentrations and lowest at 1.4% (v/v) 1-butanol. However, the fact that the final OD_{600} of the cultures with 0.6 and 0.8 % (v/v) of 1-butanol at 12 h did not differ noticeably from that of the control indicated that the level of stress subjected upon *B. subtilis* at these concentrations might be insignificant or insufficient over this 12-h time course.

From the results, because the lowest concentration of 1-butanol that moderately and continuously disrupted the growth of *B. subtilis* was 1 % (v/v), this condition was selected for the metabolomics analysis. Since *B. subtilis* entered early stationary phase at 6 h in the presence of 1 % (v/v) 1-butanol, this time point was selected, because by this time the cells would likely have already accumulated several stress-induced metabolites in respond to 1-butanol. At a 6-h time point, the OD₆₀₀ values of the 1-butanol-free control samples were approximately 1.7- to 2.0-fold higher than the samples cultured with 1 % (v/v) 1-butanol.

Untargeted metabolomics of *B. subtilis* **168 under 1-butanol stress** Untargeted metabolomics was performed on *B. subtilis* 168 cells cultured in the presence of 1 % (v/v) 1-butanol for 6 h, along with those cultured without 1-butanol as the control. Hydrophobic metabolites, such as fatty acids, were then extracted from the cells using 2:1 (v/v) ratio CHCl₃/MeOH, and the extracts were then concentrated and subjected to LC–MS analysis using an untargeted metabolomics platform (Vinayavekhin and Saghatelian 2010).

To identify differentially changed metabolites associated with the 1-butanol stress response, the XCMS program (Smith et al. 2006) was used to compare the metabolite profiles of the 1-butanol-treated samples with those of the



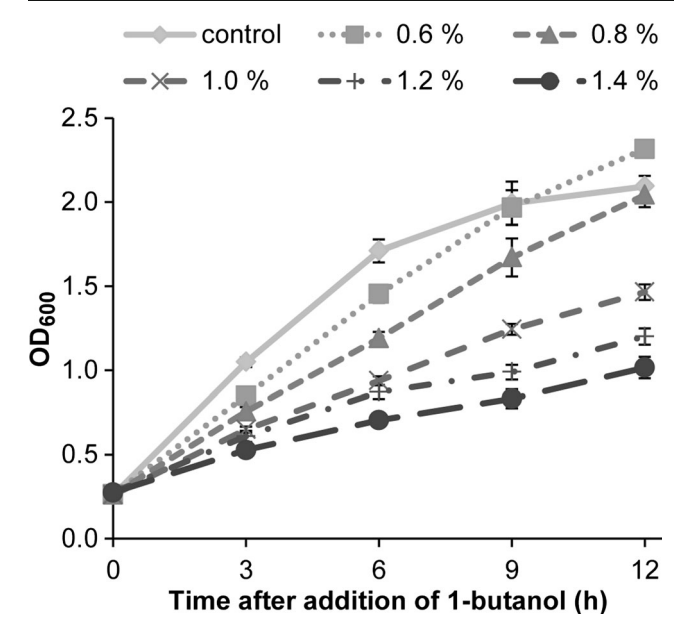


Fig. 1 Growth curves of *B. subtilis* strain 168 in SMM with different concentrations of 1-butanol. Cultures were grown to late lag phase $(OD_{600} \sim 0.2-0.3)$, before 1-butanol was added (all (v/v)) at 0 % (control; *diamonds*), 0.6 % (*squares*), 0.8 % (*triangles*), 1.0 % (*crosses*), 1.2 % (*pluses*), and 1.4 % (*circles*). Data are shown as the average $OD_{600} \pm$ standard errors of the mean, derived from three experimental replicates per concentration

untreated controls. The obtained MSII values were normalized to the ${\rm OD_{600}}$ value of each sample (aMSII) to account for differences in the cell numbers. To be certain that the differences were not merely artifacts of differing cell numbers, metabolite ions were labeled as likely to be involved in the 1-butanol stress response only if they were elevated or decreased by fourfold or more with statistical significance (p < 0.05) compared to in the control cells (Fig. 2). The differential levels of the ions could clearly be observed in the extracted ion chromatograms (Fig. 3). At the end, the unbiased comparative analyses identified 34 and 21 ions with increasing levels and 30 and 7 ions with decreasing levels in the 1-butanol-treated samples in the positive and negative ion modes, respectively (Figs. 2 and 3 and Supplementary Information (SI) Tables S1–S4).

Characterization of metabolite ions potentially involved in the 1-butanol stress response To connect the observation to biological significance, the statistically significant changing metabolite ions need to be characterized for their structures. Upon using the accurate mass of each of the ions with the asyet unidentified adducts to search on the METLIN (Smith et al. 2005) database (SI, Tables S1–S4), we found so many hits to known metabolites that unfortunately it was impossible to extract any useful information. Therefore, the data was used for assigning possible molecular formulas to the ions instead.

To obtain more structural clues, we obtained tandem mass spectra of all the involved ions. The resulting MS/MS spectra were interpreted manually one by one to construct the likely

structures from all the identifiable fragments (SI, Tables S1–S4 and Fig. S1). As a result, the most probable identification could be assigned to 27 and 18 ions with increasing levels and 27 and 7 ions with decreasing levels in the 1-butanol-treated samples in the positive and negative ion modes, respectively (SI, Tables S1–S4). Together, 86 % of the changing ions could be given potential identification. While several ions originated from the same metabolites and differed only by their ion adducts, the number of potentially identifiable ions was higher than previously anticipated for an untargeted metabolomics analysis.

In general, the characterized ions belonged to five classes of metabolites (Table 2, Fig. 3, and SI Tables S1–S4). The classes with elevated levels in the 1-butanol-treated samples were phosphatidylethanolamine (PE), diglucosyldiacylglycerol (DGDAG), and phosphatidylserine (PS), whereas diacylglycerol (DAG) and lysyl phosphatidylglycerol (lysylPG) showed decreased levels. Although the MS/MS method did not allow distinction between the *sn*-1 acyl substituents from those at the *sn*-2 position, they were useful for identification of the acyl chains present in the molecules. Notably, we found that all the differentially changed metabolites contained only *saturated* fatty acyl chains and that most comprised 15:0/15:0, 16:0/15:0, or 17:0/15:0 acyl chains (listed in random order without regarding the *sn*-1 or *sn*-2 positions).

To further confirm the identification of some of the glycerolipids and phospholipids, synthetic standards of PE (16:0/16:0), PS (16:0/16:0), and DAG (16:0/16:0) were examined. As expected, if the identification was correct, the MS/MS fragmentation data of the standards (SI, Table S6 and Fig. S1) exhibited the same patterns as those of the bacterial samples (SI, Tables S1–S4 and Fig. S1). In addition, while coinjection experiments were not performed due to the fact that the commercially available synthetic standards contained different acyl chains from those that were most abundant in our *B. subtilis* samples, the standards were found to elute off of the columns at a sufficiently close retention time to the corresponding classes of metabolites in the natural samples (SI, Tables S1–S6). Together, the data with synthetic standards supported our prior identification of the metabolites.

Mapping metabolites to biosynthetic pathways The five classes of glycerolipids and phospholipids that showed significantly altered cellular levels are known constituents of cell membranes. The biosynthetic pathways of these lipids are shown in Fig. 4 (Matsuoka et al. 2011; Salzberg and Helmann 2008), which begins with phosphatidic acid (PA). In the pathways, PA reacts with cytidine triphosphate (CTP) catalyzed by CDP-diglyceride synthase (CdsA) to produce cytidine diphosphate-DAG (CDP-DAG) as an intermediate. Subsequently, the CDP-DAG intermediate has two possible fates. In the first, it reacts with serine to give PS under the catalysis of phosphatidylserine synthase (PssA), which is then



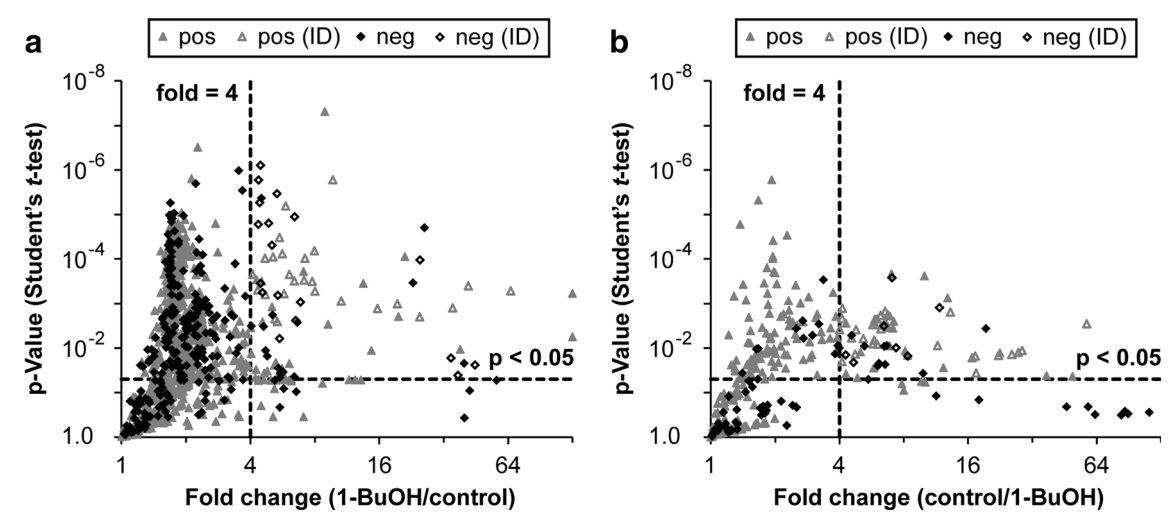


Fig. 2 Results from the untargeted metabolomics analyses of hydrophobic cell components from *B. subtilis* 168 cells cultured in the absence (control) or presence of 1 % (ν / ν) 1-butanol (1-BuOH) for 6 h. Each metabolite ion with an average MSII above 30,000 counts in the **a** 1-BuOH or **b** control group is plotted as its statistical significance against

the fold change of **a** 1-BuOH over the **b** control or vice versa. Positiveand negative-mode MS ions are indicated by *gray filled triangles* and *black filled diamonds*, respectively, with the *open symbols* representing statistically significant changing ions that could be characterized in this study

Fig. 3 Representative differential detected ions between 1-butanolstressed and unstressed B. subtilis cells and their characterization as glycerolipids and phospholipids. a Extracted ion chromatograms of representative ions that showed highly elevated levels with m/zvalues of 692.5207, 887.5686, and 734.4967 or highly decreased levels with m/z values of 586.5382 and 851.6091 in the 1butanol-treated samples (1-BuOH; dashed line) compared to the untreated control (solid line). Based on a accurate mass and b MS/MS spectra, they were characterized as PE (17:0/15:0), DGDAG (15:0/15:0), PS (17:0/ 15:0), DAG (17:0/15:0), and lysylPG (17:0/15:0), respectively, which are all membrane lipids. Precursor ions are denoted as diamonds in the MS/MS spectra. For a complete list of the changing ions, as well as identification of ions in the MS/ MS spectra, see SI Tables S1-S4

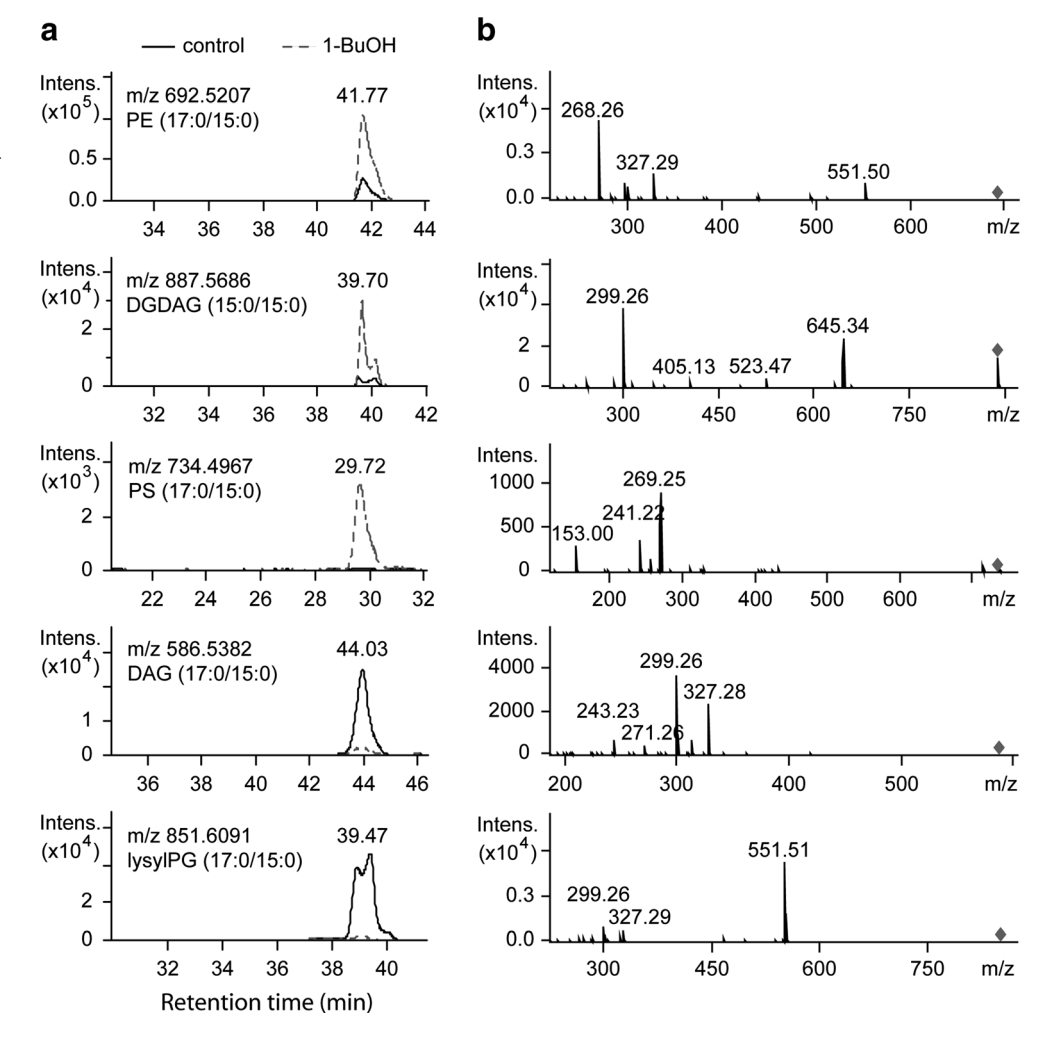




Table 2 Relative levels of representative membrane lipids, measured by metabolomics analysis of *B. subtilis* 168 cultured with and without $1\% (\nu/\nu)$ 1-butanol for 6 h

Lipid class and acyl chain	Ion	m/z	RT (min)	Fold ^{a,b}
Elevated lipids in 1-butanol-tre	ated samples ^c			
PE				
15:0/15:0	$[M + H]^+$	664.5	40.6	5.6***
16:0/15:0	$[M + H]^+$	678.5	41.2	9.7***
17:0/15:0	$[M + H]^+$	692.5	41.7	7.2***
DGDAG				
15:0/15:0	$[M + Na]^+$	887.6	39.7	8.0***
16:0/15:0	$[M + Na]^+$	901.6	40.7	5.3***
PS				
15:0/15:0	$[M-H]^-$	706.5	28.6	34.6*
16:0/15:0	$[M-H]^-$	720.5	29.5	44.8*
17:0/15:0	$[M-H]^-$	734.5	30.4	37.4*
Decreased lipids in 1-butanol-tr	reated samples ^c			
DAG				
15:0/15:0	$[M + NH_4]^+$	558.5	42.9	6.2***
16:0/15:0	$[M + NH_4]^+$	572.5	43.2	11.5**
17:0/15:0	$[M + NH_4]^+$	586.5	43.9	6.3***
LysylPG				
15:0/15:0	$[M + H]^+$	823.6	37.7	27.5*
16:0/15:0	$[M + H]^+$	837.6	38.4	17.3*
17:0/15:0	$[M + H]^+$	851.6	39.1	13.2***
Other Lipids (fold ≤ 2 or $p > 0$.	05)			
CL				
15:0/15:0/15:0/15:0	$[M - H]^-$	1295.9	39.0	0.5*
16:0/16:0/15:0/15:0	$[M - H]^-$	1323.9	40.1	1.4
17:0/17:0/15:0/15:0	$[M - H]^-$	1352.0	41.1	2.0*
CDP-DAG				
15:0/15:0	$[M - H]^-$	924.5	24.9	1.1
16:0/15:0	$[M - H]^-$	938.5	25.6	1.4
17:0/15:0	$[M - H]^-$	952.5	26.3	1.0
PA				
15:0/15:0	$[M - H]^-$	619.4	26.0	1.1
16:0/15:0	$[M - H]^-$	633.5	26.8	1.9***
17:0/15:0	$[M - H]^-$	647.5	27.6	1.3
PG				
15:0/15:0	$[M - H]^-$	693.5	33.2	0.9
16:0/15:0	$[M - H]^-$	707.5	34.1	1.4*
17:0/15:0	$[M - H]^-$	721.5	35.0	1.2
PGP				
15:0/15:0	$[M - H]^-$	773.4	21.7	1.4
16:0/15:0	$[M - H]^-$	787.5	22.4	2.3
17:0/15:0	$[M - H]^{-}$	801.5	23.0	1.5
MGDAG				
16:0/15:0	$[M + Na]^+$	739.5	41.9	1.0
17:0/15:0	$[M + Na]^+$	753.5	42.3	1.2

^a Fold value represents the ratio of the average aMSII of 1-butanol-treated samples and that of the control and vice versa (in italics)

decarboxylated by phosphatidylserine decarboxylase (Psd) to PE. In the second, in the presence of phosphatidylglycerophosphate synthase (PgsA), CDP-DAG reacts with glycerol phosphate to yield phosphatidylglycerol phosphate (PGP) and then phosphatidylglycerol (PG). In turn, PG can also serve as the starting material in the synthesis of either lysylPG, catalyzed by phosphatidylglycerol lysyltransferase (MprF), or cardiolipins (CL) catalyzed by the CL synthase enzymes (ClsA, ClsB, and potentially YwiE).

The other pathway utilizes PA as the precursor for the synthesis of lipoteichoic acid (LTA), which is a major component of the cell wall of Gram-positive bacteria (Matias and Beveridge 2008). In this pathway, PA is first dephosphorylated by an as-yet unknown enzyme to form DAG, which in turn is then converted to monoglucosyldiacylglycerol (MGDAG) and DGDAG by the enzyme UgtP. In the final step, the LTA synthase enzymes (YfnI and YflE) then mediate coupling between DGDAG and PG to produce LTA as well as DAG as a by-product in the process that is then either reused for synthesizing DGDAG or phosphorylated by DgkB to revert to its precursor, PA.

Relative levels of other lipids in membrane lipid biosynthetic pathways Since many other lipids in the membrane lipid biosynthetic pathways showed no significant changes in their levels in the untargeted metabolomics analysis, we questioned if this was because these lipids were not detected in our platform or because their levels remained truly unaltered under 1-butanol stress. From the untargeted metabolomics analysis above, the data suggested that most glycerolipids and phospholipids in B. subtilis were made up of 15:0/15:0, 16:0/15:0, and 17:0/15:0 acyl chains. Therefore, the levels of other membrane lipids that contained these acyl substituents were evaluated by searching for CL, CDP-DAG, PA, PG, PGP, and MGDAG in the LC–MS chromatograms. Based on the accurate mass measurements and retention times, we could identify an ion peak that likely corresponded to each of these metabolites. To be certain of the identification, the matches were further validated using tandem mass spectra, which were obtained for at least one metabolite in each class whenever possible (e.g., when MSII of the metabolite was high enough) (SI, Tables S1–S4 and Fig. S1). In addition, commercially available standards of CL from bovine heart (mostly 18:2/18:2/18:2/18:2) and PG (14:0/14:0) were also acquired to compare their MS/MS fragmentation patterns and approximate retention times (SI, Table S6 and Fig. S1). Because we could characterize most peaks in the tandem mass spectra, and because the fragmentation patterns as well as the retention time of the synthetic and natural samples were comparable for CL and PG, this supported the identification of the ion peaks derived from these membrane lipids.

To quantify the membrane lipids, the levels of these ions in the 1-butanol-treated samples were compared to those in



^b Student's t test: *p < 0.05; **p < 0.01; ***p < 0.005; N = 3–4

^c Ions identified from untargeted metabolomics analysis; only the three most abundant ions in each class of lipids are presented here (see SI Tables S1–S4 for a more complete list)

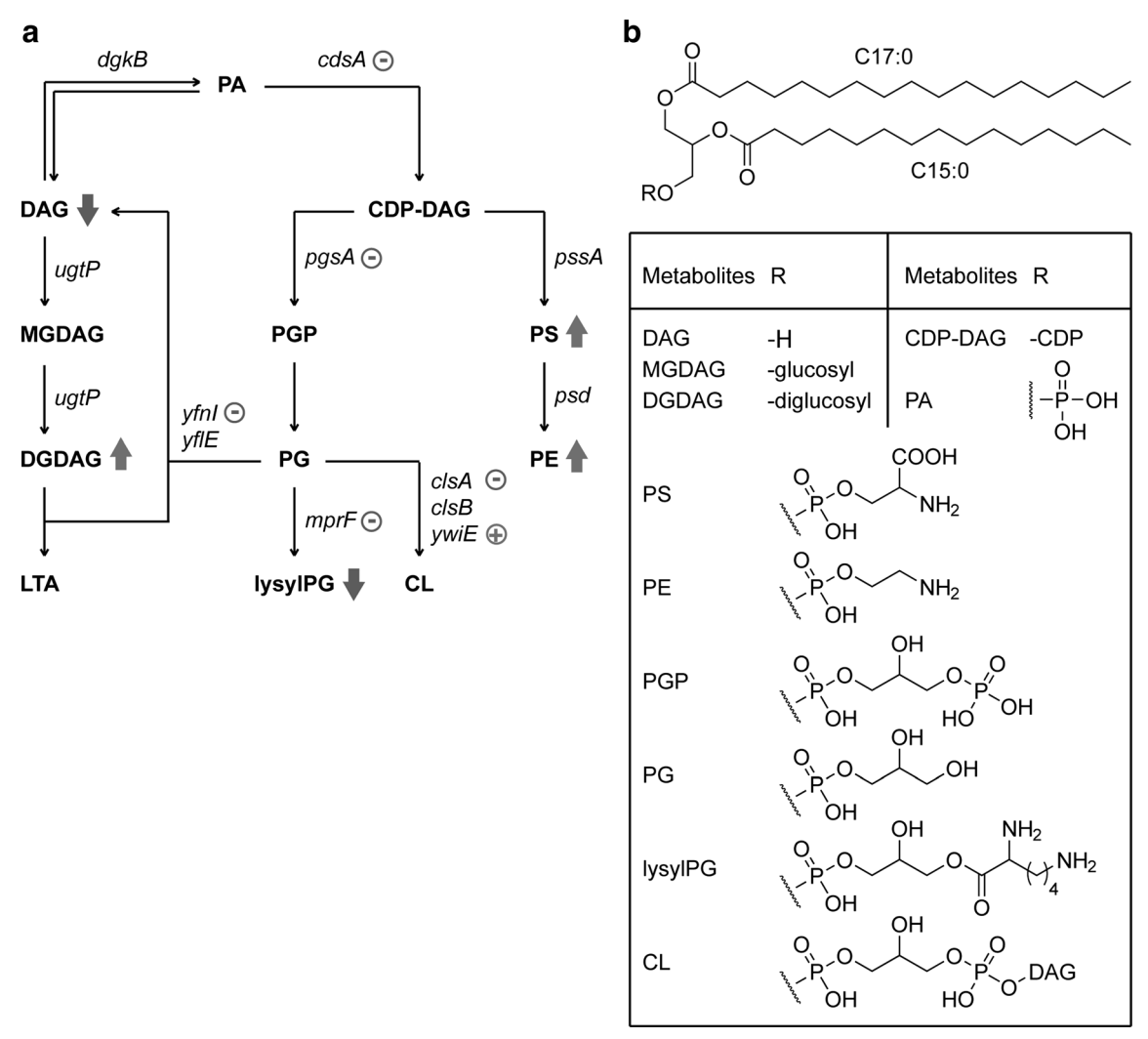


Fig. 4 Biosynthesis of membrane lipids in *B. subtilis*. a Pathways showing the key intermediates and enzyme-encoding genes for the biosynthesis of membrane lipids, starting from PA. The *block arrows* indicate lipids in the metabolomics analysis that had significantly elevated (*upward arrows*) or decreased (*downward arrows*) levels

under 1-butanol stress, whereas the *arithmetic symbols* represent up-(*pluses*) or down- (*minuses*) regulated gene transcript expression levels as determined from the qrtRT-PCR analysis. **b** Chemical structures of all the lipids shown in the pathways in **a**. All are derivatives of DAG

control groups, similar to the untargeted analysis above. As expected when the metabolites were not associated with 1-butanol stress response, all lipids under examination either changed statistically insignificantly (p > 0.05) or had two-fold or lower changes (Table 2 and SI Table S5). The data therefore confirmed that 1-butanol only caused a significant alteration in the levels of PE, DGDAG, PS, DAG, and lysylPG, but not *any* of the other lipids in the two biosynthetic pathways.

Expression levels of the key enzyme-encoding genes in membrane lipid biosynthetic pathways, as determined by qrtRT-PCR analysis How the stress-induced metabolites correlated to the regulation of the genes in the membrane lipid biosynthetic pathways of *B. subtilis* was examined by two-

stage qrtRT-PCR analysis on the total mRNA isolated from *B. subtilis* 168 cells grown under the same conditions as those for the untargeted metabolomics experiments. The relative mRNA expression level was determined for the genes in the membrane lipid biosynthetic pathways (Fig. 4: *cdsA*, *pssA*, *psd*, *pgsA*, *mprF*, *clsA*, *clsB*, *ywiE*, *dgkB*, *ugtP*, *yfnI*, and *yflE*).

The presence of 1-butanol significantly downregulated five of these 11 target genes, *cdsA* (3.4-fold), *pgsA* (1.9-fold), *mprF* (2.7-fold), *clsA* (2.5-fold), and *yfnI* (1.5-fold), and upregulated one, *ywiE* (22.3-fold), whereas the rest of the genes remained unaltered (Fig. 5). Interestingly, while *ywiE* was the only gene in the pathways found to be significantly upregulated, it had by far the highest magnitude (22.3-fold) of change. Together with the metabolomics data (Fig. 4), the results demonstrated an agreement between the



gene transcript expression level and detected metabolite levels.

Cell morphologies of B. subtilis 168 under 1-butanol stress Mutant B. subtilis cells with an altered membrane lipid composition have been shown to display aberrant cell morphologies (Salzberg and Helmann 2008), and therefore, whether the differential levels of glycerolipids and phospholipids observed in our studies led to changes in the cell morphology under 1-butanol stress was examined using SEM analysis. The studies clearly demonstrated the lengthening of stationary-phase cells after being exposed to 1.4 % (v/v) of 1butanol for 12 h in LB medium (the same medium as in the previous literature and at the concentration that resulted in a similar growth rate of B. subtilis as in SMM). The cells showed an almost twofold increased length (3.91 \pm 0.66 vs. $1.98 \pm 0.27 \,\mu\text{m}$) compared to the control cells (Fig. 6). Taken together, the findings suggested a potential correlation between the cell morphology, glycerolipid and phospholipid composition, and 1-butanol stress.

Discussion

Organic solvent-tolerant bacteria have the potential to be utilized in industrial and environmental biotechnology applications that range from biofuel and chemical production to biocatalysis and bioremediation (Nicolaou et al. 2010). With these premises, various studies have previously been conducted to elucidate the mechanisms of organic solvent tolerance (Torres et al. 2011). Some of the response mechanisms include the induction of stress proteins (Petersohn et al. 2001), inhibition of sporulation (Bohin et al. 1976), deactivation of organic solvents (Bustard et al. 2002), changes in cell morphology (Neumann et al. 2005; Nielsen et al. 2005), modification of the cell surface and cell membrane (Aono and Kobayashi 1997; Kabelitz et al. 2003; Weber and de Bont 1996), and solvent excretion through efflux pumps (Matsumoto et al. 2002). The knowledge of these mechanisms helps accelerate the acquisition of bacterial strains with a higher tolerance to organic solvents by allowing the genetic engineering of relevant pathways or by changing the levels of key culture factors that are altered when the organisms adapt to stress (Zingaro and Papoutsakis 2012).

1-Butanol is one of the organic solvents that have been used widely in industry. However, because 1-butanol is highly toxic to microorganisms, the possibilities of applying microbial fermentation to produce or transform 1-butanol to other important chemicals or for bioremediation are still quite limited in scope. In the hope of obtaining bacteria with an enhanced tolerance to 1-butanol in the near future, the present study was aimed at elucidating the metabolic responses of

B. subtilis in a 1-butanol-stressed environment using an untargeted metabolomics approach.

Accordingly, *B. subtilis* was exposed to 1-butanol during the early growing condition (late lag phase), which was earlier than in most previous reports. During this vulnerable early stage of growth, the bacteria are able to tolerate lower concentrations of 1-butanol than when 1-butanol is added at a later stage with an already high cell density (Kataoka et al. 2011). However, the late lag to early log phase condition was chosen in this study, because the common practice in fermentation process is to have the toxic substrates present as early as possible and the toxic products gradually formed.

We used an untargeted metabolomics analysis since, in contrast to targeted analysis that limits its scope to selected metabolites, untargeted analysis can detect and quantitate all ionizing metabolites based on their MSII, allowing measurement of both known and novel metabolites simultaneously (Saghatelian et al. 2004). The untargeted metabolomics analysis identified the zwitterionic PE, neutral PS, and neutral DGDAG to be differentially upregulated in 1-butanolstressed B. subtilis, whereas the positively charged lysylPG and neutral DAG were downregulated. If the whole-cell measurement of lipids in this work were directly correlated with the amount of these lipids in the B. subtilis membrane, it would mean that there is a decrease in the ratio of ionic to neutral lipids under 1-butanol stress. However, this interpretation does not explain our findings, because one would expect ionic lipids to repel with the nonpolar alkyl chain of 1-butanol better than neutral lipids.

Alternatively, the metabolomics data also indicates an increase in the ratio of neutral and anionic to cationic membrane lipids under 1-butanol stress. While no report has previously demonstrated the importance of maintaining this ratio, an increase in the anionic phospholipid contents has been shown previously to allow the adaptation of B. subtilis in a high salinity environment (Lopez et al. 2006), whereas cationic lipids generally played a role in attenuating the membrane perturbation of cationic compounds (Kilelee et al. 2010). Since 1-butanol is a neutral compound, both anionic and cationic lipids should not provide any extra protection for B. subtilis via charge-charge repulsion with the uncharged solvent. Thus, we speculated that if the altered amount of these charged lipids did not affect growth of the organism, their production might become unnecessary and was reduced in this environment, as observed in the case of the cationic lysylPG. On the other hand, the presence of the major anionic membrane lipid, PG, is essential for overall viability of the organism (Lopez et al. 2006), and therefore, its levels might be kept unaltered. Yet, it is also possible that the charged membrane lipids themselves might not interact directly with 1-butanol at all but affect the activities of integral membrane proteins, such as transporters, instead (Lee 2004). In any cases, more data



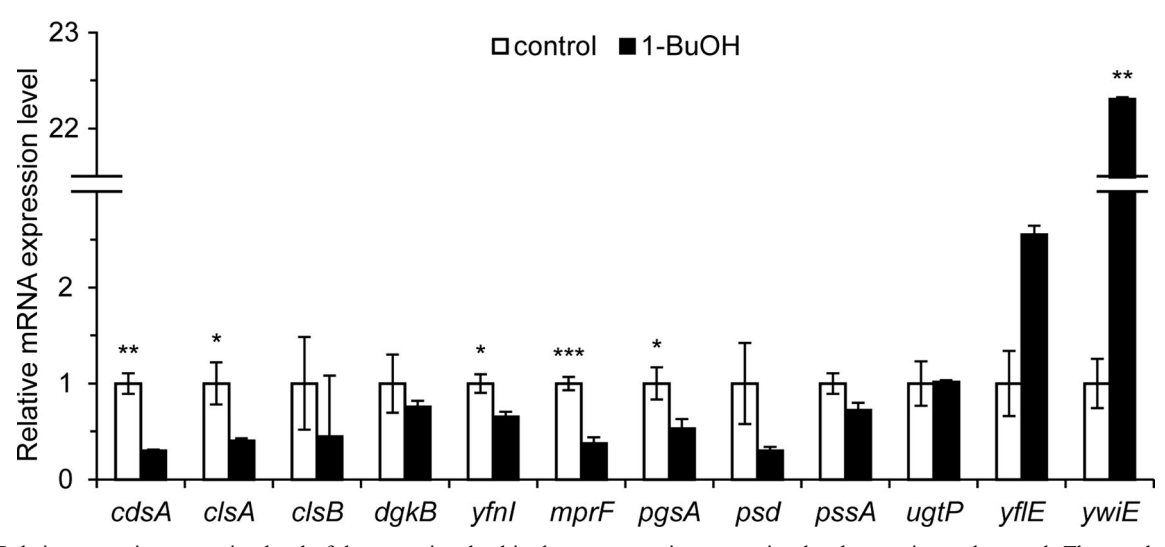


Fig. 5 Relative transcript expression level of the genes involved in the biosynthesis of membrane lipids in *B. subtilis* after treatment without (control; *white bars*) or with 1 % (v/v) 1-butanol (1-BuOH; *black bars*) for 6 h. The mRNA expression level was determined by two-stage qrtRT-PCR using the $2^{-\Delta\Delta Ct}$ method and standardized against the gyrB

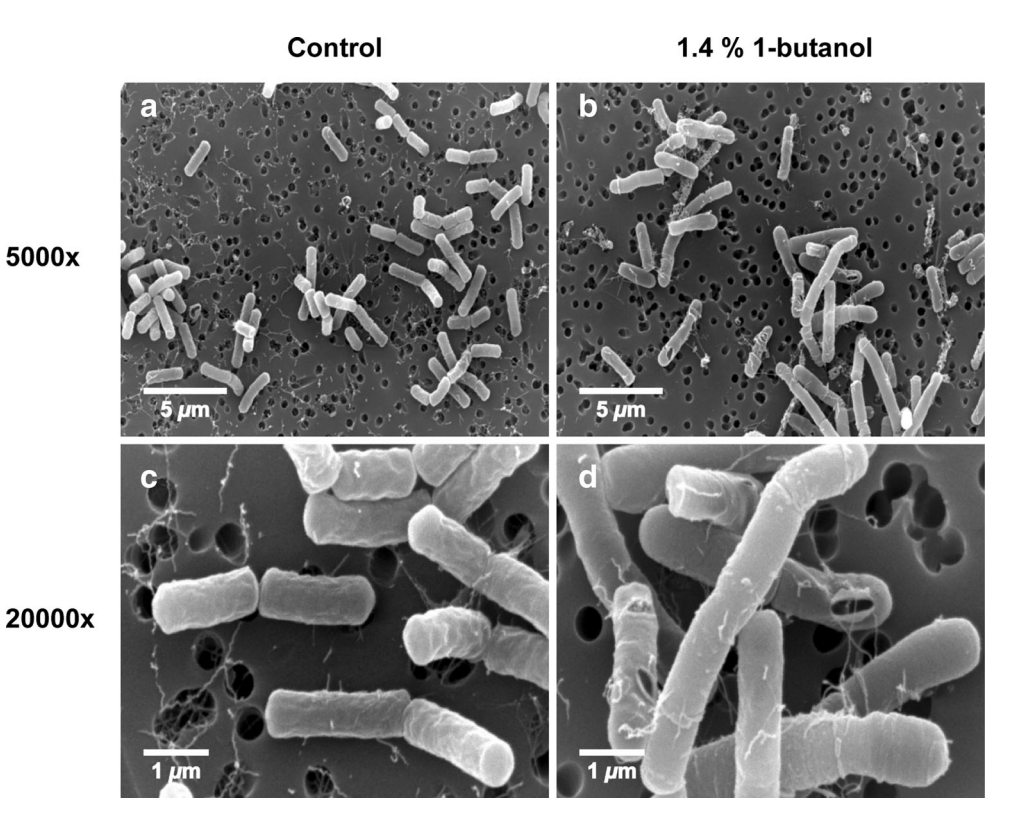
transcript expression level as an internal control. The graph indicates the fold changes in the indicated mRNA levels in 1-butanol-treated samples relative to that in the control. Data are shown as the average \pm standard errors of the mean, derived from three independent experiments. Student's t test: *p < 0.05; **p < 0.01; ***p < 0.005

points with other neutral organic solvents are needed, before any generalization can be drawn upon.

One of the known mechanisms of bacteria for dealing with organic solvent stress involves changing their membrane fluidity, which in many cases, can be achieved by changing their saturated-to-unsaturated fatty acid composition. For example, ethanol stress was reported to cause an increased level of unsaturated fatty acids in the membrane of *E. coli* (Ingram

1976) and *S. cerevisiae* (Beaven et al. 1982) and to increase the level of saturated fatty acids in *B. subtilis* (Rigomier et al. 1980) and *C. acetobutylicum* (Borden and Papoutsakis 2007; Lepage et al. 1987). Interestingly, we did not detect these changes in our metabolomics experiments with either the fatty acids themselves or as acyl chains of glycerolipids or phospholipids. One of the factors that may account for this discrepancy is that the earlier literature only described changes in

Fig. 6 Representative SEM images of *B. subtilis* 168 cells after being cultured **a**, **c** without or **b**, **d** with 1.4 % (ν/ν) of 1-butanol in LB medium for 12 h. 1-Butanol was supplemented into the *B. subtilis* 168 cultures during the late lag phase (OD600 ~ 0.2–0.3). Images shown are at **a**, **b** ×5000 (*scale bar* is 5 μm) and **c**, **d** ×20,000 (*scale bar* is 1 μm) magnification





fatty acid contents in *B. subtilis* under stress induced by methanol or ethanol, but not 1-butanol (Rigomier et al. 1980). Despite all three compounds being short-chain alcohols, they could affect lipid metabolism differently. For example, some fatty acid compositions were only modified by ethanol stress but remained unchanged with methanol stress (Rigomier et al. 1980). Alternatively, our results might simply be specific to the choices of the *B. subtilis* strain, growth medium, and conditions employed in this study. Further experiments are needed to test their generality.

The LC-MS/MS analyses of differentially altered lipids suggested that the most abundant acyl chains present were 15:0/15:0, 16:0/15:0, and 17:0/15:0. Although the results might look surprising without any a priori knowledge of the acyl chains of B. subtilis, the data was consistent with a previous report on the fatty acid distribution of the total membrane lipid extracts from B. subtilis, which indicated C15:0 as the most frequently found acyl chain (Clejan et al. 1986). Additional support for this observation also comes from a study on the lipid composition during various growth stages of B. subtilis by matrix-assisted laser desorption/ionization coupled to time-of-flight/time-of-flight (MALDI-TOF/TOF) mass spectrometry (Gidden et al. 2009). In this work, the authors reported the detection of sodiated PE, PG, lysylPG, and DGDAG in B. subtilis lipid extracts and applied tandem MS to identify the exact acyl chain combinations for DGDAG as observed here.

The LC–MS platform as used in this study was not without faults, however, since the system could not separate nor distinguish branched-chain lipids from straight-chain lipids. Since *B. subtilis* has previously been described to have C15:0 and C17:0 fatty acyl chains as mostly the iso- and anteisoderivatives (Clejan et al. 1986), it was likely that these branched-chain isomers constituted major components of our detected lipids. Nevertheless, except for the case of DGDAG above, our results demonstrated for the first time that glycerolipids and phospholipids in *B. subtilis* comprised mostly of 15:0/15:0, 16:0/15:0, and 17:0/15:0 acyl chains. Furthermore, the extensive list of MS/MS spectra of these lipids (SI) could serve as informative guides for the identification and characterization of these glycerolipids and phospholipids in the future.

Assuming that the levels of gene transcript expression correlate linearly with the activity of their encoded enzymes, the observed changes in the levels of glycerolipids and phospholipids could be partially explained by the changes in the relative mRNA expression levels. While the levels of the immediate enzymes for synthesis of PS and PE, PssA and Psd, were unaffected by 1-butanol, the level of PgsA, which also utilized CDP-DAG as its substrate, was decreased (Fig. 4). Consequently, more CDP-DAG might flux in the direction of PS and PE causing in their increased levels. On the other hand, the decreased levels of lysylPG could simply be due to the fact that the level of *mprF* was reduced.

Without differential expression of ugtP, the changes in the levels of DAG and DGDAG might seem uncorrelated to gene expression levels at first. However, because the YfnI enzyme can use DGDAG and PG as its substrate to release LTA and DAG as products (Wormann et al. 2011), the downregulation of the yfnI gene should lead to the heightened levels of substrates and lowered levels of products, which is consistent with that observed for DGDAG and DAG, respectively. Interestingly, the main LTA synthase enzyme (YflE), an ortholog of YfnI (Grundling and Schneewind 2007; Schirner et al. 2009), exhibited no significant change in its transcript expression levels. The transcription of *vfnI* is regulated by the sigma factor σ^{M} , which is involved in various stress tolerance responses, such as high salt and ethanol (Jervis et al. 2007; Thackray and Moir 2003). Albeit in the opposite direction, our work suggested that YfnI is potentially associated with the 1-butanol stress response as well. More importantly, while there are enzyme-encoding genes that were not evaluated in this study, especially in the intersecting pathways, the qrtRT-PCR data already demonstrated a strong correlation between gene regulation and metabolite production.

The *B. subtilis* 168 cells were shown to elongate almost twofold under 1-butanol stress in our studies. There are two membrane lipid-related genes that might be linked to the regulation of cell length, namely the *ugtP* and *yflE* genes. Deletion of the former gene was shown to shorten cells (Salzberg and Helmann 2008). The UgtP enzyme converts DAG into MGDAG and DGDAG in the membrane lipid biosynthetic pathway, and therefore, in the *ugtP* mutant, the levels of DAG and DGDAG should be elevated and decreased, respectively. While no significant changes in the transcript levels of *ugtP* were found in this study, the DAG and DGDAG levels were decreased and increased, respectively, under 1-butanol stress, corroborating the observed cell morphologies.

The deletion of the *yflE* gene was previously shown to increase the cell or cell chain length of *B. subtilis* (Schirner et al. 2009). Although YflE is the major LTA synthase enzyme in *B. subtilis*, another LTA synthase enzyme, YfnI, and not YflE showed a marked change in transcript expression levels under 1-butanol stress. A single deletion in the *yfnI* gene did not lead to the same morphological effects as the *yflE* mutant, but it is possible that its downregulation might affect the amount or structure of LTA (Wormann et al. 2011) or the same metabolites in the pathway as the *yflE* mutant, leading to the observed morphologies. Nevertheless, it is also possible that the observed longer cell phenotype under 1-butanol stress might be unrelated to these genes, and further experiments are required to pin down any effects of these genes on 1-butanol tolerance of *B. subtilis*.

In total, applying untargeted metabolomics to study the hydrophobic or lipid-soluble cell components of *B. subtilis* under 1-butanol stress led to the identification of a moderate number of stress-associated membrane lipids. Using a



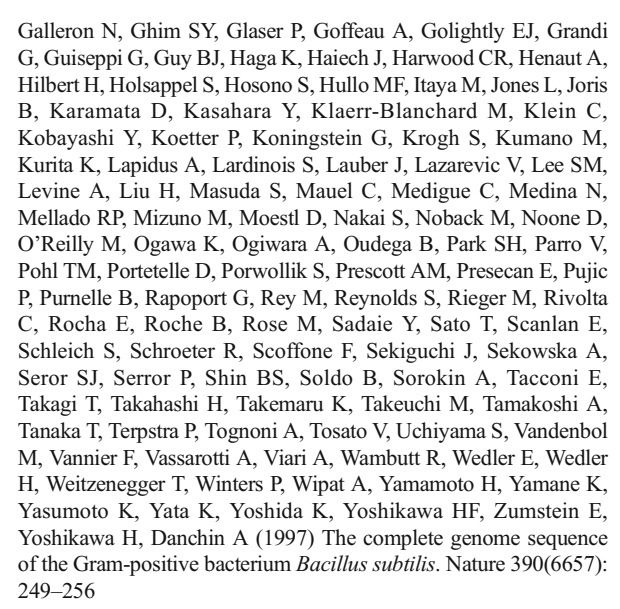
combination of accurate mass determination, tandem mass spectra, and partial comparison with synthetic standards, more than 85 % of the ions could be characterized and were found to belong to five classes of glycerolipids and phospholipids in the membrane lipid biosynthetic pathways. These methods also revealed for the first time that the most frequently found acyl chains of these lipids in B. subtilis were 15:0/15:0, 16:0/ 15:0, and 17:0/15:0. The downstream targeted grtRT-PCR and SEM analyses further supported this discovery. The former revealed six lipid metabolism genes with significant altered transcript expression levels that were strongly correlated with the observed metabolite changes, while the latter showed cell elongation morphologies that were potentially associated with the pathways. Together, this study revealed changes in the composition of glycerolipids and phospholipids in B. subtilis in response to 1-butanol stress. Future work will aim to determine the relevance of these changes in glycerolipids and phospholipids levels on 1-butanol tolerance. More generally, the results highlighted the importance of metabolite identification in metabolomics experiments, as well as the utility of linking metabolites to metabolic pathways in uncovering novel biological insights.

Acknowledgments We thank Sitthiporn Associates Co., Ltd. for providing us with the Waters Alliance e2695 high performance LC instrument; the Food Research and Testing Laboratory, Faculty of Science, Chulalongkorn University for access to the nitrogen concentrator; the Thai Government Stimulus Package 2 (TKK2555) for the financial support to acquire the Bruker MicrOTOF Q-II mass spectrometer; Poompat Aroonsri for his initial help with the project; and Dr. Robert Douglas John Butcher (Publication Counseling Unit, Chulalongkorn University) for his thorough checking of English usage and constructive comments in preparing this manuscript. This work was supported by the Thailand Research Fund (TRG5780194) and the Ratchadapisek Somphot Fund of Chulalongkorn University. The opinions expressed in this paper are the sole responsibility of the authors and do not necessarily reflect those of the Thailand Research Fund or Chulalongkorn University.

Conflict of interest The authors declare that they have no conflict of interest.

References

- Aono R, Kobayashi H (1997) Cell surface properties of organic solventtolerant mutants of *Escherichia coli* K-12. Appl Environ Microbiol 63(9):3637–3642
- Beaven MJ, Charpentier C, Rose AH (1982) Production and tolerance of ethanol in relation to phospholipid fatty-acyl composition in Saccharomyces cerevisiae NCYC 431. J Gen Microbiol 128(7): 1447–1455
- Kunst F, Ogasawara N, Moszer I, Albertini AM, Alloni G, Azevedo V, Bertero MG, Bessieres P, Bolotin A, Borchert S, Borriss R, Boursier L, Brans A, Braun M, Brignell SC, Bron S, Brouillet S, Bruschi CV, Caldwell B, Capuano V, Carter NM, Choi SK, Codani JJ, Connerton IF, Cummings NJ, Daniel RA, Denizot F, Devine KM, Dusterhoft A, Ehrlich SD, Emmerson PT, Entian KD, Errington J, Fabret C, Ferrari E, Foulger D, Fritz C, Fujita M, Fujita Y, Fuma S, Galizzi A,



- Boch J, Kempf B, Bremer E (1994) Osmoregulation in *Bacillus subtilis*: synthesis of the osmoprotectant glycine betaine from exogenously provided choline. J Bacteriol 176(17):5364–5371
- Bohin JP, Rigomier D, Schaeffer P (1976) Ethanol sensitivity of sporulation in *Bacillus subtilis*: a new tool for the analysis of the sporulation process. J Bacteriol 127(2):934–940
- Borden JR, Papoutsakis ET (2007) Dynamics of genomic-library enrichment and identification of solvent tolerance genes for *Clostridium acetobutylicum*. Appl Environ Microbiol 73(9):3061–3068. doi:10. 1128/AEM.02296-06
- Bustard MT, Whiting S, Cowan DA, Wright PC (2002) Biodegradation of high-concentration isopropanol by a solvent-tolerant thermophile, *Bacillus pallidus*. Extremophiles 6(4):319–323. doi:10.1007/ s00792-001-0260-5
- Clejan S, Krulwich TA, Mondrus KR, Seto-Young D (1986) Membrane lipid composition of obligately and facultatively alkalophilic strains of *Bacillus* spp. J Bacteriol 168(1):334–340
- Connor MR, Liao JC (2009) Microbial production of advanced transportation fuels in non-natural hosts. Curr Opin Biotechnol 20(3):307–315. doi:10.1016/j.copbio.2009.04.002
- Durre P (2011) Fermentative production of butanol—the academic perspective. Curr Opin Biotechnol 22(3):331–336. doi:10.1016/j.copbio.2011.04.010
- Fischer CR, Klein-Marcuschamer D, Stephanopoulos G (2008) Selection and optimization of microbial hosts for biofuels production. Metab Eng 10(6):295–304. doi:10.1016/j.ymben.2008.06.009
- Fortman JL, Chhabra S, Mukhopadhyay A, Chou H, Lee TS, Steen E, Keasling JD (2008) Biofuel alternatives to ethanol: pumping the microbial well. Trends in Biotechnology 26(7):375–381. doi:http:// dx.doi.org/10.1016/j.tibtech.2008.03.008
- Gidden J, Denson J, Liyanage R, Ivey DM, Lay JO (2009) Lipid compositions in *Escherichia coli* and *Bacillus subtilis* during growth as determined by MALDI-TOF and TOF/TOF mass spectrometry. Int J Mass Spectrom 283(1–3):178–184. doi:10.1016/j.ijms.2009.03.005
- Green EM (2011) Fermentative production of butanol—the industrial perspective. Curr Opin Biotechnol 22(3):337–343. doi:10.1016/j. copbio.2011.02.004
- Grundling A, Schneewind O (2007) Synthesis of glycerol phosphate lipoteichoic acid in *Staphylococcus aureus*. Proc Natl Acad Sci U S A 104(20):8478–8483. doi:10.1073/pnas.0701821104
- Ingram LO (1976) Adaptation of membrane lipids to alcohols. J Bacteriol 125(2):670–678



- Jervis AJ, Thackray PD, Houston CW, Horsburgh MJ, Moir A (2007) SigM-responsive genes of *Bacillus subtilis* and their promoters. J Bacteriol 189(12):4534–4538. doi:10.1128/Jb.00130-07
- Kabelitz N, Santos PM, Heipieper HJ (2003) Effect of aliphatic alcohols on growth and degree of saturation of membrane lipids in Acinetobacter calcoaceticus. FEMS Microbiol Lett 220(2):223–227
- Kataoka N, Tajima T, Kato J, Rachadech W, Vangnai AS (2011) Development of butanol-tolerant *Bacillus subtilis* strain GRSW2-B1 as a potential bioproduction host. AMB Express 1(1):10. doi: 10.1186/2191-0855-1-10
- Kilelee E, Pokorny A, Yeaman MR, Bayer AS (2010) Lysyl-phosphatidylglycerol attenuates membrane perturbation rather than surface association of the cationic antimicrobial peptide 6W-RP-1 in a model membrane system: implications for daptomycin resistance. Antimicrob Agents Chemother 54(10):4476–4479. doi:10.1128/AAC.00191-10
- Kongpol A, Kato J, Vangnai AS (2008) Isolation and characterization of *Deinococcus geothermalis* T27, a slightly thermophilic and organic solvent-tolerant bacterium able to survive in the presence of high concentrations of ethyl acetate. FEMS Microbiol Lett 286(2):227–235. doi:10.1111/j.1574-6968.2008.01273.x
- Lee AG (2004) How lipids affect the activities of integral membrane proteins. Biochim Biophys Acta 1666(1–2):62–87. doi:10.1016/j. bbamem.2004.05.012
- Lepage C, Fayolle F, Hermann M, Vandecasteele JP (1987) Changes in membrane lipid composition of *Clostridium acetobutylicum* during acetone-butanol fermentation: effects of solvents, growth temperature and pH. J Gen Microbiol 133(1):103–110
- Liu S, Qureshi N (2009) How microbes tolerate ethanol and butanol. New Biotechnology 26(3–4):117–121. doi:10.1016/j.nbt.2009.06.984
- Lopez CS, Alice AF, Heras H, Rivas EA, Sanchez-Rivas C (2006) Role of anionic phospholipids in the adaptation of *Bacillus subtilis* to high salinity. Microbiology 152(Pt 3):605–616. doi:10.1099/mic.0. 28345-0
- Matias VR, Beveridge TJ (2008) Lipoteichoic acid is a major component of the *Bacillus subtilis* periplasm. J Bacteriol 190(22):7414–7418. doi:10.1128/JB.00581-08
- Matsumoto M, de Bont JA, Isken S (2002) Isolation and characterization of the solvent-tolerant *Bacillus cereus* strain R1. J Biosci Bioeng 94(1):45–51
- Matsuoka S, Hashimoto M, Kamiya Y, Miyazawa T, Ishikawa K, Hara H, Matsumoto K (2011) The *Bacillus subtilis* essential gene dgkB is dispensable in mutants with defective lipoteichoic acid synthesis. Genes Genet Syst 86(6):365–376
- Nakano MM, Dailly YP, Zuber P, Clark DP (1997) Characterization of anaerobic fermentative growth of *Bacillus subtilis*: identification of fermentation end products and genes required for growth. J Bacteriol 179(21):6749–6755
- Neumann G, Veeranagouda Y, Karegoudar TB, Sahin O, Mausezahl I, Kabelitz N, Kappelmeyer U, Heipieper HJ (2005) Cells of Pseudomonas putida and Enterobacter sp. adapt to toxic organic compounds by increasing their size. Extremophiles 9(2):163–168. doi:10.1007/s00792-005-0431-x
- Ni Y, Sun Z (2009) Recent progress on industrial fermentative production of acetone-butanol-ethanol by *Clostridium acetobutylicum* in China. Appl Microbiol Biotechnol 83(3):415–423. doi:10.1007/s00253-009-2003-y
- Nicolaou SA, Gaida SM, Papoutsakis ET (2010) A comparative view of metabolite and substrate stress and tolerance in microbial bioprocessing: from biofuels and chemicals, to biocatalysis and bioremediation. Metab Eng 12(4):307–331. doi:10.1016/j.ymben. 2010.03.004

- Nielsen LE, Kadavy DR, Rajagopal S, Drijber R, Nickerson KW (2005) Survey of extreme solvent tolerance in Gram-positive cocci: membrane fatty acid changes in *Staphylococcus haemolyticus* grown in toluene. Appl Environ Microbiol 71(9):5171–5176. doi:10.1128/AFM 71.9.5171-5176.2005
- Petersohn A, Brigulla M, Haas S, Hoheisel JD, Volker U, Hecker M (2001) Global analysis of the general stress response of *Bacillus subtilis*. J Bacteriol 183(19):5617–5631. doi:10.1128/JB.183.19.5617-5631.2001
- Rigomier D, Bohin JP, Lubochinsky B (1980) Effects of ethanol and methanol on lipid metabolism in *Bacillus subtilis*. J Gen Microbiol 121(1):139–149
- Saghatelian A, Trauger SA, Want EJ, Hawkins EG, Siuzdak G, Cravatt BF (2004) Assignment of endogenous substrates to enzymes by global metabolite profiling. Biochemistry 43(45):14332–14339
- Salzberg LI, Helmann JD (2008) Phenotypic and transcriptomic characterization of *Bacillus subtilis* mutants with grossly altered membrane composition. J Bacteriol 190(23):7797–7807. doi:10.1128/JB. 00720-08
- Schirner K, Marles-Wright J, Lewis RJ, Errington J (2009) Distinct and essential morphogenic functions for wall- and lipo-teichoic acids in *Bacillus subtilis*. EMBO J 28(7):830–842. doi:10.1038/emboj.2009.
- Smith CA, O'Maille G, Want EJ, Qin C, Trauger SA, Brandon TR, Custodio DE, Abagyan R, Siuzdak G (2005) METLIN: a metabolite mass spectral database. Ther Drug Monit 27(6):747–751
- Smith CA, Want EJ, O'Maille G, Abagyan R, Siuzdak G (2006) XCMS: processing mass spectrometry data for metabolite profiling using nonlinear peak alignment, matching, and identification. Anal Chem 78(3):779–787. doi:10.1021/ac051437y
- Spizizen J (1958) Transformation of biochemically deficient strains of Bacillus subtilis by deoxyribonucleate. Proc Natl Acad Sci U S A 44(10):1072–1078
- Thackray PD, Moir A (2003) SigM, an extracytoplasmic function sigma factor of *Bacillus subtilis*, is activated in response to cell wall antibiotics, ethanol, heat, acid, and superoxide stress. J Bacteriol 185(12):3491–3498. doi:10.1128/Jb.185.12.3491-3498.2003
- Torres S, Pandey A, Castro GR (2011) Organic solvent adaptation of Gram positive bacteria: applications and biotechnological potentials. Biotechnol Adv 29(4):442–452. doi:10.1016/j.biotechadv.2011.04. 002
- Vinayavekhin N, Saghatelian A (2009) Regulation of alkyldihydrothiazole-carboxylates (ATCs) by iron and the pyochelin gene cluster in *Pseudomonas aeruginosa*. ACS Chem Biol 4(8): 617–623. doi:10.1021/cb900075n
- Vinayavekhin N, Saghatelian A (2010) Untargeted metabolomics. Current protocols in molecular biology/edited by Frederick M Ausubel [et al] Chapter 30:Unit 30 1 1–24. doi:10.1002/0471142727.mb3001s90
- Vinayavekhin N, Saghatelian A (2011) Discovery of a protein-metabolite interaction between unsaturated fatty acids and the nuclear receptor Nur77 using a metabolomics approach. J Am Chem Soc 133(43): 17168–17171. doi:10.1021/ja208199h
- Weber FJ, de Bont JA (1996) Adaptation mechanisms of microorganisms to the toxic effects of organic solvents on membranes. Biochim Biophys Acta 1286(3):225–245
- Wormann ME, Corrigan RM, Simpson PJ, Matthews SJ, Grundling A (2011) Enzymatic activities and functional interdependencies of *Bacillus subtilis* lipoteichoic acid synthesis enzymes. Mol Microbiol 79(3):566–583. doi:10.1111/j.1365-2958.2010.07472.x
- Zingaro KA, Papoutsakis ET (2012) Toward a semisynthetic stress response system to engineer microbial solvent tolerance. MBio 3(5). doi:10.1128/mBio.00308-12

